

Doctoral Thesis

# Water driven transport processes in agricultural systems across scales

submitted in satisfaction of the requirements for the degree of  
Doctor of Science in Civil Engineering  
of the TU Wien, Faculty of Civil Engineering

as part of the  
Vienna Doctoral Program on Water Resource Systems

by

Dipl. Ing. **Alexander Eder**

Matr.Nr.: 0040142

- Examiner: Univ.Prof. Dipl.-Ing. Dr. techn. **Günter Blöschl**  
Institut für Wasserbau und Ingenieurhydrologie  
Technische Universität Wien  
Karlsplatz 13/222, 1040 Wien
- Examiner: Univ.Prof. Dipl.-Ing. Dr. techn. **Matthias Zessner**  
Institut für Wassergüte und Ressourcenmanagement  
Technische Universität Wien  
Karlsplatz 13/226, 1040 Wien
- Examiner: Assoc.Prof. Dr. **Alberto Viglione**  
Department of Environment, Land and Infrastructure Engineering (DIATI)  
Polytechnic University of Turin  
Corso Duca degli Abruzzi 24, 10129 Turin, Italy

Vienna, May 202

---



Die approbierte gedruckte Originalversion dieser Dissertation ist an der TU Wien Bibliothek verfügbar.  
The approved original version of this doctoral thesis is available in print at TU Wien Bibliothek.

Dissertation

# Wasserbezogene Transportprozesse in landwirtschaftlich genutzten Systemen auf unterschiedlichen Skalen

ausgeführt zum Zwecke der Erlangung des akademischen Grades eines  
Doktors der technischen Wissenschaften  
eingereicht an der Technischen Universität Wien, Fakultät für Bauingenieurwesen

als Teil des Doktoratskolleg für  
Water Resource Systems

von

Dipl. Ing. **Alexander Eder**

Matr.Nr.: 0040142

- Gutachter: Univ.Prof. Dipl.-Ing. Dr. techn. **Günter Blöschl**  
Institut für Wasserbau und Ingenieurhydrologie  
Technische Universität Wien  
Karlsplatz 13/222, 1040 Wien
- Gutachter: Univ.Prof. Dipl.-Ing. Dr. techn. **Matthias Zessner**  
Institut für Wassergüte und Ressourcenmanagement  
Technische Universität Wien  
Karlsplatz 13/226, 1040 Wien
- Gutachter: Assoc.Prof. Dr. **Alberto Viglione**  
Department of Environment, Land and Infrastructure Engineering (DIATI)  
Polytechnic University of Turin  
Corso Duca degli Abruzzi 24, 10129 Turin, Italy

Wien, im Mai 2021

---



Die approbierte gedruckte Originalversion dieser Dissertation ist an der TU Wien Bibliothek verfügbar.  
The approved original version of this doctoral thesis is available in print at TU Wien Bibliothek.

---

## Abstract

Agricultural land use often causes higher erosion rates and higher release of nutrients compared to other land uses, potentially resulting in land degradation and reduced water quality. Among other parameters, suspended sediments and solutes, such as dissolved organic carbon and nitrogen, control the water quality and therefore the usability of water and the ecological status of water bodies. Furthermore, a considerable part of greenhouse gas emissions, especially  $N_2O$ , are indirect soil emissions via leaching and runoff caused by agricultural activities. Understanding the water driven transport processes of sediments and nutrients and their export from agricultural catchments is therefore important for both land and water resources management. The aim of this thesis is to explore these processes, in particular the flow paths, concentrations and loads of sediments, dissolved organic carbon and nitrogen.

In Chapter 2, the short-term dynamics of sediments during rainfall-runoff events and their impact on sediment load calculations were investigated. Due to a high variability in the relationship between runoff and sediment concentration, both during and between individual events and various hysteresis effects, instantaneous sediment concentrations and event loads are difficult to estimate. Therefore, five methods for calculating the instantaneous sediment concentrations in the stream and the resulting sediment loads were tested on 19 events in the hydrological open-air laboratory (HOAL) in Petzenkirchen, Lower Austria. Calibrated turbidity measurements (i) with high temporal resolution were used as a benchmark. A generalized rating curve approach of all data pairs (ii) between runoff and sediment concentration of the water samples resulted a considerable bias for both event specific sediment concentrations and total sediments loads. Fitting of event-specific rating curves (iii) still misrepresented instantaneous sediment concentrations within the events, but gave load estimations that were in a range of 5% of the benchmark. Two approaches accounting explicitly for hysteresis, applied to sediment concentrations of water samples (iv) and turbidity measurements (v), exhibited the best fit and provided load estimates that were within a range of 0–1% of the benchmark sediment concentrations. Testing the various hysteresis effects against event parameters such as event rainfall, maximum rainfall intensity and initial soil water content suggested a relationship with these parameters, which renders them useful for estimating concentrations based on this hysteresis model approach.

As an open issue of the hysteresis model approach, the within-event time patterns of sediment concentrations usually differed from those of the associated precipitation. It was hypothesised that this phenomenon may be related to different sediment sources such as the stream bed itself, which was subsequently investigated in Chapter 3. To understand resuspension of stream bed sediments at the reach scale we artificially flooded the small stream of the HOAL

---

Petzenkirchen by pumping sediment-free water into the stream ( $\sim 17 \text{ m}^3$ ,  $57 \text{ l s}^{-1}$ ). Two short floods were produced and flow, sediment and bromide concentrations were measured at three sites with high temporal resolution. Hydrologically, the two flood events were almost identical, however, a considerably smaller sediment load was resuspended and transported during the second event due to depletion of stream bed sediments. The results indicate that the first peak of the sedigraphs of natural events in this stream is indeed caused by the resuspension of streambed sediments, accounting for up to six percent of the event sediment load depending on total flow volume.

In Chapter 4, the fate of the quantity of dissolved organic carbon (DOC) and the composition of dissolved organic matter (DOM) in an agricultural hillslope - stream network system was explored. We measured DOC and DOM quality (by fluorescent spectrophotometry and PARAFAC analyses) of soil samples on three land use units (arable, grassland, forest), and of water samples from the stream and from seven tributaries (inlet, tile drains, spring). Soil DOC shows the highest concentrations in summer due to high temperatures. In contrast, DOC concentrations in the tributaries are lower in summer than in winter by between 19% and 31% due to higher microbial biomass and respiration. DOM composition of the soil eluate differs between land use units which, however, is not reflected by the DOM composition in the tributaries. DOM is related to DOC and to catchment soil moisture; wetter soils lead to more refractory terrestrial DOM and less labile, protein-like DOM. We estimated the DOC import from the tributaries into the stream as 125 kg during base flow conditions in the period February to December 2017 and the instream DOC production as 38 kg, considering mass balance and exchange with groundwater. Instream processes modify DOM quality over short flow distances.

Chapter 5 is dedicated to nitrogen, another important nutrient. This analysis goes beyond the water bodies, additionally exploring atmospheric interactions. Specifically, the indirect nitrogen losses from agricultural areas and their contribution to greenhouse gases emission were evaluated by using 22 lysimeters, covering a wide range of soils, climatic conditions and management practices in Austria. The components of the nitrogen mass balance of the lysimeters were directly measured for several years. Both grassland and arable land plots gave significantly smaller values of  $\text{Frac}_{\text{LEACH}}$  than the default value of 0.3 recommended by the International Panel on Climate Change (IPCC) for estimating annual emissions.  $\text{Frac}_{\text{LEACH}}$  is a factor that represents the fraction of nitrogen losses compared to total nitrogen inputs and sources. For grassland,  $\text{Frac}_{\text{LEACH}}$  values of only 0.02 were found which varied very little over the entire observation period. For arable sites,  $\text{Frac}_{\text{LEACH}}$  values were higher (around 0.25) and showed significant variability between years due to variations in crop rotation, fertilization rates, and yields. The new  $\text{Frac}_{\text{LEACH}}$  estimate for Austria of 0.15 has been used in the National Inventory Report submitted annually to the IPCC since 2016.

This thesis contributes in both methodological and practical ways to the current knowledge of water related transport processes. The improved estimation method that accounts for the within-event dynamics of sediment transport gives more accurate estimates of sediment loads

---

than the existing methods. These can support the evaluation of erosion protection measures and the optimization of land management in order to maintain the quality and ecological state of water bodies, while taking into account the viability of agricultural operations. The investigation of the transport processes of dissolved organic carbon and its composition has resulted in an enhanced understanding of the role of land use and other environmental factors in these processes, which can also support decision-making in the interaction between agriculture and water management. Finally, the analysis of nitrogen goes one step further. The new, more precise values of the factor representing nitrogen losses results in a reduction of the estimates of indirect soil emissions in Austria by 50% to 1,46 Gg N<sub>2</sub>O (laughing gas), corresponding to a CO<sub>2</sub> equivalent of 435 Gg per year and thus also has enormous economic relevance due to the reduced target level of the overall emissions.



Die approbierte gedruckte Originalversion dieser Dissertation ist an der TU Wien Bibliothek verfügbar.  
The approved original version of this doctoral thesis is available in print at TU Wien Bibliothek.

---

## Zusammenfassung

Die landwirtschaftliche Nutzung der Böden führt im Vergleich zu anderen Nutzungen in der Regel zu höheren Erosionsraten und einem höheren Nährstoffaustrag, und damit potentiell zu Bodendegradation und zur Beeinträchtigung der Wasserqualität. Neben anderen Parametern bestimmen die Konzentrationen von Feststoffen (suspendierte Sedimente) und gelösten Stoffen, wie zum Beispiel gelöstem organischen Kohlenstoff oder Stickstoff, das Ausmaß der Beeinträchtigung und damit die Nutzbarkeit des Wassers und den ökologischen Zustand der Gewässer. Darüber hinaus tragen indirekte Bodenemissionen durch Auswaschung und oberflächlichen Abfluss auf landwirtschaftlichen Flächen zur Emission von Lachgas ( $N_2O$ ) und anderen Treibhausgasen bei. Für eine effiziente, ausgewogene Bewirtschaftung der Landschaft und der Wasserressourcen ist deshalb die Kenntnis der wasserbezogenen Transportprozesse von Sedimenten und Nährstoffen im landwirtschaftlichen Kontext essentiell. Ziel dieser Arbeit ist es, diese Transportprozesse zu untersuchen, insbesondere die Fließpfade, Konzentrationen und Frachten von Sedimenten, gelöstem organischen Kohlenstoff und Stickstoff.

In Kapitel 2 wurden die kurzfristige Dynamik des Sedimenttransportes während Niederschlags-Abfluss-Ereignissen und ihre Auswirkungen auf die Berechnung des Sedimentaustrags untersucht. Aufgrund der hohen Variabilität in der Beziehung von Abfluss und Sedimentkonzentration, sowohl während als auch zwischen einzelnen Ereignissen, und Hysteresiseffekten, ist die Berechnung der aktuellen Sedimentkonzentrationen und des Sedimentaustrages nur mit großen Unsicherheiten möglich. Deshalb wurden fünf Methoden zur Berechnung der Sedimentkonzentrationen im Bach und der daraus resultierende Sedimentaustrag an 19 Ereignissen im Hydrologischen Freiluftlabor (HOAL) in Petzenkirchen, Niederösterreich, getestet. Als Benchmark dienten zeitlich hoch aufgelöste, kalibrierte Trübungsmessungen (i). Die Verwendung einer allgemeinen Beziehung aller Datenpaare (ii) zwischen Abfluss und Sedimentkonzentration der Wasserproben führte zu systematischen Abweichungen von Konzentrationen und Frachten des Sedimentaustrags im Vergleich zum Benchmark. Die Anpassung ereignisspezifischer Beziehungen (iii) führte zwar auch zu erheblichen Abweichungen bei den Konzentrationen, die Frachten konnten jedoch mit einer Genauigkeit von etwa 5% ermittelt werden. Durch die Berücksichtigung der Hysterese in der Beziehung konnte die Genauigkeit sowohl bei der Verwendung von Wasserproben (iv) als auch bei der Trübungsmessung (v) weiter gesteigert werden (0–1% Abweichung vom Benchmark-Sedimentaustrag). Die Parameter zur Beschreibung der Hysterese (Richtung und Größe) wurden in Bezug zu Ereignischarakteristika gesetzt und sind abhängig vom Ereignisniederschlag, der maximalen Niederschlagsintensität und dem Anfangsbodenwassergehalt. Sie erlauben eine zutreffende Vorhersage des Sedimentkonzentrationsverlaufs basierend auf Ereignisparametern.

Eine offene Frage bei der Verwendung des Hysterese-modells war die im Vergleich zum Niederschlagsverlauf unterschiedliche zeitliche Entwicklung der Sedimentkonzentration, die mit der Aktivierung unterschiedlicher Sedimentquellen zusammenhängen könnte. In Kapitel 3 wird deshalb untersucht, ob das Bachbett eine dieser Sedimentquellen ist. Um die Resuspension von Bachbett-Sedimenten zu verstehen, wurde der Bach des HOAL Petzenkirchen künstlich geflutet, indem sedimentfreies Wasser in den Bach gepumpt wurde ( $\sim 17 \text{ m}^3$ ,  $57 \text{ l s}^{-1}$ ). Es wurden zwei kurze Wellen erzeugt und der Abfluss sowie die Sediment- und Bromidkonzentrationen an drei Stellen mit hoher zeitlicher Auflösung gemessen. Hydrologisch waren die beiden Wellen nahezu identisch, jedoch wurde während der zweiten Welle aufgrund der bereits im ersten Versuch verlagerten Sedimente eine erheblich geringere Sedimentfracht resuspendiert und transportiert. Die Ergebnisse zeigen, dass der erste Peak der Sedigraphen von natürlichen Ereignissen in diesem Bach tatsächlich durch die Resuspension von Sedimenten im Flussbett verursacht wird und diese je nach Gesamtabflussvolumen bis zu sechs Prozent der Sedimentaustrags des Ereignisses ausmacht.

In Kapitel 4 wurde der Transport von gelöstem organischem Kohlenstoff (DOC) und die Veränderung seiner Zusammensetzung (DOM) untersucht. Bodenproben von drei unterschiedlichen Landnutzungseinheiten (Ackerland, Grünland, Wald) und Wasserproben von den Zuflüssen zum Bach (Dränagen, Quellen) sowie vom Bach selbst wurden hinsichtlich DOC Gehalte und DOM Qualität, die mittels Fluoreszenzspektrophotometrie und PARAFAC Analysen bestimmt wurde, untersucht. Der Boden weist im Sommer aufgrund hoher Temperaturen die höchsten Konzentrationen an DOC auf. Im Gegensatz dazu sind die DOC Konzentrationen in den Zuflüssen zum Bach im Sommer aufgrund höherer mikrobieller Biomasse und Veratmung um 19% bis 31% niedriger als im Winter. Die verschiedenen Landnutzungseinheiten weisen eine unterschiedliche DOM Zusammensetzung auf, die aber in den Zuflüssen (aus unterschiedlichen Landnutzungseinheiten) nicht mehr zu erkennen ist. Die DOM Zusammensetzung der Zuflüsse ist neben der Höhe der DOC Konzentration auch von der Bodenfeuchte im Einzugsgebiet abhängig. Feuchtere Böden führen zu höheren Anteilen schwer abbaubaren, terrestrischem DOM und geringeren Anteilen von labilem, proteinartigem DOM. Der DOC Import von den Zuflüssen betrug im Zeitraum von Februar bis Dezember 2017 bei Basisabflussbedingungen 125 kg. Für den Bach selbst wurden mittels Massenbilanz und unter Berücksichtigung von DOC Austausch mit dem Grundwasser eine DOC Produktion von 38 kg berechnet. Um- und Abbauprozesse innerhalb des Baches reduzieren den Anteil labilen DOMs bereits innerhalb einer kurzen Fließstrecke.

Das Kapitel 5 widmet sich dem Stickstoff als weiteren wichtigen Nährstoff. Hier ist, über die Gewässer hinausgehend, auch der Zusammenhang mit der Atmosphäre von Interesse. Es wurden die indirekten Stickstoffverluste aus landwirtschaftlich genutzten Flächen und ihr Beitrag zur Treibhausgasemission mit Hilfe von 22 Lysimetern bewertet, die ein breites Spektrum von Böden, klimatischen Bedingungen und Bewirtschaftungspraktiken in Österreich abdecken. Die Bilanzglieder der Stickstoffkreislaufes wurden mit den Lysimetern über mehrere Jahre direkt gemessen. Sowohl für Grünland als auch für ackerbaulich genutzte Flächen wurden

---

geringere  $Frac_{LEACH}$ -Werte bestimmt, als vom Zwischenstaatlicher Ausschuss für Klimaänderungen (IPCC) zur Berechnung der jährlichen Emissionen empfohlen wird (0.3).  $Frac_{LEACH}$  ist ein Faktor, der den Anteil der jährlichen Stickstoffverluste den gesamten jährlichen Stickstoffeinträgen inklusive Mineralisierungspotential gegenüberstellt. Für Grünland wurde ein mittlerer  $Frac_{LEACH}$ -Wert von nur 0,02 berechnet mit geringer räumlicher und zeitlicher Variabilität. Die  $Frac_{LEACH}$ -Werte für Ackerflächen betragen im Mittel 0,25 mit einer deutlichen Variabilität zwischen den Jahren aufgrund der unterschiedlichen Fruchtfolgen, den Düngungsgaben und Erträgen. Der neue berechnete  $Frac_{LEACH}$  Wert für Österreich von 0,15 wird seit 2016 zur Erstellung des nationalen Inventurberichts verwendet, der jährlich dem IPCC vorgelegt wird.

Diese Arbeit hat eine Reihe neuer Erkenntnisse über wasserbezogene Transportprozesse in landwirtschaftlichen Systemen erzielt, die auch aus praktischer Sicht wesentlich sind. Die hier entwickelte Berechnungsmethode der Dynamik des Sedimenttransportes während Ereignissen und die darauf aufbauende Austragsberechnung sind genauer als die existierenden Verfahren. Sie können als Grundlage für die Bewertung von Erosionsschutzmaßnahmen und die Optimierung der Landbewirtschaftung dienen, um die Qualität und Funktionsfähigkeit der Gewässer zu erhalten, bei gleichzeitiger Berücksichtigung der Wirtschaftlichkeit der landwirtschaftlichen Betriebe. Die Untersuchung der Transportprozesse von gelöstem organischem Kohlenstoff und dessen Zusammensetzung hat eine Einschätzung der Rolle der Landnutzung und anderer Umweltfaktoren für diese Prozesse ergeben, die ebenfalls Entscheidungsprozesse im Zusammenspiel Landwirtschaft-Wasserwirtschaft unterstützen kann. Die Untersuchung des Stickstoffs schließlich geht einen Schritt weiter. Die neuen, genaueren Werte des Faktors, der die Stickstoffverluste beschreibt, reduziert die Rechenwerte der indirekten Bodenemissionen Österreichs um 50% auf 1,46 Gg  $N_2O$  (Lachgas), entsprechend einem  $CO_2$ -Äquivalent von 435 Gg pro Jahr, und hat damit auch eine enorme wirtschaftliche Bedeutung.



Die approbierte gedruckte Originalversion dieser Dissertation ist an der TU Wien Bibliothek verfügbar.  
The approved original version of this doctoral thesis is available in print at TU Wien Bibliothek.

---

*I am very grateful to my supervisor Prof. Günter Blöschl for his patient, and highly motivating guidance. His commitment to the establishment of the doctoral program on water resource systems brought me enormous advantages and offered the opportunity to build up a network beyond the subject of hydrology.*

*I would like to thank Prof. Matthias Zessner and Prof. Alberto Viglione for their critical review of my thesis.*

*I wish to thank Dr. Peter Strauß for the suggestion to do a PhD and the scientific orientation of the Federal Agency for Water Management, which enabled me to write this thesis.*

*Many thanks also go to all my co-authors, my working colleagues at the Federal Agency for Water Management and my fellow students for their direct and indirect contribution to my doctoral thesis.*

*Last but not least, I would like to thank my family for their support, patience and inspiration - just for being there.*



Die approbierte gedruckte Originalversion dieser Dissertation ist an der TU Wien Bibliothek verfügbar.  
The approved original version of this doctoral thesis is available in print at TU Wien Bibliothek.

---

# Content

<b>Abstract .....</b>	<b>3</b>
<b>Zusammenfassung.....</b>	<b>3</b>
<b>Content .....</b>	<b>3</b>
<b>Chapter 1 Introduction .....</b>	<b>7</b>
<b>Chapter 2 Hysteresis effects in sediment transport.....</b>	<b>11</b>
Abstract .....	11
2.1 Introduction .....	12
2.2 Materials and methods .....	13
2.2.1 Catchment description.....	13
2.2.2 Instrumentation .....	14
2.2.3 Event separation .....	14
2.2.4 Suspended sediment concentration (ssc).....	15
2.2.5 Catchment sediment load (CSL) .....	16
2.3 Results and Discussion .....	16
2.3.1 Event Separation.....	16
2.3.2 Suspended sediment concentrations.....	17
2.3.3 Rating curves .....	18
2.3.4 Hysteresis model – ssc.....	20
2.3.5 Catchment sediment load (CSL) .....	25
2.4 Conclusions .....	26
<b>Chapter 3 Resuspension of stream bed sediments.....</b>	<b>29</b>
Abstract .....	29
3.1 Introduction .....	30
3.2 Study site.....	32
3.3 Experimental setup.....	34
3.4 Results .....	35

3.5 Discussion .....	39
3.5.1 Source and magnitude of re-suspended sediments.....	39
3.5.2 Comparison with natural events .....	41
3.6 Conclusions .....	44
<b>Chapter 4 Pathways of dissolved organic carbon .....</b>	<b>45</b>
Abstract .....	45
4.1 Introduction .....	46
4.2 Material and Methods .....	47
4.2.1 Study area .....	47
4.2.2 Sampling, preparation and analyses.....	49
4.2.3 Definition of base flow conditions .....	50
4.2.4 Exfiltration-infiltration model.....	51
4.3 Results .....	52
4.3.1 Spatiotemporal Variations of DOC.....	52
4.3.2 DOC: from the tributaries to the catchment outlet.....	55
4.3.3 Spatiotemporal variations of DOM Quality .....	58
4.3.4 DOM quality: from source to catchment outlet .....	61
4.4 Discussion .....	62
4.4.1 Land use impacts on DOC and DOM quality .....	62
4.4.2 Temporal variations of DOC and DOM quality.....	64
4.4.3 Main drivers of DOC at the catchment outlet .....	65
4.5 Summary and Conclusions.....	66
<b>Chapter 5 Indirect nitrogen losses due to leaching.....</b>	<b>69</b>
Abstract .....	69
5.1 Introduction .....	69
5.2 Methodology .....	71
5.2.1 Site description .....	73
5.3 Results and discussion.....	77
5.3.1 Correction of leaching rates .....	77
5.3.2 Calculation of $Frac_{LEACH}$ (only leaching).....	78
5.3.3 Nitrogen loss.....	80

---

5.3.4 Calculation of $\text{Frac}_{\text{LEACH}}^a$ (leaching and runoff).....	83
5.4 Conclusions .....	84
<b>Chapter 6 Summary of the results and overall conclusions .....</b>	<b>85</b>
<b>Acknowledgements.....</b>	<b>89</b>
<b>Bibliography .....</b>	<b>91</b>



Die approbierte gedruckte Originalversion dieser Dissertation ist an der TU Wien Bibliothek verfügbar.  
The approved original version of this doctoral thesis is available in print at TU Wien Bibliothek.

# Chapter 1

## Introduction

The water quality of streams, lakes and aquifers is controlled by numerous physical, chemical and biological processes along the various pathways of the water from the land surface to the ocean. These processes depend on each other and a large number of environmental factors, making it difficult to understand the temporal dynamics of the transport and transformation of substances. These substances can either be of particular form, such as sediments and attached phosphorus, or dissolved, such as nitrogen and dissolved organic carbon (DOC). The loads transported and the concentrations at a particular location and time determine the usability of water and the ecological state of water bodies. Additionally, these processes are closely linked to the climate, for example through uptake and emission of carbon and nitrogen compounds from the land surface.

While the hydrological response to rainfall is well documented, there is still a lack of knowledge concerning the fate of substances. For instance, the same rainfall can activate different flow paths – including percolation through the soil towards the groundwater and direct surface runoff into the stream - depending on initial catchment soil moisture, vegetation soil treatment and other factors. Depending on which path is triggered, and to what extent, the same rainfall will, therefore, result in different spatial and temporal patterns of the transported substances. While it is difficult to measure transport processes within a catchment in a representative way due to the enormous spatial variability (Walling, 1988; Prosser et al., 2001a), monitoring in streams is a common and efficient way of quantifying the bulk export from the catchment. However, the spatial and temporal resolution of the measurements determines the degree to which individual processes can be unravelled. Ideally, a sufficiently small scale is chosen to estimate all terms of the mass balance accurately, which will help in attributing changes in the transport behaviour in response to changing catchment or rainfall-runoff characteristics.

A major control of water driven transport processes is land use, especially agricultural land use (Kronvang et al., 1997; Graeber et al., 2012; Prasuhn and Moni, 2003). Streams in intensively used agricultural catchments are frequently characterised by increased transport of suspended solids during rainfall events, which may affect stream water quality considerably. Most of the annual sediment transport usually takes place during a few events (Kronvang et al., 1997), and thus the short-term dynamics within storm events are important controls of the overall sediment loads exported from a catchment. Traditionally, these dynamics are reflected by a large scatter in the relationship between suspended sediment concentration (SSC) and discharge including hysteresis effects (Walling and Teed, 1971). However, hysteresis is usually not considered in load estimation techniques. Nevertheless, it has been suggested that the presence of hysteresis, and in particular its shape, may be an important indicator of different processes of runoff, location of sediment sources and sediment transport (Krueger et al., 2009, Seeger et al., 2004, Terajima et al., 1997, Williams, 1989). Often, there is a temporal shift between discharge and sediment peak, resulting in either clockwise or counter-clockwise hysteresis when plotting flow against sediment concentrations, and multiple peaking

sedigraphs are often associated with single peaking hydrographs (Kronvang et al., 1997; Brasington and Richards, 2000; Peticrew et al. 2007; Yeshaneh et al. 2013). Many authors relate these observations to the activation of different sediment sources such as the resuspension from streambed sediments (Williams, 1989; Kronvang et al., 1997; Lenzi and Marchi, 2000; Regües et al., 2000; Eder et al., 2010).

Besides sediments, agricultural activities deliver significant amounts of dissolved organic matter (DOM) to stream ecosystems, changing basic metabolic processes in the water and affecting the ecological state and the health of aquatic systems (Fasching and Battin, 2012; Findlay et al., 2001, 2003; Piscart et al., 2009; Rouhani et al., 2021). The amount of DOC and composition of terrestrial DOM influence benthic microbial growth and respiration as well as CO<sub>2</sub> outgassing from streams (Findlay et al., 2003; Piscart et al., 2009; Williams et al., 2010).

The flow paths of dissolved organic matter are more diverse than those of sediments, as they tend to include subsurface flow (both in the unsaturated zone and in groundwater), while the transport of sediments is mainly limited to surface runoff, sometimes with some contribution from fast subsurface stormflow through drainage pipes (Kronvang et al., 1997).

DOM is a mixture of various compounds with molecular weights ranging from simple carbohydrates to complex molecules of different aromaticity (Bolan et al., 2011), which can be determined by distinct spectrophotometric properties in terms of both absorption and fluorescence (Baker et al., 2003; Chen et al., 2003; Hudson et al., 2007). Recent advances in fluorescent spectrophotometry have provided a new tool for rapidly identifying DOM fluorophores via excitation–emission matrices (Chen et al., 2003; Fellman et al., 2010) for distinguishing bioavailable from refractory DOM components (Bolan et al., 2004; Findlay et al., 2001; Marschner and Kalbitz, 2003).

In natural streams, refractory DOM originating from terrestrial sources usually dominates over autochthonous, labile DOM from algal primary production (Osburn et al., 2017). Agricultural activities may significantly alter this DOM composition (Graeber et al., 2012). Both enhanced benthic primary production, resulting from increased nutrient supply and light penetration, and increased manure inputs with high amino acids contents may shift the composition towards the dominance of labile components (Fellman et al., 2009).

Comparative studies of soil and stream DOM often show contradictory results (Graeber et al., 2012) since the processes that drive the modifications are not very well understood. The inconsistency of these findings may be related to differences in land use practices (e.g. fertilization, tillage) and environmental conditions (e.g. climate, vegetation), the significance of the different flow paths (surface runoff, soil pore water, tile drainage water) and different investigation methods. In order to understand the impacts of agriculture on DOM concentrations, composition and processing in streams, an approach is needed that combines measurements of soil DOM, the corresponding DOM in tributaries and changes in the instream DOM along stream reaches.

Another very relevant substance in agricultural systems subject to water driven transport through the soil is nitrogen. Applied to enhance plant growth, some of the nitrogen is leached as nitrate, nitrite or ammonia, depending on the environmental conditions. These nitrogen losses can be represented as a fraction relative to all nitrogen added to or mineralized in soils, a parameter that is termed  $Frac_{LEACH}$  (IPCC 2006). A part of the lost nitrogen is transformed to

laughing gas ( $N_2O$ ), which is a listed greenhouse gas with global warming potential 296 times higher than carbon dioxide ( $CO_2$ ) over a 100 year time scale. Therefore, these nitrogen losses (indirect soil emissions) are part of the annual national inventory reports (NIP), which Austria has to compile and submit to the United Nations Framework Convention on Climate Change (UNFCCC). The Intergovernmental Panel on Climate Change (IPCC) has established guidelines with internationally agreed methodologies intended to be used by the countries for estimating greenhouse gas inventories in their reports to the UNFCCC (IPCC 2006). Mosier et al. (1998) suggested a value of 0.3 for  $Frac_{LEACH}$ , which is the value recommended in the IPCC Guidelines (IPCC 2000, 2006) as a default value. Lower values than 0.3 for  $Frac_{LEACH}$  can be used if more specific data are available (IPCC 2006). Many countries have indeed established country-specific values since research studies usually suggest lower values of  $Frac_{LEACH}$  (Environment Protection Agency Ireland 2011; Del Prado et al. 2006; Ryan et al. 2006; Neill 1989; Thomas et al., 2005). In Austria, the default value of 0.3 has been used in the past as no accurate estimates had been available. However, in the light of the studies in other countries there is reason to believe that this value overestimates the actual fraction of indirect soil emissions.

Given the research gaps in agricultural systems discussed above, the aim of this thesis is to better understand the water driven transport processes of sediments, dissolved organic carbon and nitrogen in terms of their flow paths from the field to the stream, and the associated concentrations and loads. In particular, the thesis addresses the following research questions in Chapters 2 to 5:

How does hysteresis of the concentration-discharge relationship affect the estimation of suspended sediment concentrations and sediment loads, and can the direction and shape of hysteresis be related to event characteristics? (Chapter 2)

What is the magnitude of re-suspension of fine sediments from the stream bed of a small stream during rain events, what is their source and is the early peak in the sedigraphs of natural events due to the re-suspension of sediments from the stream bed? (Chapter 3)

How do DOC concentrations and DOM composition change from the soil to the tributaries and along the stream to the catchment outlet and which factors control the spatial patterns and seasonal dynamics of DOC and DOM composition of these ecosystem components? (Chapter 4)

Is it feasible to use plot-scale lysimeters for estimating nitrogen losses and  $Frac_{LEACH}$  for different land uses, and is the Austrian overall  $Frac_{LEACH}$  smaller than the IPCC proposed of 0.3? (Chapter 5)

Finally, Chapter 6 provides an overview of the results and an overall conclusion.



Die approbierte gedruckte Originalversion dieser Dissertation ist an der TU Wien Bibliothek verfügbar.  
The approved original version of this doctoral thesis is available in print at TU Wien Bibliothek.

## Chapter 2

# Hysteresis effects in sediment transport

The present chapter corresponds to the following scientific publication in its original form:

*Eder A., P. Strauss, T. Krueger and J.N. Quinton, 2010. "Comparative calculation of suspended sediment loads with respect to hysteresis effects (in the Petzenkirchen catchment, Austria)". Journal of Hydrology, 389 (1-2), pp. 168-176. <https://doi.org/10.1016/j.jhydrol.2010.05.043>.*

### Abstract

Streams in intensively used agricultural catchments are frequently characterised by high transport of suspended solids during rainfall events. Due to a high variability in runoff, the sediment concentration relationship during and between different events and various hysteresis effects, instantaneous sediment concentrations and event loads are difficult to calculate. We tested the applicability of turbidity measurements for calculating instantaneous sediment concentrations and loads in a small agricultural catchment in Austria. We calibrated quasi-continuous turbidity measurements using additional water sampling and employed these calibrated sediment concentrations as benchmark sediment concentrations. Four different methods to calculate instantaneous sediment concentrations were tested on 19 events. A generalized rating curve approach resulted in a considerable bias for both event specific sediment concentrations and total sediments loads. Fitting of event-specific rating curves still misrepresented instantaneous sediment concentrations for the different events, but gave load estimations that were in a range of 5% of the benchmark values. Two approaches accounting explicitly for hysteresis exhibited the best fit and provided load estimations that were in a range of 0–1% deviation to the benchmark sediment concentrations. Nevertheless, several limitations to the hysteresis model approach were identified. Testing the various hysteresis effects against other event parameters such as total rainfall amount, maximum rainfall intensity and initial soil water content revealed interactions to these parameters that could predefine parameter values of the hysteresis model approach.

## 2.1 Introduction

Streams in intensively used agricultural catchments are frequently characterised by increased transport of suspended solids during rainfall events, which may affect stream water quality considerably. Most of the annual sediment transport usually takes place during a few events (Kronvang et al., 1997), and thus the short-term dynamics of storm events are important in sediment loading.

Traditionally, these dynamics are characterised by empirical relationships between suspended sediment concentration (ssc) and discharge. These relationships are normally not homogenous in time, neither within nor between events. This causes a large scatter of ssc–discharge data pairs, which can often be explained by short- (within events) and long-term (between events) hysteresis effects (Walling and Teed, 1971). However, hysteresis is usually not taken into account in load estimation techniques. Nevertheless, it has been suggested that the hysteresis effect, and in particular its shape, may be an important indicator of different processes of runoff, location of sediment sources and sediment transport (Krueger et al., 2009, Seeger et al., 2004, Terajima et al., 1997, Williams, 1989). To account for the hysteresis effect of sediment concentration within single events, Krueger et al. (2009) introduced an empirical hysteresis model based on a concept used by House and Warwick (1998) to describe solute dynamics in rivers.

To identify within-event sediment behaviour, discontinuous water sampling or, more common in recent years, continuously measuring turbidity devices are employed (Lewis, 1996, Brasington and Richards, 2000, Stubblefield et al., 2007, Wass and Leeks, 1999). It has been shown that quasi-continuous turbidity recording may avoid significant uncertainty due to interpolation and extrapolation of low-frequency measurements (Grayson et al., 1996, Lewis, 1996) and to allow the investigation of the short-term dynamics of sediment transport (Kronvang et al., 1997, Stubblefield et al., 2007, Brasington and Richards, 2000, Nistor and Church, 2005, Chikita et al., 2002). However, problems in deriving a relationship between turbidity and ssc exist. Particularly, variations in the response of turbidity probes due to differences in particle size, sediment mineralogy and the colour of dissolved organic material (Gippel, 1995) as well as their sensitivity to clogging of the measurement window have been reported (Gurnell, 1987).

The aim of this paper is threefold: (1) we test the applicability of turbidity measurements for calculating continuous sediment concentrations in a stream draining a small agricultural catchment in Austria; (2) we compare five methods of estimating sediment concentrations to highlight hysteresis effects and their importance for identifying runoff generation processes; and (3) we assess the significance of hysteresis for estimating catchment sediment loads.

## 2.2 Materials and methods

### 2.2.1 Catchment description

The Petzenkirchen catchment (Fig. 2.1) is situated in the western part of Lower Austria and it has a size of 64 ha. The climate can be characterised as humid with a mean annual temperature of 9.3 °C and a mean annual rainfall of 716 mm. Temperature, rainfall and rainfall intensity have their peak during summertime. The elevation of the catchment ranges from 268 to 323 m above sea level (a.s.l.) with a mean slope of 8%. The form factor of the catchment (width/length) is 0.3, while the river density (length of river in km/area of catchment in km<sup>2</sup>) is 0.8. The dominant soil types are Cambisols and Planosols (FAO, 1998) with medium to poor infiltration capacities. Due to shallow low permeability soil and the use of the catchment area as agricultural land, sub-surface drainage systems were installed in the 1950s. The drainage systems influence both discharge and sediment concentration behaviour in the stream. The estimated drainage area from the drainage system is about 15% of the total catchment and can be divided into two bigger drainage systems in the southwestern part of the creek and four smaller drainage systems on the northeastern part (Fig. 2.1). Additionally, the upper most 25% of the stream length were piped in the 1950s to enlarge the agricultural production area. At present, 87% of the catchment area is arable land, 5% is used as pasture, 6% is forested and 2% is paved.

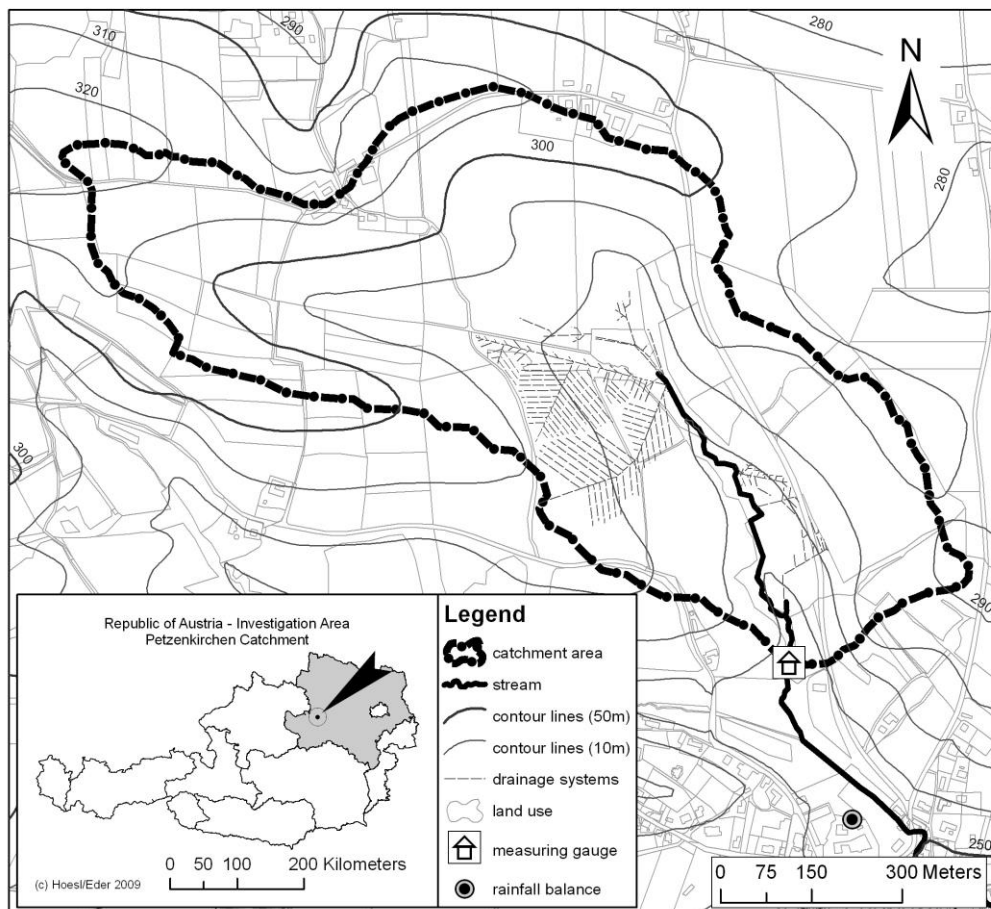


Fig. 2.1: Petzenkirchen Catchment

### 2.2.2 Instrumentation

Discharge, suspended sediment concentration and turbidity were monitored at the outlet of the Petzenkirchen catchment (Fig. 2.1). Discharge was measured every minute, indirectly with a calibrated H-flume in combination with a pressure transducer (OTT PS 1). The H-flume was self-made after instructions in BOS (1974) and had a maximum flow capacity of 400 l s<sup>-1</sup>. The flow calming section upstream of the measuring point had a length of 3 m. Water samples (ws) were taken with an automatic suction sampler (Manning S 4040) at set intervals (see below) triggered by increasing flow rates (starting from 9.1 l s<sup>-1</sup>). The inlet of the suction tube was placed into the small swirl zone directly after the flume to ensure good mixing of the sampled volume. The volume of the swirl zone is approximately 500 l, which means a mean residence time of 250 s at low flow conditions. The sampler minimises mixing of samples by a 17 s of purge cycle before and after the filling of the samples. Within an event, samples were taken at constant time intervals ranging from 3.75 min to 24 h. The intervals were chosen in advance of an event according to the weather forecast to ensure an optimal sampling distribution. In addition, manual sampling took place once per week. All water samples were filtered through 0.45 µm membrane filters and oven-dried to obtain sediment concentrations (ssc<sub>ws</sub>) gravimetrically. An in-stream turbidity device (WTW: ViSolid 700 IQ) was used to collect quasi-continuous turbidity data at 3 min intervals. The measurement range for this device was from 0 to 25 g l<sup>-1</sup> with a resolution of 0.01 g l<sup>-1</sup>. The device uses a scattered light measurement, which records the reflectance of total suspended solids. The reflectance was transformed into suspended sediment concentration (turb) using the default calibration equation, supplied by the manufacturer. The turbidity probe was installed into the swirl zone next to the suction tube of the automatic sampler to guarantee both similar measuring conditions and required distance of the optical sensor to fixed surrounding structures.

Rainfall was recorded with a rainfall balance (OTT Pluvio) situated about 200 m away from the catchment outlet. Readings were taken every 0.1 mm of rainfall.

Surrogate measurements of catchment soil water content were obtained from TDR-probes located in a lysimeter station close to the catchment at the beginning of events.

### 2.2.3 Event separation

An automated recursive digital filter (Nathan and McMahon, 1990, Arnold et al., 1995) was applied to the whole time series to identify periods of direct flow. Due to noisy discharge data, a moving average filter with a window size of 5 min was first used to smooth the data. The equation of the recursive digital filter is given by

$$q_t = \beta \cdot q_{t-1} + (1 + \beta)/2 \cdot (Q_t - Q_{t-1}) \quad (2.1)$$

where  $q_t$  is the filtered quick response (event water) at time step  $t$  and  $Q_t$  is the original stream flow. The value of the filter parameter  $\beta$  was manually set to 0.95 after visual data inspection. For our study, we defined an 'event' as beginning when stream discharge increased above base flow, to the time when only base flow contributed to discharge, although there may still have been increased base flow sediment concentrations. Subsequently, the maximum discharge of

an event had to be at least  $5 \text{ l s}^{-1}$ . The difference between the maximum discharge and the antecedent discharge had to be greater than  $2 \text{ l s}^{-1}$  and the maximum turbidity had to reach values above  $100 \text{ mg l}^{-1}$  to define an event. These constraints were necessary to avoid a large number of low-flow events with low suspended sediment concentrations in the stream water.

#### 2.2.4 Suspended sediment concentration (ssc)

Quasi-continuous suspended sediment concentrations were calculated comparing five different methods:

- a) Calibration of turbidity data against suspended sediment concentration of water samples ( $\text{ssc}_{\text{ws}}$ ):  $\rightarrow \text{ssc}_{\text{tu}}$

Gippel (1995) states that, in general, the best correlations were obtained in areas where sediment properties were likely to be relatively constant (oceanic environments and small catchments), where field instruments were used, and where the concentration of suspended sediments covered a wide range. The Petzenkirchen catchment fulfils all of the requirements. Both linear and exponential relations between water samples and turbidity were tested via statistical regression analysis.

Results of this method were used as benchmark, when the different methods were compared.

- b) Rating curve generated from all  $\text{ssc}_{\text{ws}}$ -discharge data pairs:  $\rightarrow \text{ssc}_{\text{R}}$

A power-law rating curve is usually employed to describe this kind of relationship (e.g. in Campbell and Bauder, 1940) for annual catchment sediment load estimation. Following Asselman (2000), we did not transform the power-law logarithmically to avoid transformation bias. Instead, the power-law function was fitted to all  $\text{ssc}_{\text{ws}}$ -discharge data pairs using non-linear least-square regression. The rating curve has the form

$$\text{ssc}_{\text{R}} = a \cdot q^b \quad (2.2)$$

where **a** and **b** are the fitting parameters,  $\text{ssc}_{\text{R}}$  is the suspended sediment concentration and **q** represents the discharge.

- c) Rating curve generated from  $\text{ssc}_{\text{ws}}$ -discharge data pairs for single individual events:  $\rightarrow \text{ssc}_{\text{RE}}$

The power-law function was fitted to individual events in the same way as in (b) to account for the potential of rating curve heterogeneity between events.

- d) Hysteresis model after Krueger et al. (2009) with discharge records and  $\text{ssc}_{\text{ws}}$  as input for individual events:  $\rightarrow \text{ssc}_{\text{Hws}}$

Krueger et al.'s model was tested to include the hysteresis behaviour of discharge-ssc relationships during single events. Krueger et al. introduced a term incorporating the steepness of the rising and falling limbs of the hydrograph during single events to characterise the hysteresis effect of sediment dynamics. They modified Eq. 2.1 to

$$ssc_H = a \cdot q^b + c \cdot dq/dt \quad (2.3)$$

where  $c$  is an additional fitting parameter and  $dq/dt$  is the steepness of the hydrograph (for similar use of  $dq/dt$  see Paustian and Beschta, 1979, Terajima et al., 1997, House and Warwick, 1998 and Ide et al. (2008)). This allows to account for sediment peaks that arrive at the catchment outlet in advance (clockwise) or after (counter-clockwise) the hydrograph peak. Eq. 2.3 was fitted to discharge–ws data by non-linear least-square regression for individual events.

- e) Hysteresis model after Krueger et al. (2009) with discharge records and calibrated turbidity records ( $ssc_{tu}$ ) as input for individual events:  $\rightarrow ssc_{Htu}$

The hysteresis model (Eq. 2.3) was fitted to the calibrated turbidity–discharge data pairs for single events in the same way as in (d) to display possible differences induced by the availability of data pairs (low-resolution  $ssc_{ws}$  versus high-resolution  $ssc_{tu}$ ).

The validity of all model fits was quantified by the Nash–Sutcliffe efficiency (Nash and Sutcliffe, 1970) with respect to the calibrated turbidity record ( $ssc_{tu}$ ) as a benchmark. Please note that for this study no explicit consideration of possible data uncertainties in a model rejectionist framework (such as in Krueger et al. (2009)) was attempted. Instead, the five different methods of calculating  $ssc$  were compared in a classic non-linear optimisation setting, which allows gauging their relative merits. However, a future study to fully assess the uncertainties in these methods is envisaged.

### 2.2.5 Catchment sediment load (CSL)

Measured and calculated suspended sediment concentrations were used to estimate catchment sediment load for the observed events and to compare the different methods of generating continuous suspended sediment concentrations.

## 2.3 Results and Discussion

### 2.3.1 Event Separation

The mean flow during the study period (2005 - 2008) was  $3.9 \text{ l s}^{-1}$ , while the minimum discharge was  $0.2 \text{ l s}^{-1}$  and the maximum flow was  $293 \text{ l s}^{-1}$ . The highest discharge ever observed was around  $2000 \text{ l s}^{-1}$  (estimate from waterline on the embankment) in 2002. In total, event separation led to 82 runoff events with rainfall, discharge and turbidity data available. In 19 of the 82 events, suspended sediment data were available as well. These 19 events formed the database for subsequent analyses. Tab. 2.1 gives an overview of the characteristics of these events.

The method used for event separation was determined as appropriate, because temporal extension of the events showed only minor effect on sediment load calculations due to very low sediment concentrations before and after the defined events. However, the definition of the

beginning and ending of an event is important, especially for sediment load calculations on event basis.

Tab. 2.1: Event number (No.), date of event, event duration (dur in h), event maximum discharge ( $q_{\max}$  in  $\text{l s}^{-1}$ ), rainfall amount (I in mm), maximum rainfall intensity within 10 minutes ( $I_{10}$  in  $\text{mm h}^{-1}$ ), initial soil water content at 10 cm depth ( $\theta_{10}$  in %) and estimated catchment sediment load ( $\text{CSL}_{\text{tu}}$  in kg)

No.	Date	Duration (h)	$q_{\max}$ ( $\text{l s}^{-1}$ )	I (mm)	$I_{10}$ ( $\text{mm h}^{-1}$ )	$\theta_{10}$ (%)	$\text{CSL}_{\text{tu}}$ (kg)
E 1	09.03.2006	37.3	16.2	5.6	2.4	35.5	148
E 2	28.03.2006	19.2	37.3	17.3	4.8	35.3	724
E 3	17.05.2006	2.8	8.4	4.2	8.4	26.4	4
E 4	02.06.2006	23.8	21.9	26.9	6.6	35.6	126
E 5	18.09.2006	3.1	18.4	23.7	76.2	22.5	231
E 6	01.01.2007	16.7	11.3	13.0	7.2	35.4	83
E 7	18.01.2007	20.3	38.8	26.1	10.2	35.0	1006
E 8	27.02.2007	17.8	14.3	12.9	3.0	35.8	177
E 9	23.03.2007	21.7	24.0	16.4	9.6	35.4	213
E 10	05.09.2007	25.9	60.6	66.2	6.6	28.4	1369
E 11	07.11.2007	24.8	36.2	19.3	9.0	34.1	377
E 12	21.04.2008	5.1	19.7	19.4	21.6	29.1	69
E 13	03.06.2008	15.6	17.7	27.2	22.8	25.6	90
E 14	25.06.2008	3.6	8.4	10.9	24.6	24.8	24
E 15	26.06.2008	3.4	10.4	12.3	31.8	24.5	26
E 16	12.07.2008	1.8	50.1	13.8	48.0	24.0	1609
E 17	20.07.2008	7.2	7.3	14.5	11.4	26.3	73
E 18	23.07.2008	18.0	10.8	25.7	7.8	28.4	146
E 19	24.07.2008	7.8	59.2	12.8	9.0	34.0	706

### 2.3.2 Suspended sediment concentrations

Turbidity records, transformed with the default calibration equation to suspended sediment concentrations (turb) as described above, ranged from zero to  $25 \text{ g l}^{-1}$ , the upper detecting limit of the turbidity probe. Maximum suspended sediment concentration of the automatic water sampler ( $\text{ssc}_{\text{ws}}$ ) was  $27.3 \text{ g l}^{-1}$ , but this was a unique value. For the linear fit correlation (Pearson) between  $\text{ssc}_{\text{ws}}$  and turb was 0.91 (Fig. 2.2).

The slope of  $0.631 \pm 0.024$  (95% confidence intervals) of the linear regression in Fig. 2.2 indicates that the internal default calibration equation of the turbidity probe was not sufficient to deliver absolute suspended sediment concentrations. A meaningful use of turbidity devices was bound to some limitations, i.e. simultaneous water sampling for calibration (Lewis, 1996, Brasington and Richards, 2000) and regular cleaning of the optical window Gurnell (1987). Furthermore, the turbidity records required a plausibility check, manual data correction and calibration before they could be considered a valuable advance in sediment observation. On the other hand using turbidity devices, we could avoid the typical representational problems of automated water sampling (Fig. 2.3), i.e. sampling intervals that are either too large to resolve sediment peaks or too short leading to an exhaustion of sampling bottles in advance of the peak. Obviously, the total suspended sediment concentration consists of either material, which has been eroded from somewhere in the catchment including the stream bank or material, which

has been re-suspended during increase of flow. Unfortunately, we are not able to distinguish these sources at present.

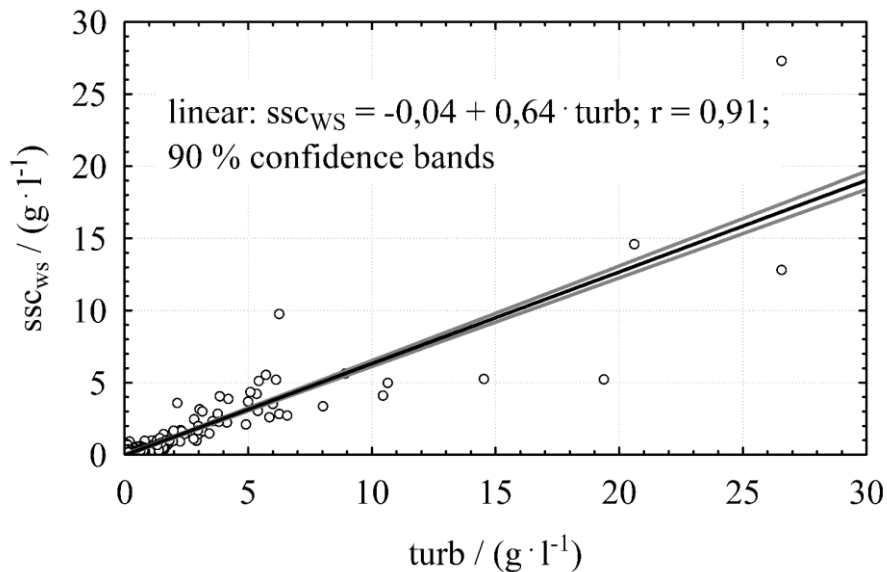


Fig. 2.2: Relationship between suspended sediment concentration of the water sampler ( $ssc_{ws}$ ) and default turbidity values ( $turb$ ).

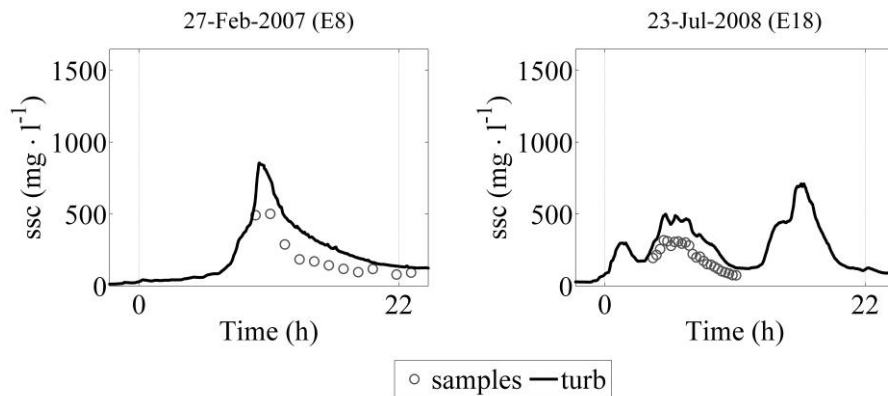


Fig. 2.3: Missing sediment peak due to large sampling intervals on the left and use of all sampling bottles before the end of a long lasting event (right).

### 2.3.3 Rating curves

In general, the relationship between discharge and sediment concentration data showed a large scatter (Fig. 2.4). A number of variables may influence the variation of this relationship: (i) rainfall characteristics like duration, intensity, time to peak and spatial distribution; (ii) initial catchment conditions like soil water content and its spatial distribution, land use, management practises and stadium of plant development; (iii) flow characteristics at the beginning of an event like discharge and sediment concentration. The fit to the scattered data was consequently characterised by a low correlation coefficient of 0.32 (Fig. 2.4) and led to overestimated suspended sediment concentrations for most of the events (Fig. 2.5 - left) and an underestimation of suspended sediment concentration for a few heavy storm events (Fig. 2.5-right). However, these events tend to contribute most to annual sediment loads and therefore

annual loads are often underestimated using these forms of average rating curves (Kronvang, 1997).

Fitting event-specific rating curves (Fig. 2.4), demonstrates the enormous variability of sediment – discharge relationships within the same catchment. Tab. 2.2 provides information on model parameters, correlation coefficients of the model fits (with respect to  $ssc_{ws}$ ) and model efficiencies (with respect to the  $ssc_{tu}$ ) for each event. The correlation coefficients of the event-specific rating curves ranged from 0.04 to 0.99. It should be noted that some of these fits were extremely poor, whereas the validity of other fits might have been positively biased by the low number of water samples and the timing of sampling during an event.

Nevertheless, applying event-specific rating curves resulted in higher correlation coefficients overall compared to the general rating curve.

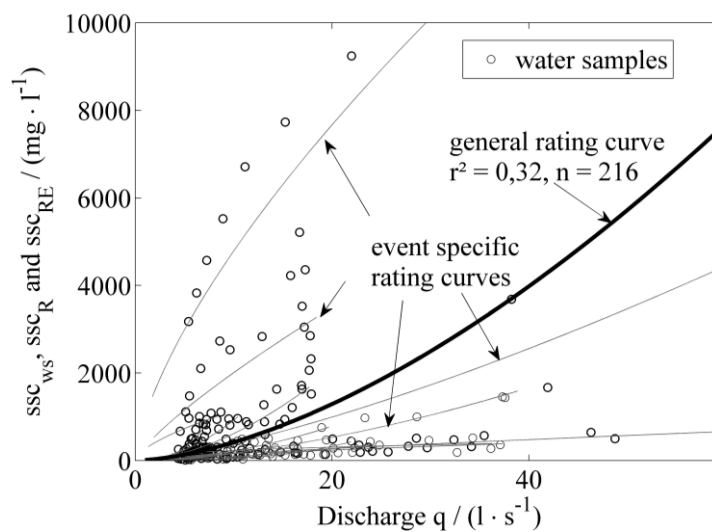


Fig. 2.4: Suspended sediment concentration of the water samples ( $ssc_{ws}$ ) against discharge, general rating curve generated from all water samples – discharge data pairs ( $ssc_R$ ) and event specific rating curves ( $ssc_{RE}$ ).

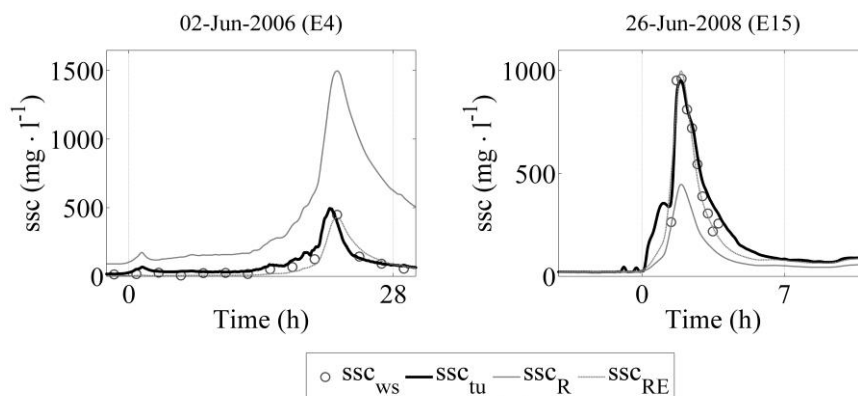


Fig. 2.5: Calculated suspended sediment concentrations ( $ssc_R$  – general rating curve,  $ssc_{RE}$  – event specific rating curve) compared to suspended sediment concentration of the water samples ( $ssc_{ws}$ ) and calibrated turbidity records ( $ssc_{tu}$ ).

Tab. 2.2: Model parameters of equation 2 (a and b), number of data points (n), correlation coefficients of the model fits to the water samples ( $r_R$  and  $r_{RE}$ ) and Nash-Sutcliffe efficiencies with respect to the turbidity record for both general ( $E_R$ ) and event specific ( $E_{RE}$ ) rating curves.

	General rating curve					Event specific rating curves				
	$a_R$	$b_R$	$n_R$	$r_R$	$E_R$	$a_{RE}$	$b_{RE}$	$n_{RE}$	$r_{RE}$	$E_{RE}$
E 1	9.90	1.63	216	0.57	-32.75	0.01	3.72	3	1.00	-0.14
E 2	9.90	1.63	216	0.57	-271.56	23.49	0.77	9	0.54	-0.30
E 3	9.90	1.63	216	0.57	-12.46	3.09	1.67	6	0.63	0.36
E 4	9.90	1.63	216	0.57	-18.24	0.05	2.96	12	0.97	0.62
E 5	9.90	1.63	216	0.57	-1.39	317.67	0.80	17	0.55	0.10
E 6	9.90	1.63	216	0.57	0.41	11.77	1.25	6	0.21	0.76
E 7	9.90	1.63	216	0.57	-4.66	3.86	1.64	11	0.97	0.70
E 8	9.90	1.63	216	0.57	0.26	1.22	2.11	10	0.47	0.29
E 9	9.90	1.63	216	0.57	-37.83	2.00	1.64	14	0.75	0.69
E 10	9.90	1.63	216	0.57	-193.53	23.69	0.81	16	0.80	0.52
E 11	9.90	1.63	216	0.57	-20.56	89.07	0.41	5	0.27	0.45
E 12	9.90	1.63	216	0.57	-0.43	3.14	1.84	10	0.96	0.88
E 13	9.90	1.63	216	0.57	0.90	10.60	1.76	24	0.76	0.92
E 14	9.90	1.63	216	0.57	-0.54	262.50	0.64	6	0.50	0.40
E 15	9.90	1.63	216	0.57	0.17	11.11	1.92	10	0.95	0.88
E 16	9.90	1.63	216	0.57	-1.37	999.24	0.68	12	0.85	0.21
E 17	9.90	1.63	216	0.57	-0.43	3.45	2.77	13	0.81	0.70
E 18	9.90	1.63	216	0.57	0.17	12.64	1.45	24	0.39	0.02
E 19	9.90	1.63	216	0.57	-1.77	16.71	1.36	5	0.84	0.37

The model efficiencies ( $E_R$  and  $E_{RE}$ ) of the simulated suspended sediment concentrations ( $ss_{CR}$  and  $ss_{CRE}$ ) with respect to the calibrated turbidity record ( $ss_{tu}$ ) depended on the correlation coefficients of the model fit to the water samples and the magnitudes of hysteresis. The mostly negative values of the Nash-Sutcliffe coefficient for the general rating curve ( $E_R$ ) confirm that it cannot be used to calculate suspended sediment concentrations for single events. Better results were obtained with event-specific rating curves, illustrated by raised efficiencies ( $E_{RE}$ ), although half of the events yielded  $E_{RE}$  values below 0.5. There is, therefore, scope for model improvement.

### 2.3.4 Hysteresis model – ssc

The hysteresis model was applied to both water samples ( $ss_{ws}$ ) and calibrated turbidity data ( $ss_{tu}$ ) sets. Tab. 2.3 gives the model parameters, the model efficiencies and the actual direction of hysteresis.

Taking in account the hysteresis effect in suspended sediment calculations led to increasing efficiencies ( $E_{H,ws}$ ) in nine of nineteen events compared to the event specific rating curves. In six cases, efficiency did not change and in 4 events efficiency declined, which indicates some limitations of the hysteresis model's approach. No improvement could be obtained for events with a low number of data points, which do not represent the full dimension of the hysteresis (E1), multi-peak events with different numbers of sediment and discharge peaks (E6, E11, E19), and noisy events without smoothing the data (see Fig. 2.6).

Tab. 2.3: Model parameters of equation 3 (a, b and c), number of data points (n), correlation coefficients of the hysteresis model fits to  $ssc_{ws}$  ( $r_{Hws}$ ) and  $ssc_{tu}$  ( $r_{Htu}$ ), Nash-Sutcliffe efficiencies with respect to the turbidity record for both hysteresis model applications ( $E_{Hws}$  and  $E_{Htu}$ ), and direction of the hysteresis loop (cl – clockwise, ac – counter clockwise, 8 – eight-shaped and – no hysteresis).

	Hysteresis model water samples ( $ssc_{ws}$ )						Hysteresis model turbidity data ( $ssc_{tu}$ )					Direction of hysteresis
	$a_{Hws}$	$b_{Hws}$	$c_{Hws}$	$n_{Hws}$	$r_{Hws}$	$E_{Hws}$	$a_{Htu}$	$b_{Htu}$	$c_{Htu}$	$n_{Htu}$	$E_{Htu}$	
E 1	0.01	3.84	-989	3	1.00	-1.21	1.35	1.80	2435	2236	0.91	cl
E 2	1.46	1.56	3187	9	0.92	0.19	37.67	0.66	2885	1151	0.51	cl
E 3	5.17	1.39	-168	6	0.83	0.57	4.29	1.49	-222	166	0.59	8
E 4	0.04	3.04	1390	12	0.99	0.89	0.59	2.08	1678	1426	0.95	cl
E 5	342.89	0.79	-1268	17	0.59	0.26	809.65	0.41	-2720	186	0.46	ac
E 6	290.63	-0.18	2049	6	0.97	-1.03	1.60	2.26	62	1001	0.96	-
E 7	4.31	1.61	-286	11	0.98	0.68	2.83	1.68	1770	1216	0.85	cl
E 8	0.16	2.89	1925	10	0.67	0.39	1.28	2.29	3288	1066	0.80	cl
E 9	0.53	2.08	1412	14	0.86	0.81	2.44	1.58	1226	1301	0.85	cl
E 10	23.41	0.82	-75	16	0.80	0.51	65.94	0.58	451	1556	0.75	cl
E 11	0.21	2.28	2273	5	0.70	0.17	1.73	1.68	-80	1486	0.99	-
E 12	2.93	1.87	70	10	0.96	0.87	5.00	1.68	-134	306	0.89	8
E 13	10.39	1.77	-192	24	0.76	0.91	8.21	1.79	268	936	0.97	8
E 14	153.00	0.92	-1021	6	0.97	0.71	66.03	1.40	-568	216	0.85	8
E 15	9.59	1.98	-244	10	0.96	0.86	33.06	1.43	-123	206	0.95	8
E 16	941.64	0.70	-756	12	0.87	0.32	2946.66	0.44	-3013	111	0.72	ac
E 17	1.64	3.15	-4240	13	0.91	0.68	1.90	3.26	-2778	431	0.88	ac
E 18	11.58	1.48	4975	24	0.93	0.24	16.73	1.45	3677	1081	0.50	cl
E 19	4.99	1.71	1561	5	1.00	0.27	13.42	1.32	1237	466	0.89	cl

Examples for valid and failed fits of the hysteresis model are displayed in Fig. 2.6. The diagrams on the left side show discharge, calibrated turbidity records ( $ssc_{tu}$ ), the suspended sediment concentrations of the water samples ( $ssc_{ws}$ ) and the calculated suspended sediment concentrations of the hysteresis model ( $ssc_{Hws}$ ). On the right diagram, the corresponding hysteresis loops can be seen. Limitations of the modelling approach can be classified into not enough data (Fig. 2.6- middle panel), different number of discharge and sediment peaks (Fig. 2.6- lower panel), noisy data and a conspicuous sagging of subsequent sediment peaks compared to discharge peaks in multi-peak events.

The highest Nash-Sutcliffe efficiencies were obtained when the hysteresis model was fitted to calibrated turbidity data. The higher number of data pairs, which resolved the shape of hysteresis better, led to efficiencies ( $E_{Htu}$ ) ranging from 0.50 to 0.99. Even multi-peak events with small loops inside another hysteresis loop were predicted well, although the validity of fit decreased slightly due to smaller subsequent sediment peaks compared to the discharge peaks. This underlines the importance of a sufficient quantitative data set and continuous monitoring when dynamic behaviour of sediment transport is the point of interest.

In case the hysteresis model fitted the data reasonably well, parameter  $c$  of equation 2.3 directly reflected the behaviour of sediment concentration during an event, i.e. the direction and extent of the hysteresis loop (Tab. 2.3). Positive values of  $c$  correspond to clockwise hysteresis (cl), while high negative  $c$  values are an indication for counter clockwise loops (ac), and  $c$  values around zero correspond to an eight-shaped form (8) or nearly no hysteresis (-). Nine events showed a clockwise hysteresis (E1, E2, E4, E7, E8, E9, E10; E18, E19) and five events showed an eight-shaped hysteresis (E3, E12, E13, E14, E15). Only in three cases (E5, E16, E17), a counter clockwise loop was observed. Two events showed nearly no hysteresis (E6, E11).

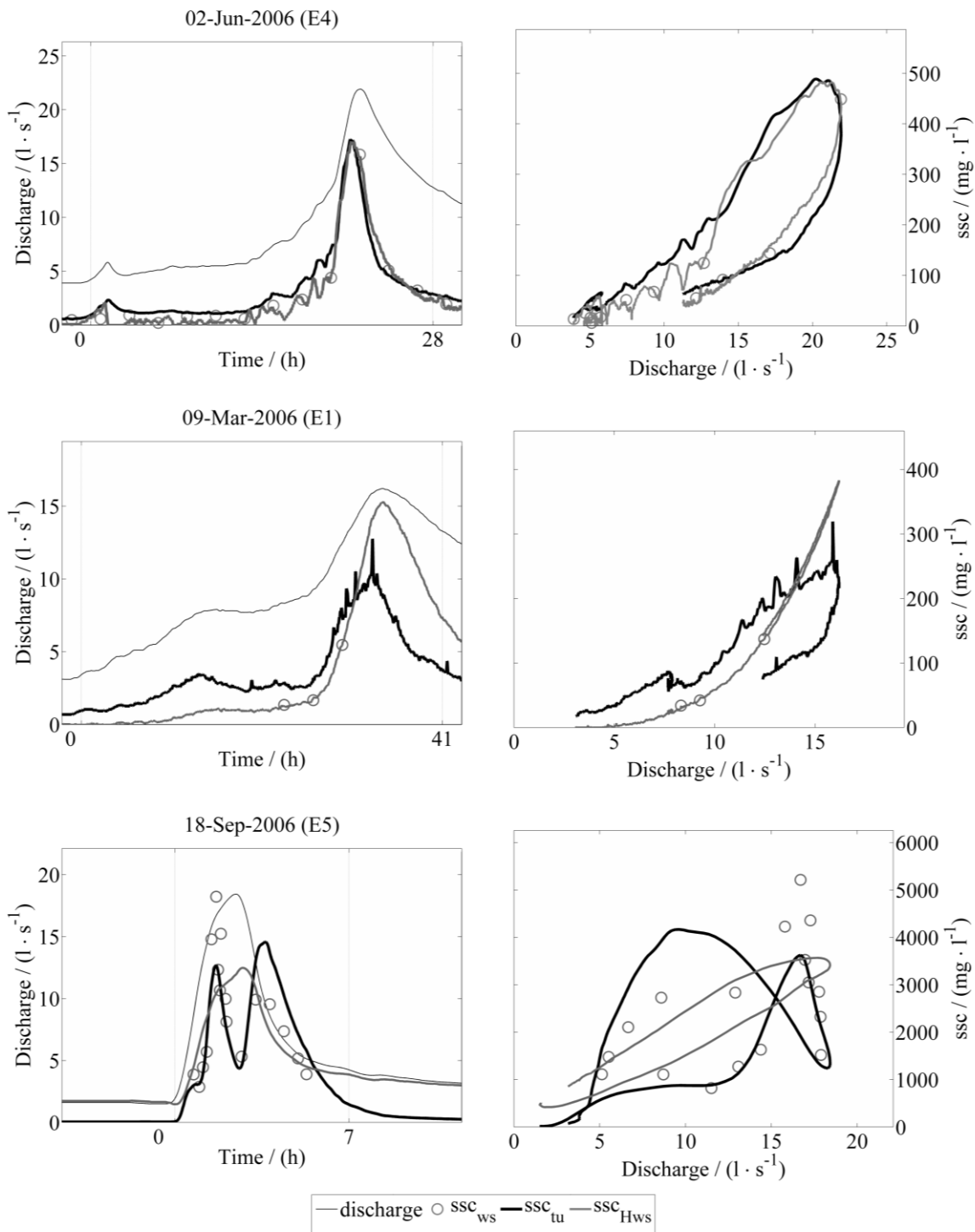


Fig. 2.6: Discharge, suspended sediment concentration of the water samples ( $SSC_{ws}$ ), calibrated turbidity data ( $SSC_{tu}$ ) and calculated suspended sediment concentrations of the hysteresis model ( $SSC_{Hws}$ ) on the left and the corresponding hysteresis loops on the right. a) good simulation, b) not enough data, c) different number of discharge and sediment peaks.

In a next step, we evaluated values for  $c$  against various event characteristics. Fig. 2.7 shows correlations between  $c$  and different event characteristics and its corresponding hysteresis direction.

Clockwise hysteresis required rainfalls with long duration (Brasington and Richards, 2000) and low intensity, high total runoff and high initial soil moisture. Counter clockwise hysteresis occurred at small events with high rainfall intensity and very dry soil conditions. This can be explained by the significantly higher flood wave celerity compared to the flow velocity that carries the bulk of suspended sediment (Williams, 1989, Brasington and Richards, 2000). Counter clockwise hysteresis in events with long duration, observed by Seeger et al. (2004), was not detected in the Petzenkirchen catchment.

In case of long lasting events with low intensities, wave velocity was not fast enough to appear in advance of the bulk of sediment. On the contrary, the peak of sediment concentration appeared in front of the discharge peak. A possible explanation of clockwise hysteresis is the exhaustion of easily available sediments close to the stream (Williams, 1989). At low intensity rainfall events, only saturation excess runoff is expected. It is in areas at the bottom of the slope, close to the stream, that contribute first to discharge due to higher initial soil water contents. Therefore, sediment coming from these areas would contribute first to sediment discharge. A further source of early sediment may be the stream bed (Williams, 1989, Kronvang et al., 1997, Lenzi and Marchi, 2000), where sediments are available due to increasing shear stress. Additionally, the stream bank could contribute to the sediment source (Kronvang et al., 1997) from sediments deposited at the end of former events. A further continuation of rainfall may cause an increasing area to contribute to discharge and sediment delivery. However, the easily available sediments close to the stream may already be exhausted, leading to reduced sediment input from areas that contribute since the beginning of the event.

An explanation for the variable extent of hysteresis may be the heterogeneity of rainfall characteristics and different initial conditions in terms of soil moisture, discharge, land use, management practices and plant development. For example, areas with lower soil water contents, perhaps with actively growing crops, will contribute later and less water in comparison to those with higher water contents, for example area after harvest.

Eight-shaped hysteresis combined both directions of hysteresis and occurred at low total amounts of runoff, medium rainfall intensities and medium soil water contents. All events with eight-shaped hysteresis had the clockwise loop at low discharges followed by a counter clockwise hysteresis. Seeger et al. (2004) mentioned the same phenomena. Possible explanations can be: (i) a sediment flush from the streambed and its banks, (ii) a delayed contribution of a sub-catchment, (iii) storage in small basins and their later connection after filling or (iv) influences of drainage. Kronvang et al. (1997) measured a sediment contribution from drainages of up to 69 % in an arable catchment. Its temporal delay is caused by the passage through the soil, even when preferential flow paths through the soil exist.

Further investigations of the contribution of drainages on sediment transport and the influence of soil moisture and vegetation will be done when more events have been recorded.

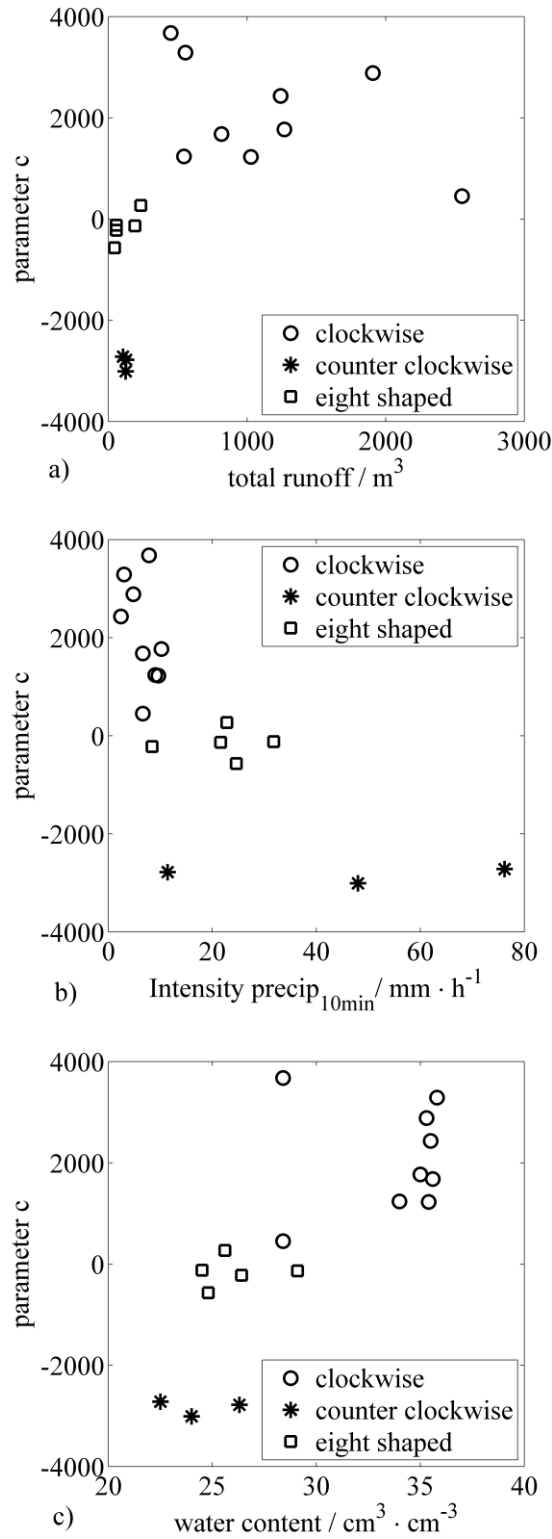


Fig. 2.7: Correlation between parameter  $c$  of the hysteresis model (equation 3) and total rainfall amount (a), maximum rainfall intensity within 10 minutes (b) and initial soil water content (c), together with the corresponding hysteresis direction of the event (clockwise, counter clockwise and eight-shaped).

### 2.3.5 Catchment sediment load (CSL)

Calculations of catchment sediment loads for single events employing the different model approaches are given in Tab. 2.4. Calibrated turbidity records ( $ss_{tu}$ ) produced event loads between 4 kg and 1609 kg, which will again be used as a benchmark. Calculations with the general rating curve ( $ss_R$ ) led to a mean overestimation of 152 % with a maximum of 660 % and a minimum of -78 % compared to  $ss_{tu}$  for the same events (Fig. 2.8). Nearly no differences in prediction of sediment load occurred between the event specific loading function ( $ss_{RE}$ ) and the hysteresis model ( $ss_{Hws}$ ). Values varied from 4 kg to 1258 kg and from 4 kg to 1254 kg, respectively. The variation of suspended loads compared to  $CSL_{tu}$  ranged from 47 % to -42 % and from 61 % to -44 %, with a mean difference of -5 % and -1 %, respectively. Although  $ss_{Hws}$  was calculated with higher accuracy compared to  $ss_R$ , there is no indication for a better prediction of total suspended sediment load. This seems to be due to a systematic averaging out of the deficiencies of the  $ss_{RE}$  model described above over a full event. The most accurate results were obtained with the application of the hysteresis model using the calibrated turbidity data ( $ss_{Htu}$ ), with maximum calculation errors between 1 % and -1 %.

Tab. 2.4: Measured ( $CSL_{tu}$  – calibrated turbidity data) and calculated ( $CSL_R$  – general rating curve,  $CSL_{RE}$  event specific rating curve,  $CSL_{Hws}$  – Hysteresis model fitted to water samples,  $CSL_{Htu}$  – Hysteresis model fitted to turbidity data) catchment sediment loads on event basis.

	$CSL_{tu}$	$CSL_R$	$CSL_{RE}$	$CSL_{Hws}$	$CSL_{Htu}$
<i>Event loads in kg</i>					
E 1	148	638	172	200	148
E 2	724	4809	610	645	722
E 3	4	11	4	4	4
E 4	126	548	110	117	124
E 5	231	68	245	257	234
E 6	83	124	65	84	83
E 7	1006	2812	1171	1157	1007
E 8	177	255	103	99	177
E 9	213	946	197	198	213
E 10	1369	10411	1166	1181	1373
E 11	377	1787	334	367	378
E 12	69	119	67	67	69
E 13	90	71	107	107	89
E 14	24	5	29	26	24
E 15	26	11	23	23	26
E 16	1609	379	1258	1254	1622
E 17	73	20	54	51	72
E 18	146	120	106	110	146
E 19	706	1627	1039	1138	708
<b>Σevents</b>	<b>7200</b>	<b>24760</b>	<b>6859</b>	<b>7083</b>	<b>7217</b>

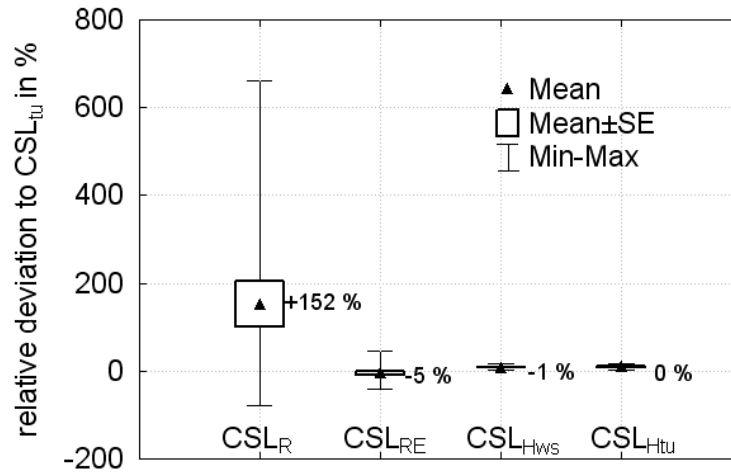


Fig. 2.8: Relative errors of catchment sediment load for the tested calculation methods (CSL<sub>R</sub> – general rating curve, CSL<sub>RE</sub> – event specific rating curve, CSL<sub>Hws</sub> – hysteresis model applied to water samples, CSL<sub>Htu</sub> – hysteresis model applied to calibrated turbidity data) compared to measured catchment sediment load (CSL<sub>tu</sub>).

## 2.4 Conclusions

We used quasi-continuous turbidity measurements and additional water sampling as the best available representation of instantaneous sediment concentrations in the stream draining the Petzenkirchen catchment, Austria. However, the necessity of probe calibration indicated that even with the effort of additional water sampling there is still considerable uncertainty associated with the estimation of in-stream sediment concentrations.

Transport of suspended sediment in streams underlies a wide range of influencing factors. Their variability caused enormous variation of the ssc – flow relationship in this study and therefore biased ssc calculations considerably when a general rating curve approach was used. We obtained better results when using rating curves on an event basis, but omitting hysteresis effects still misrepresented instantaneous ssc calculations.

Of the 19 events that were analysed, nine showed a clockwise hysteresis, five were eight-shaped and three followed a counter clockwise loop. For two events, nearly no hysteresis was detected. We used the model parameter  $c$  of the Krueger et al. (2009) hysteresis model to classify the direction and extent of hysteresis. Variable rainfall intensities, antecedent soil water content and total runoff amounts were identified as most relevant for the hysteresis direction. High  $c$  values, i.e. large clockwise hysteresis loops, were caused by long enduring events with low intensities and higher initial soil moisture. Small but intense events and drier soil conditions entailed counter clockwise hysteresis and therefore high negative  $c$  values. Eight-shaped hysteresis loops are mixed forms that happened during events with medium rainfall intensity and medium initial soil water content, but total runoff had to be very low.

Although several limitations to successfully applying the hysteresis model have been identified, parameter  $c$  of the Krueger et al. (2009) model provided additional information about the hysteresis behaviour of suspended sediment concentrations in the study catchment.

Specifically, we found that the value of parameter  $c$  directly reflected direction and extent of the hysteresis loop, depending on various event characteristics.

In contrast, for the calculation of total loads of suspended sediment, application of a single event rating approach was already sufficient to obtain reliable event loads with respect to the observed benchmark turbidity data. However, application of a general rating curve led to mean deviations of more than 150%, making this a highly questionable solution for calculating reliable sediment loads, even when calculating annual sediment loads.



Die approbierte gedruckte Originalversion dieser Dissertation ist an der TU Wien Bibliothek verfügbar.  
The approved original version of this doctoral thesis is available in print at TU Wien Bibliothek.

# Chapter 3

## Resuspension of stream bed sediments

The present chapter corresponds to the following scientific publication in its original form:

*Eder A., M. Exner-Kittridge, P. Strauss and G. Blöschl, 2014. „Re-suspension of bed sediment in a small stream; Results from two flushing experiments”. Hydrol. Earth Syst. Sci. 18, pp. 1043–1052. <https://doi.org/10.5194/hess-18-1043-2014>.*

### Abstract

Streams draining small watersheds often exhibit multiple peaking sedigraphs associated with single peaking hydrographs. The process reasons of the multiple sediment peaks are not fully understood but they may be related to the activation of different sediment sources such as the streambed itself where deposited sediments from previous events may be available for resuspension. To understand resuspension of stream bed sediments at the reach scale we artificially flooded the small stream of the HOAL Petzenkirchen catchment in Austria by pumping sediment-free water into the stream. Two short floods were produced and flow, sediment and bromide concentrations were measured at three sites with high temporal resolution. Hydrologically, the two flood events were almost identical. The peak flows decreased from 57 to 7.9 l s<sup>-1</sup> and the flow volumes decreased from 17 to 11.3 m<sup>3</sup> along the 590 m reach of the stream. However, a considerably smaller sediment load was resuspended and transported during the second flood due to depletion of stream bed sediments. The exception was the middle section of the stream where more sediment was transported during the second flood event which can be explained by differences between flow velocity and wave celerity and the resulting displacement of sediments within the stream. The results indicate that the first peak of the sedigraphs of natural events in this stream is indeed caused by the resuspension of streambed sediments, accounting for up to six percent of the total sediment load depending on total flow volume.

### 3.1 Introduction

Understanding the sediment export from agricultural catchments is important for both land and water resources management. Erosion, land degradation and the transport of phosphorus are closely related to the sediment export (Kovacs et al., 2012). The occurrence of contaminants and particle bound elements such as phosphorous in the stream can be related to the abundance of fine sediments (Mudroch and Azcue, 1995; Quinton et al., 2003). While it is difficult to measure erosion within a catchment in a representative way due to the enormous spatial variability in catchments (Walling, 1988; Prosser et al., 2001a), monitoring the sediment concentrations in streams is a common way of indirectly measuring the bulk erosion from the catchment. However, in many environments sediment losses measured on the field scale are much higher than the sediment loads measured in the stream (e.g. Millington, 1981). This is because much of the sediment is deposited prior to reaching the stream or deposited in the stream network itself prior to reaching the catchment outlet (Merrit et al., 2003; De Rose et al., 2003).

There are many processes influencing the erosion, transport, deposition and remobilisation of sediments. Most of these factors vary significantly between events even if the hydrograph shape is similar. There is seasonal variation due to vegetation dynamics and antecedent soil moisture, variation due to different runoff mechanisms (infiltration excess vs. saturation excess) and variation due to differences in the rainfall intensities and spatial rainfall patterns (Soler et al., 2008; Lana-Renault, 2009; Giménez et al., 2012). In large catchments not all of these process variations may be visible in the sedigraph because of long pathways and the averaging of component processes, so there tends to be a close correspondence between sedigraphs and hydrographs. However, in small catchments many scientists have observed massive differences between the timing and shape of the hydrographs and the sedigraphs. Often, there is a temporal shift, resulting in either clockwise or counter-clockwise hysteresis when plotting flow against sediment concentrations, and multiple peaking sedigraphs are often associated with single peaking hydrographs (Kronvang et al., 1997; Brasington and Richards, 2000; Petticrew et al. 2007; Eder et al., 2010; Yeshaneh et al. 2013). As an example, Fig. 3.1 shows a hydrograph and the associated sedigraph of the HOAL catchment in Petzenkirchen where small sediment peaks often occur in advance of the main sediment and discharge peak. Seeger et al. (2004) observed similar early sediment peaks in a small headwater catchment in the Spanish Pyrenees.

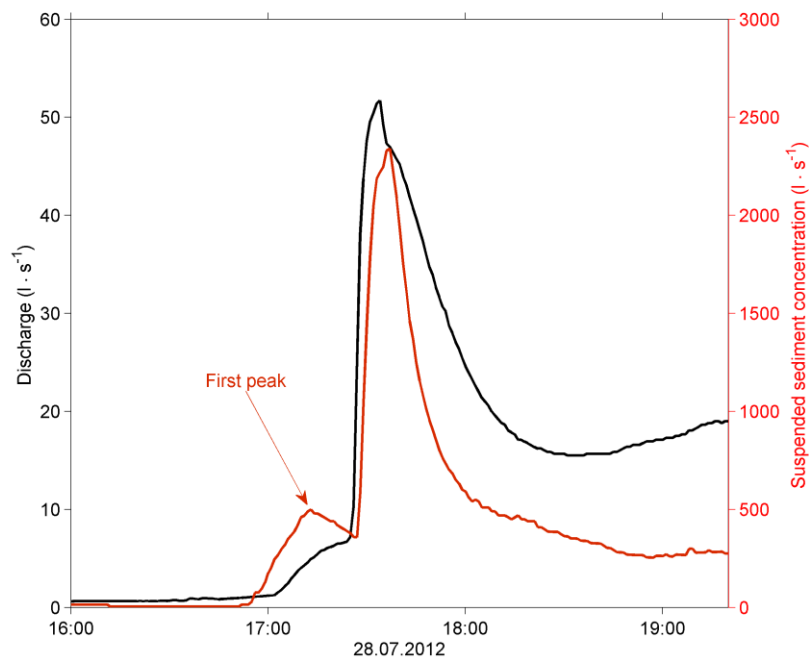


Fig. 3.1.: Natural event with single peaking hydrograph and double peaking sedigraph in the HOAL Petzenkirchen catchment (0.64 ha) on 28 July, 2012.

Many authors relate these observations to the activation of different sediment sources such as the resuspension from streambed sediments (Williams, 1989; Kronvang et al., 1997; Lenzi and Marchi, 2000; Regües et al., 2000; Eder et al., 2010). Although the movement of bedload for streambed stability analyses is well investigated, the behaviour of fine sediments, often simplified as washload, is less well investigated (Petticrew et al., 2007). However, it is the latter that reflects the amount of eroded sediments from the fields in agricultural catchments. Also, little information is available on the resuspension of fine sediments from the bed of small streams that were deposited during the tailing limb of the previous events and the transportation out of the catchment. Much of the difficulty in analysing these processes is related to the hydrological variability between events. Each and every event is different, which makes it very difficult to unravel the individual factors driving the processes of sedimentation and resuspension. What is needed are repeatable experiments (Blöschl and Zehe, 2005).

This paper therefore reports on reach-scale experiments of controlled water inputs into a small stream to understand the resuspension, transport and deposition processes of fine sediments. Specifically, the following science questions are addressed for an experimental catchment: (i) What is the magnitude of re-suspension of fine sediments from the stream bed? (ii) What is the source of these re-suspended sediments (catchment erosion during previous events or the channel bank)? (iii) Is the early peak in the sedigraphs of natural events due to the re-suspension of sediment from the stream bed?

### 3.2 Study site

The flooding experiments were conducted in the Hydrological Open Air Laboratory (HOAL) Petzenkirchen (Fig. 3.2). It is situated in the Western part of Lower Austria and has a size of 64 ha. It is jointly operated by the Federal Agency for Water Management and the Technical University of Vienna to study catchment processes from data with high temporal and spatial resolution. Climate in the catchment can be characterised as humid with a mean annual temperature of 9.3 °C and a mean annual rainfall of 716 mm. Temperature, rainfall and rainfall intensity have their peak during summertime. The elevation of the catchment ranges from 257 to 325 meter above sea level. 87 percent of the catchment area is arable land, five percent is used as pasture, six percent is forested and two percent is paved. The dominant soil types are Cambisols and Planosols (FAO, ISRIC and ISSS, 1998) with medium to poor infiltration capacities and underlying geology of quarternary sediments. Mean annual flow of the last decade was 3.8 l s<sup>-1</sup> but flow drops down in summertime to less than one litre per second. Maximum observed flow was around 2 m<sup>3</sup> s<sup>-1</sup> during a big flood in 2002. The stream itself has an open length of 590 meters with a medium slope of 2.4 % (Fig. 3.3). Additionally, the upper most 25 % of the stream length were piped in the 1950s to enlarge the agricultural production area. The piped section of the stream is not included in the length of 590 meters. The deposited material on the stream bed mainly consists of silt (68 percent), followed by clay (18 percent) and sand (14 percent).

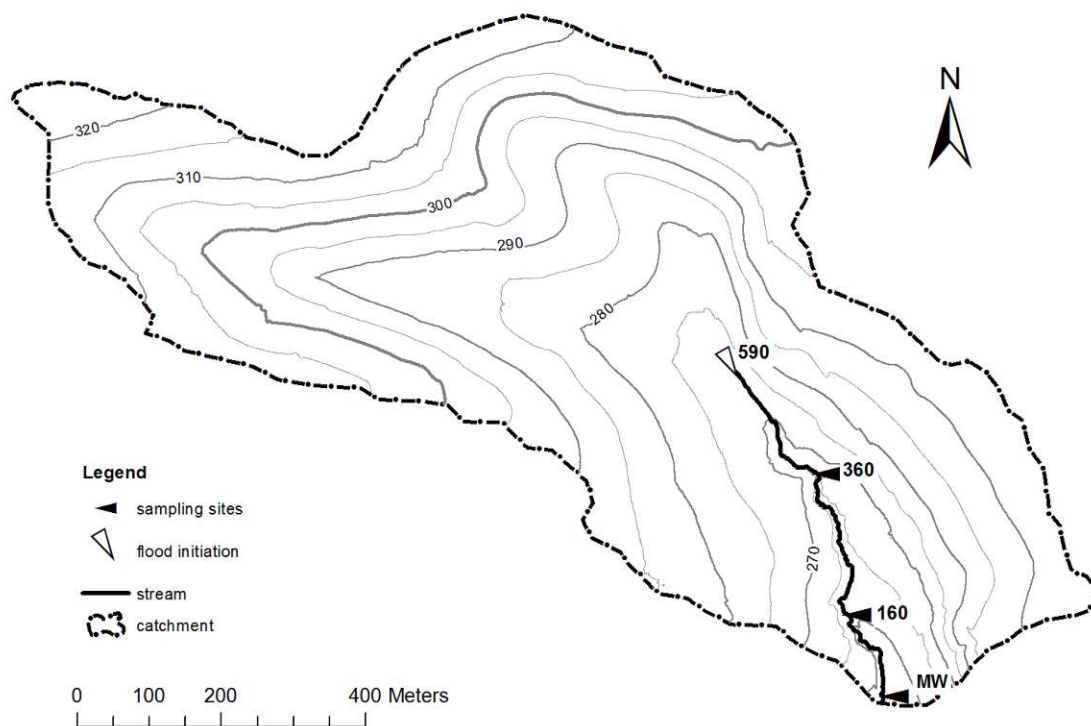


Fig. 3.2: HOAL catchment with point of flood initiation (590) and measurement sites (360, 160, and MW)

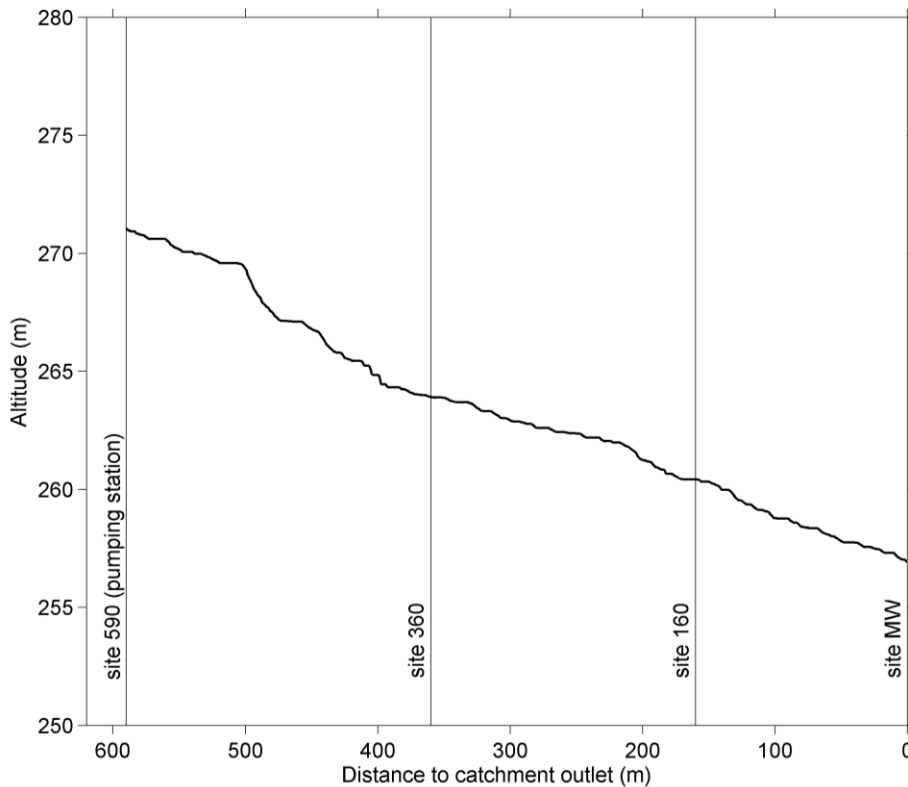


Fig. 3.3: Longitudinal section of the stream in the HOAL catchment with measurement sites.



Fig. 3.4: Upstream section of the stream in the HOAL catchment close to the pumping station (left) and downstream section close to the catchment outlet (right). Width of stream is indicated in the photos for comparison. Both photos are upstream views.

In the upstream section of the stream, bank slope ratio is almost 1:1. The stream is very narrow (Fig. 3.4, left) and a change in flow leads to a significant change in the water level. In the area of the catchment outlet the stream reaches a width of approximately one meter. The banks are very shallow (Fig. 3.4, right) and are flooded during medium sized floods. After the small river bed is flooded it takes a substantial increase in flow to produce a significant increase in water level. The longitudinal section of the stream (Fig. 3.3) shows a number of steps, followed by pools and sections with varying slopes.

Low gradient sections of the stream with small water velocities tend to be covered by deposited fine sediments whereas in the steep sections the quaternary material is visible. At the later the quaternary underground is often coated with precipitated carbon and resistant against erosion.

### 3.3 Experimental setup

Two flooding experiments were conducted in 2011 on August, 24th and August 31st respectively. Prior to the experiments, three temporary water reservoirs were set up at the beginning of the open stream (site 590 in Fig. 3.1). They were filled with stream water one day before the flooding experiments. Bromide was added to the water as a tracer. The reservoirs were fitted with three pumps with a nominal flow rate of a total of  $56.7 \text{ l s}^{-1}$ . The pumps were started with a delay of one minute and pumped water into the stream directly at site 590. Due to different sizes of the pumps (two smaller and one bigger pump) and the delayed start of each pump a stepwise initial flood was produced. The flow from the hoses was stabilised in a wooden box to minimise the stir up of sediments from the streambed. The total capacity of the reservoirs was  $24 \text{ m}^3$  but it was not possible to empty the water reservoirs completely, so the actual water volume pumped into the stream was  $16,9 \text{ m}^3$  at the first flood and  $17.1 \text{ m}^3$  at the second flood.

Flow in the stream at site 590 was measured by a calibrated H-Flume fitted with a pressure transducer where water levels were logged at 1 min intervals. For the flow measurements at site 360 and site 160, V-notch weirs were installed in the streambed. At both sites we recorded water level, turbidity, conductivity and temperature at 1 min intervals and took manual water samples at two minute intervals for the first 40 minutes after the first increase of the water level. Additionally, automated samplers were installed at these sites with a sampling interval of 20 minutes to capture the tail of the flood waves. We did not use the automated samplers directly after the first increase of the water level because the minimum sampling interval of five minutes attainable with the sampler was considered to be too long for the flow dynamics of interest. The water samples were analysed for suspended sediment concentration and bromide concentration in the laboratory. Final sediment concentrations were calculated from the readings of the turbidity probes which were calibrated with manual and automated sampler data for each single site separately.

At the catchment outlet (site MW) we measured flow with an H-flume and a pressure transducer, at one minute intervals. Turbidity, electrical conductivity and water temperatures were measured also at one minute intervals. Additionally we took water samples using the same procedures as for sites 360 and 160.

The weather and the hydraulic conditions in the stream prior to the flooding events were almost identical. Although there was some rain and discharge began to rise a few days in advance of both flooding experiments, directly before the tests base flow conditions were reached again (Fig. 3.5). It is assumed that only a negligible part of sediment was transported at the natural rainfall event between the flooding tests, because turbidity did not show a clear response to the increased flow rate.

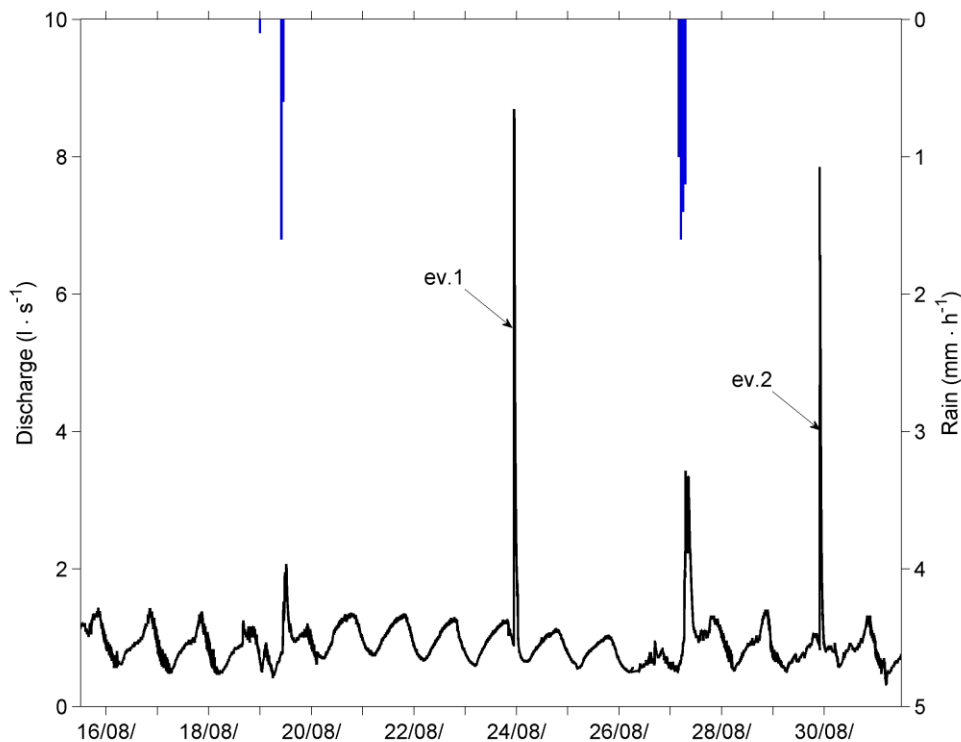


Fig. 3.5: Hyetograph and discharge at the catchment outlet (site MW) ten days before and during the flooding events in August 2011.

### 3.4 Results

The hydrographs of the two flooding experiments are shown in Fig. 3.6. For the first experiment (Fig. 3.6a) the maximum flow rate measured at the pumping station (site 590) was  $57 \text{ l s}^{-1}$  which is close to the nominal capacity of the pumps. There is a strong dispersion of the flood wave and thus a significant reduction of the maximum flow rate along the stream from  $57 \text{ l s}^{-1}$  at site 590 to 21.5, 10.0 and  $8.7 \text{ l s}^{-1}$  at sites 360, 160 and the catchment outlet, respectively. The total volume of water pumped into the stream was  $16.9 \text{ m}^3$  and decreased to 15.2, 13.3 and  $11.3 \text{ m}^3$  at sites 360, 160 and the catchment outlet, respectively. The reduction in volume along the stream (Fig. 3.8) is due to transient storage, i.e. storage in either stream channel dead zones (side pools, eddies) or exchanges through the hyporheic zone (Gooseff et al., 2007).

The hydrographs of the second experiment (Fig. 3.6b) are almost identical to the hydrographs of the first experiment. The maximum flow rates decreased from  $57 \text{ l s}^{-1}$  at the pumps to 20.7, 9.9 and  $7.9 \text{ l s}^{-1}$  at the downstream sites. The measured water volumes decreased from  $17.1 \text{ m}^3$  to 14.7, 12.9 and  $11.7 \text{ m}^3$ . The close similarity of the hydrograph characteristics is important as the flooding experiments were designed as repeated experiments to infer the differences in sediment characteristics for flood waves that are otherwise similar.

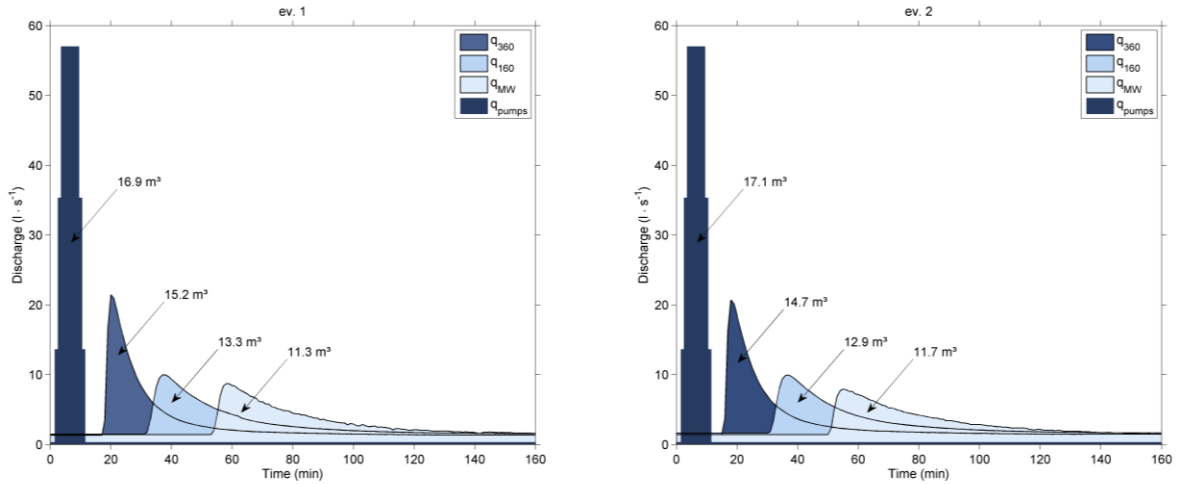


Fig. 3.6: Hydrographs of the first (ev.1) and second (ev.2) flooding experiment at the flood initiation location and three monitoring sites (see Fig. 3.2).

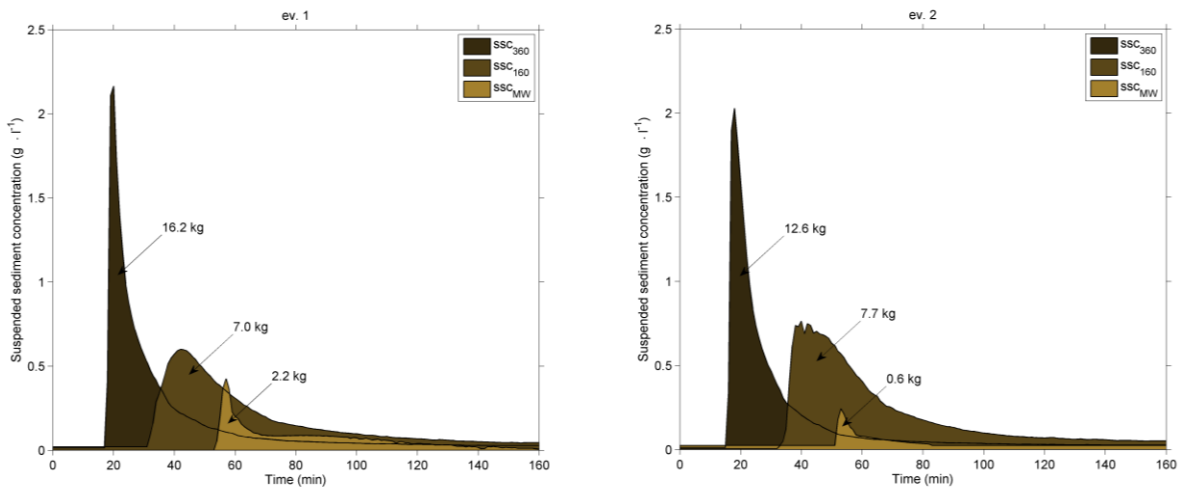


Fig. 3.7: Sedigraphs of the first (ev.1) and second (ev.2) flooding experiments at the three monitoring locations (see Fig. 2).

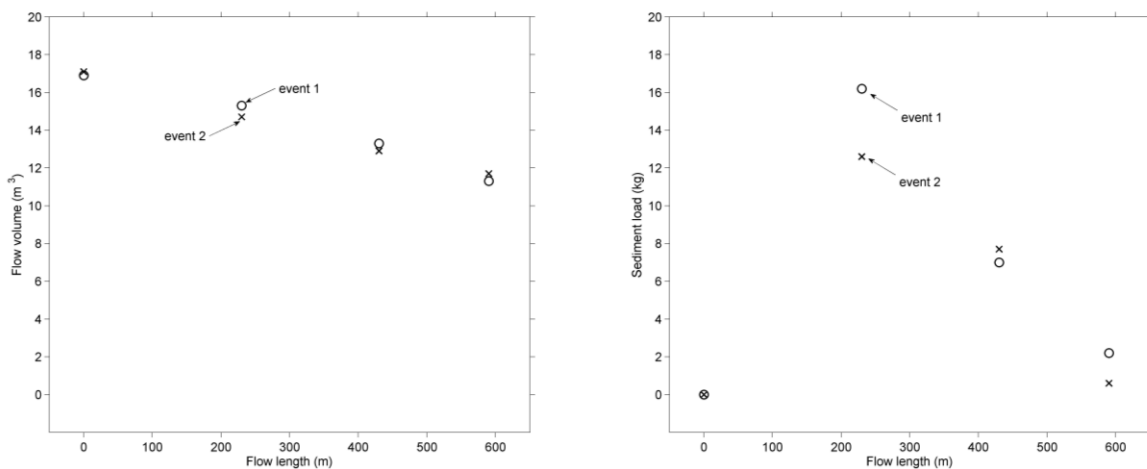


Fig. 3.8: Comparison of water volumes and sediment loads transported along the stream for the two flooding experiments (event 1 and event 2). Water flow is from left to right.

To shed light on the sources of the transported sediments Fig. 3.9 compares the time lags of the hydrograph dynamics representing wave celerities (Fig. 3.9a), the time lags of the sediment (Fig. 3.9b) and the time lags of the bromide tracer representing flow velocities (Fig. 3.9c). The first rise of the hydrograph at site 360 occurred 18 minutes after starting the pumps. It took 32 minutes to see the first rise at site 160 and 54 minutes at the MW (Fig. 3.9a). Since the hydrographs of the two experiments are almost identical, the time lags for the second event are very similar (17, 32 and 52 minutes). The first appearance of sediments is simultaneous with the first rise of the hydrograph. In the first experiment the sediment concentrations at the individual sites along the stream increased 18, 33 and 55 minutes after starting the pumps (Fig. 3.9b). In the second experiment they increased 17, 34 and 53 minutes after starting the pumps. In the first experiment the first detection of bromide occurred 20, 38 and 86 minutes after starting the pumps, and in the second experiment after 20, 41 and 75 minutes at sites 360, 160 and MW, respectively. This means that first detection of bromide occurred later than the rise of the hydrograph.

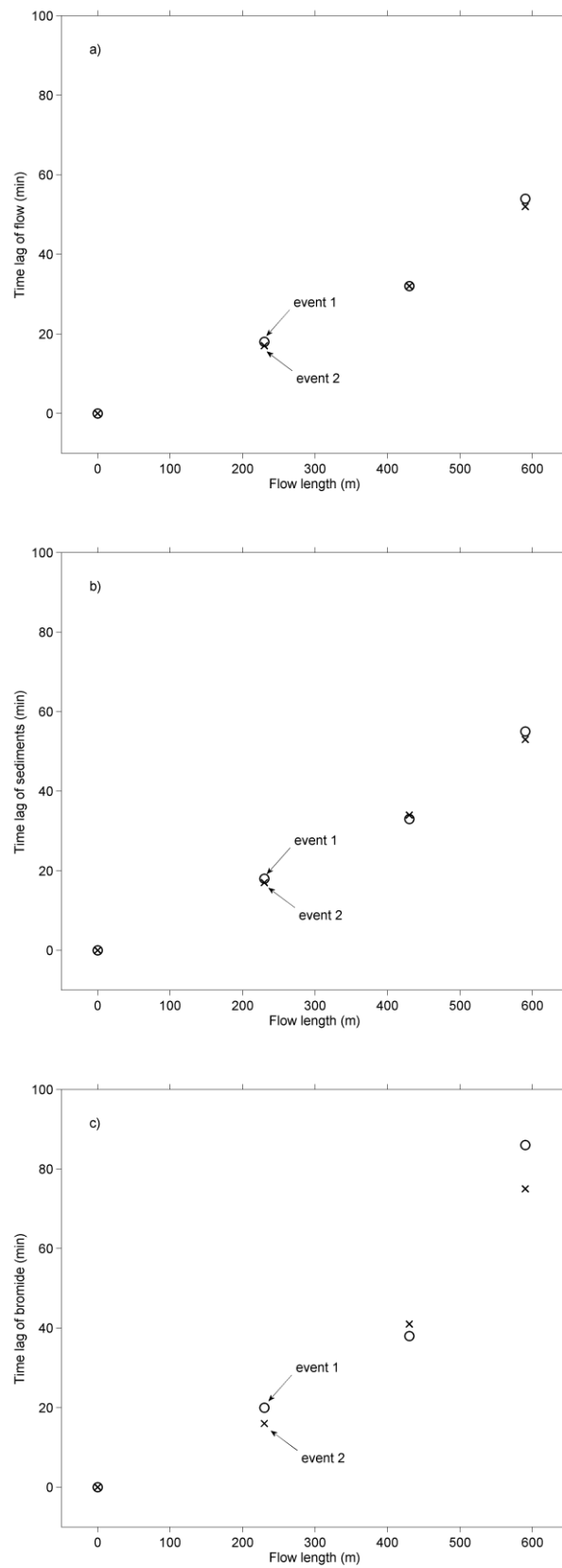


Fig. 3.9: Time lag of water (celerity) (a), sediment (b) and bromide (velocity) (c) for the two flooding experiments (event 1 and event 2) estimated from the first appearance (first rise) of the signal.

## 3.5 Discussion

### 3.5.1 Source and magnitude of re-suspended sediments

The most striking feature of the two experiments is that the hydrographs are almost identical. Indeed the experiments were designed in a way to make the two flooding events identical replicas from the perspective of water flow. In the two flooding experiments approximately equal flow maxima were measured at the individual stations along the stream. Also, the decrease of the total runoff volume is almost identical. In both experiments, apparently, exfiltration into the groundwater and surface ponding occurred as would be expected for this type of events (Wondzell et al., 2010). As shown in Fig. 3.5, there was no impact of rainfall on the base flow conditions between the two experiments, so we can safely assume that the hydrological conditions (including soil moisture and groundwater tables) were very similar. This similarity allows a comparison of sediment processes purely based on the availability of sediments in the stream. With the experimental setup it was ensured that no sediment was delivered from the fields. Therefore, the only sediment sources were the stream bed itself, stream banks or deposited sediments of previous events. Due to the fact that the stream bed is cut into the molassic subsurface and has been stable for several decades, a further deepening and thus direct erosion of the stream bed can be excluded. Bank erosion, on the other hand, is a local phenomenon and can never be excluded. However, the immediate increase in sediment concentration at the onset of the hydrograph suggests that the main source of the sediments is resuspension of previously deposited sediments, either from the stream bed or from the flood plains. This is also supported by the finding that significant less sediment was transported during the second flooding experiment although hydraulic conditions were identical. Thus, the sediment deposits on the stream bed have been depleted during the first experiment.

The estimated hydraulic conditions at maximum discharge at the measurement sites (Tab. 3.2) indicate transport of sediments with a maximum diameter of 45 mm at the upper section, declining to 10 mm at the middle section where minimum shear stress occurred due to lowest topographic gradient (Tab. 3.1). For the estimations mean section slope, mean section velocities and characteristic stream widths were applied and Shields parameter was assumed to be 0.05. Using simple Kresser equation (Kresser, 1964) for fine silt (0.002 to 0.006 mm) the critical velocity for suspension is  $0.15 \text{ m s}^{-1}$  which was exceeded at maximum discharge at the upper and the middle section. This means a transport in suspended form of both fine silt and silt at these sections during high flow conditions. Only at the downstream part velocity was always lower than the critical value. The maximum diameter of suspended sediment was 0.004 mm for the given transport velocity of  $0.12 \text{ m s}^{-1}$ .

Tab. 3.1: Wave celerities estimated from the hydrograph dynamics, velocities of sediment transport estimated from the sedigraphs and flow velocities estimated from the bromide tracer samples. All estimates are for the first appearance (first rise) of the signal as in Fig. 9.

	Event 1				Event 2		
	Mean topographic gradient	Wave celerity	Sediment velocity	Flow velocity from bromide tracer	Wave celerity	Sediment velocity	Flow velocity from bromide tracer
	( $10^{-3}$ )	( $m s^{-1}$ )	( $m s^{-1}$ )	( $m s^{-1}$ )	( $m s^{-1}$ )	( $m s^{-1}$ )	( $m s^{-1}$ )
Site 590 to 360	31	0.213	0.213	0.192	0.225	0.225	0.192
Site 360 to 160	17	0.238	0.222	0.185	0.222	0.196	0.159
Site 160 to MW	22	0.121	0.116	0.056	0.133	0.140	0.078

Tab. 3.2: Estimated hydraulic conditions at maximum discharge at the measurement sites and associated critical mean sediment diameter.

	Event 1				Event 2			
	Flow depth	Shear velocity	Shear stress	Mean critical diameter	Flow depth	Shear velocity	Shear stress	Mean critical diameter
	(m)	( $m s^{-1}$ )	( $N m^{-2}$ )	(mm)	(m)	( $m s^{-1}$ )	( $N m^{-2}$ )	(mm)
Site 360	0.17	0.19	37	45	0.16	0.19	35	44
Site 160	0.05	0.09	8	10	0.05	0.09	8	10
Site MW	0.07	0.12	14	17	0.07	0.11	13	16

The sediment load transported by the stream at the various sections decreased along the stream (Fig. 3.7). This is consistent with the decreasing discharge and flow velocities according to transport capacity concepts (eg. Merrit et al., 2003). As noted above, the sedigraphs of the two flooding experiments differed although the hydraulic conditions were identical. At site 360 the sediment load of the second experiment was 22 % smaller than that of the first experiment. At the catchment outlet the sediment load of the second experiment was even 72 % smaller than that of the first experiment.

However, contrary to our initial expectations, at the middle section (site 160) the sediment load of the second experiment increased by 10% relative to the first experiment. Possible reasons for this increase are a bank collapse upstream of the site and/or a change in the availability of sediments along the stream. The latter is supported by the bromide tracer results. The ratio between wave celerity and bromide velocity is approximately unity at the upper section and increases to 2.2 near the catchment outlet (

Tab. 3.1), indicating that transport velocity is lower than wave celerity in the downstream section. Due to the immediate rise of sediment concentrations when flow starts to increase, the sediments must originate from the streambed directly upstream of the measurement site. Because of the short duration of the flood wave and the differences between celerities and velocities, the sediments are likely transported for only a limited length and re-deposited as the transport capacities decrease when the wave recedes after its maximum. This interpretation of limited transport length is supported by travel distance studies within flumes from Parsons and Stromberg (1998) and Bryan and Brun (1999). These results, along with the data from this study, suggest that a considerable amount of fine sediments was transported during the first flooding experiment until site 160. These sediments were then easily available for the second flooding. Because of the higher ratio between celerity and velocity and lower flow rates at the downstream part less sediment was transported in this section. The sediment delivery from the upper part of the reach is limited. Furthermore, the stream has a complex geometry with small steps followed by pools which may act as temporary sediment sinks. One would expect that the influence of these pools is related to the mean exchange rate with the main stream and therefore depends on the discharge. This process reasoning suggests that the higher sediment loads at site 160 in the second experiment relative to the first are real and can be explained by the differences in sediment availability along the stream. However, the main pattern is that the sediments on the stream bed were depleted during the first experiment, leading to smaller sediment loads at the catchment outlet in the second experiment.

### 3.5.2 Comparison with natural events

A crucial point of the study was the comparison of the resuspension experiments with the first flush sediment load of natural events. The results of the experiment suggest that the first flush sediment peak of a natural rainfall-runoff events in the catchment are indeed caused by resuspension. Especially for short duration storms with high rainfall intensities the time for transporting eroded sediments from the fields to the catchment outlet is not long enough to take these sediments out of the catchment. In our experiments, the main part of the event was around 20 mins while it took the water around 80 mins to reach the catchment outlet. Most of the sediment must therefore remain somewhere on the pathway.

It is now of interest to compare the flooding experiments with natural events. Data of natural events from the years 2006 and 2007 taken from Eder et al. (2010) were used for the comparison. Relationships between sediment concentrations and discharge for both the flooding experiments and the natural events are plotted in Fig. 3.10. On average, the relationships for the flooding experiments (Fig. 3.10a) and the natural events from the years 2006 and 2007 (Fig. 3.10b) are very similar. This suggests that enough sediment is available for resuspension in the natural events. However, the relationships of the two experiments are much more consistent than those of the individual natural events because of the similarity in the hydrological conditions.

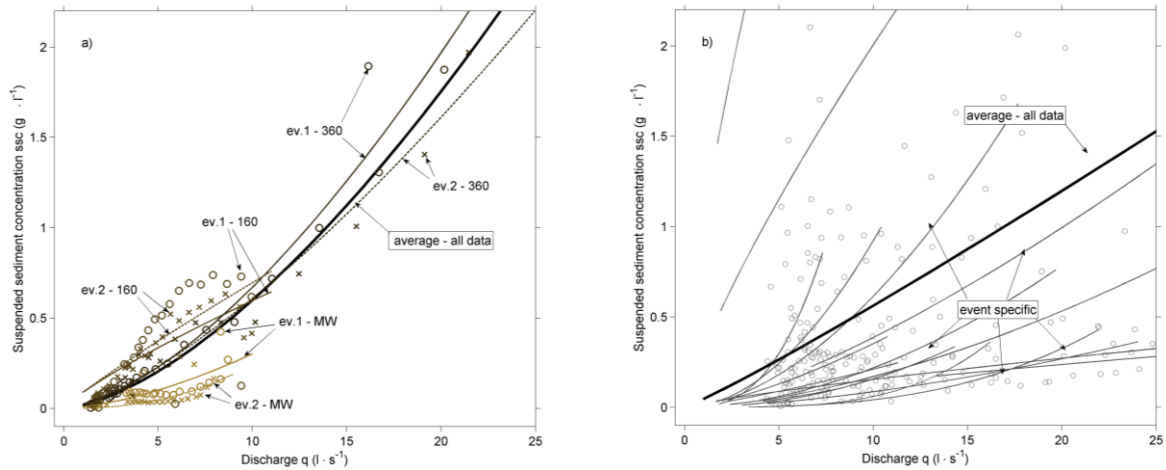


Fig. 3.10: Relationship between sediment concentrations and discharge of the flooding experiments (a) and natural events (b, modified from Eder et al., 2010) in the HOAL catchment.

For evaluating the resuspension during natural events, six events were selected where a clear first flush peak could be identified. These were used to calculate the contribution of the first flush sediments to the total sediment load (Tab. 3.3). The results indicate that the proportion of first flush (resuspension) sediment load to the total load is between 0.1 and 6 %. For comparison, the corresponding values of the flooding experiments are reported. The sediment concentrations and loads of the experiments are listed under first peak as they stem from resuspension. The total export of the two experiments was 2.2 and 1.6 kg respectively, while the first flush export of the natural events usually ranged between 0.1 and 5.6 kg with the exception of the June 2007 event. A possible reason for the extraordinary high sediment concentrations of the June 2007 event can be the planting of maize on the most sensitive fields for erosion in the catchment and the less developed plant stadium at that time of the year. Therefore, the soil was not covered and easily erodible.

Tab. 3.3: Characteristics of natural events and the flooding experiments at the outlet of the HOAL catchment (64 ha). The sediment concentrations and loads of the experiments are listed under first peak as they stem from resuspension.

	Water volume of event	Max. discharge of event	Max. sediment concentration of event	Max. sediment concentration of first peak	Sediment load of event	Sediment load of first peak	Contribution of first peak to total load
	m <sup>3</sup>	l s <sup>-1</sup>	mg L <sup>-1</sup>	mg L <sup>-1</sup>	kg	kg	%
29 Apr 2006	88.6	19	3156	1083	94.6	5.6	6.0
29 Oct 2006	92.2	15.5	570	317	20.3	0.5	2.3
1 Jan 2007	360.8	11.5	712	166	143.2	0.1	0.1
1 Mar 2007	583.7	13.3	729	373	215.1	1.8	0.8
10 Jun 2007	255.2	15.9	26565	8243	2481.3	42	1.7
28 Jul 2012	661.3	51.7	2340	499	145.9	1.1	0.8
Experiment 1	21.7	8.69	→	890	→	2.2	-
Experiment 2	21.6	7.94	→	290	→	1.6	-

As the event magnitude of the natural events increases, the relative contribution of the first flush relative to the total load decreases (Fig. 3.11). This would be expected as a result of the depletion of the sediment deposits on the stream bed during the events and the corresponding increase of total sediment load because of enlargement of sediment contributing areas. The March 2007 event exhibits a large total flow volume (584 m<sup>3</sup>) but lowest contribution of first flush peak to total sediment load. Contrary, the April 2006 event shows lowest total flow volume (88 m<sup>3</sup>) but highest relative first flush sediment load.

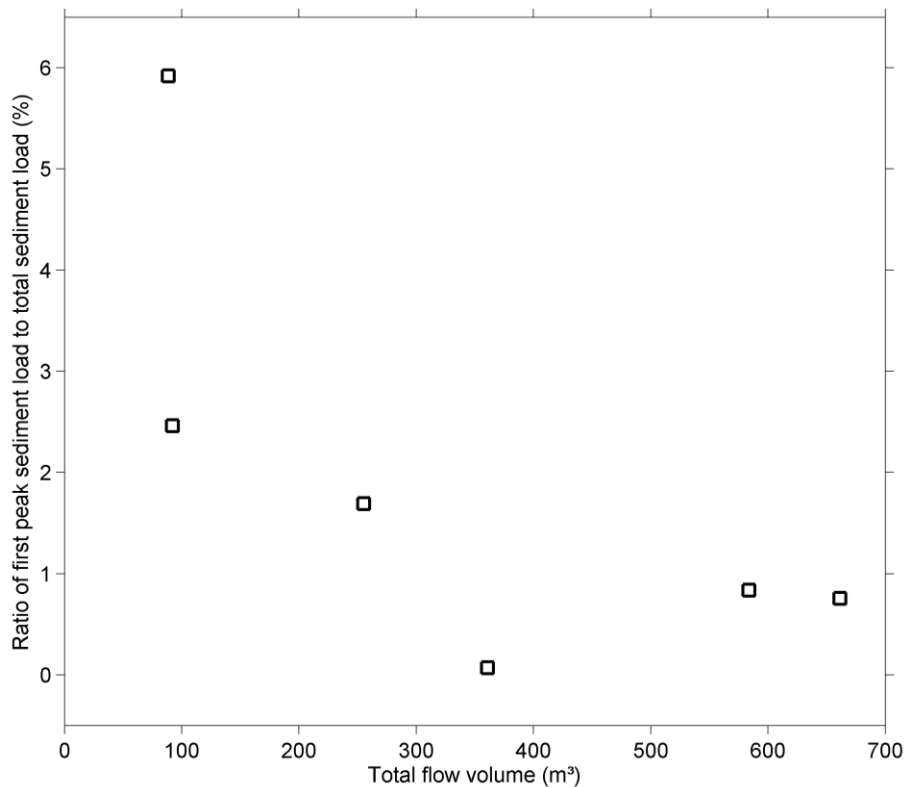


Fig. 3.11: Ratio of first flush sediment load to total sediment load of natural events as a function of total flow volume in the in the HOAL catchment (64 ha), see Tab. 3.2.

The contribution of the first flush sediment load is much smaller than the figures for bed/bank erosion reported in the literature. For example, Kronvang et al. (1997) reported a contribution of 66- 89 % for the low land river in Denmark. Therefore, it is very likely that in the case of the HOAL catchment the first sediment peak is caused by resuspension but resuspension also occurs later during the event. As long as sediments are available in the stream bed and the critical shear stress or transport capacity is high enough, resuspension will happen. Whether the sediment is exported from the catchment or just displaced within the reach depends on the event characteristics, in particular on the duration and magnitude of the event. The amount of resuspension is also affected by the deposition characteristics of the previous event, as demonstrated by the differences in the sedigraphs in this study. If a summer storm with high erosion rates but short duration transports a lot of sediments from the fields to the stream, much sediment will be available for the following event. In contrast, a long event with low intensities and low erosion rates may resuspend most of the streambed sediments and not leave much sediment for the following event. Furthermore, the grain size distribution of the

available and transported sediments will play an important role. For instance, Peticrew (2007) reported that more mass but smaller grain sizes were transported during the falling limb of the hydrograph. This could lead to a big resource for easily available sediments when the ratio between flow celerity and velocity is high.

### 3.6 Conclusions

Two flooding experiments in a stream draining a small agricultural catchment clearly indicate resuspension of fine sediments from the streambed. At the first experiment suspended sediment load decreased from 16.2 kg to 2.2 kg along the stream according to the decrease of flow. During the second experiment less sediment was resuspended and transported through the different sections of the stream (12.6 kg to 0.6 kg along the stream) due to the depletion of easily available sediments from the streambed. The evaluation of flow and travel times indicates that the first peak of the sedigraphs of natural events in this stream is indeed caused by the resuspension of streambed sediments. The sediment loads of the first peak of natural events may contribute between 0.1 and 6% of the total sediment load, depending on total flow volume.

Our future work will focus on the depletion of streambed sediments during long lasting events, including grain size analyses and hysteresis effects to more fully understand the physical processes of in-stream sediment transport. Furthermore, it would be of interest to compare the results of this study with similar experiments for different hydrological conditions.

# Chapter 4

## Pathways of dissolved organic carbon

The present chapter corresponds to the following scientific publication in its original form:

*Eder A., G. Weigelhofer, M. Pucher, A. Tiefenbacher, P. Strauss, M. Brandl and G. Blöschl, 2021. „Pathways and composition of dissolved organic carbon in a small agricultural catchment“. Submitted to Ecohydrology and Hydrobiology on April 19<sup>th</sup>, 2021.*

### Abstract

The amount and composition of organic carbon are major controls on water quality and ecological processes in streams, but the degree to which they are affected by agricultural land use is not fully understood. The objective of this study is to explore the fate of the quantity of dissolved organic carbon (DOC) and the composition of dissolved organic matter (DOM) in an agricultural hillslope - stream network system. We conducted our study in the 66 ha HOAL (Hydrological Open Air Laboratory) in Lower Austria. We collected soil samples on three land use units (arable, grassland, forest), and water samples from the stream and from seven tributaries (inlet, tile drains, spring) on a monthly basis during low flow conditions. We measured DOC of the eluate of the soil samples and DOC of the water samples, and estimated DOM components by fluorescent spectrophotometry and PARAFAC analyses. Soil DOC shows the highest concentrations in summer due to high temperatures. Carbon input from litter almost doubles soil DOC at the forest site in autumn. In contrast, DOC concentrations in the tributaries are lower in summer than in winter by between 19% and 31% due to higher microbial biomass and respiration. DOM composition of the soil eluate differs between land use units. The forest site, which has the highest DOC concentration, exhibits the largest fractions of humic-like fluorophores and less fresh and labile DOM. DOM composition in the tributaries is, in addition to DOC, controlled by catchment soil moisture; wetter soils lead to more refractory, humic-like, recalcitrant, terrestrial DOM and less labile, protein-like DOM with low molecular weight, indicating enhanced microbial activity. We estimated the DOC import from the tributaries into the stream as 125 kg during base flow conditions in the period February to December 2017 and the instream DOC production as 38 kg, considering mass balance and exchange with groundwater. Six out of seven DOM components have a positive net production along the stream, only relatively aliphatic DOM with low molecular weight is consumed (65 % of its input). These findings suggest that agricultural land use increases DOC input into streams and therefore alters their DOM quality. Instream processes modify DOM quality over short flow

distances. The process complexity along the flow path from the soil surface to the stream requires further research.

## 4.1 Introduction

Agriculture delivers significant amounts of dissolved organic matter (DOM) to stream ecosystems, changing basic metabolic processes in the water and at the water-sediment interface, and affecting the ecological state and the health of aquatic systems (Fasching and Battin, 2012; Findlay et al., 2001, 2003; Piscart et al., 2009; Rouhani et al., 2021). The amount and composition of terrestrial DOM influence benthic microbial growth and respiration as well as CO<sub>2</sub> outgassing from streams (Findlay et al., 2003; Piscart et al., 2009; Williams et al., 2010). DOM is a mixture of various compounds with molecular weights ranging from simple carbohydrates to complex molecules of different aromaticity (Bolan et al., 2011). Dissolved organic carbon (DOC) typically represents ~67% of the elemental composition of DOM (Bolan et al., 2011) and, therefore, is often used as a proxy when quantifying DOM. Due to light absorbing chromophores and fluorescent fluorophores, DOM has distinct spectrophotometric properties in terms of both absorption and fluorescence (Baker et al., 2003; Chen et al., 2003; Hudson et al., 2007). UV-visible (200 – 800 nm) optical properties of DOM have been used to determine DOM characteristics such as aromaticity (SUVA<sub>254</sub>; (Weishaar et al., 2003a)) and molecular size (Dalrymple et al., 2010). Recent advances in fluorescent spectrophotometry have provided a new tool for rapidly identifying DOM fluorophores via excitation–emission matrices (EEM; wavelengths 200 – 500 nm, (Chen et al., 2003; Fellman et al., 2010)). An EEM identifies fluorescence peaks that can be attributed to various DOM components, such as humic-, fulvic- or protein-like fluorophores (Baker et al., 2003). Thus, fluorescence methods are useful for identifying anthropogenic DOM sources in streams (Hudson et al., 2007) and for distinguishing bioavailable from refractory DOM components, the relative abundance of which determines microbial activity and organic matter processing (Bolan et al., 2004; Findlay et al., 2001; Marschner and Kalbitz, 2003).

In natural streams, refractory DOM originating from terrestrial sources usually dominates over autochthonous, labile DOM from algal primary production (Osburn et al., 2017). Agricultural activities may significantly alter this DOM composition (Graeber et al., 2012). Both enhanced benthic primary production, resulting from increased nutrient supply and light penetration, and increased manure inputs with high amino acids contents may shift the composition towards the dominance of labile components (Fellman et al., 2009). Wilson and Xenopoulos (2009) observed that pore-water DOM in agricultural soils showed lower molecular weights and less humicity than DOM in soils under native vegetation (see also Williams et al., 2012, 2010). In addition, DOM aromaticity correlated positively with soil moisture, indicating that soil drainage may increase the export of labile DOM to streams (Brockett et al., 2012).

In contrast, other studies have found a higher proportion of humic-like, structurally complex DOM in agricultural streams than in pristine streams, which may be related to the disturbance of agricultural soils by tillage (Frank and Groffman, 2009; Kalbitz et al., 2000; Marschner and Kalbitz, 2003). Comparative studies of soil and stream DOM show contradictory results

(Graeber et al., 2012) since the processes that drive the modifications are still largely unknown. The inconsistency of these findings may be related to differences in land use practices (e.g. fertilization, tillage, etc.) and environmental conditions (e.g. climate, vegetation, etc.), the significance of the different flow paths (surface runoff, soil pore water, drainage water), and different investigation methods.

Past studies have generally followed one of four sampling strategies. Some studies focused on the DOM of soil eluate (water extractable organic carbon) from different land uses (Chantigny, 2003; Ghani et al., 2007; Zsolnay, 1996), its change with depth (Cronan and Aiken, 1985; Worrall and Burt, 2007) and the impact of land management (Kalbitz et al., 2000; Steenwerth and Belina, 2008; Sun et al., 2017). A second group of studies measured DOM in soil pore water, either directly in the field with suction cups (Vinther et al., 2006) or via percolation towards drainages from individual land use units such as pastures (Ghani et al., 2007). A third group focused instead on the streams and measured DOM within the stream system, relating the measured DOM quantity and composition to the proportion of different land uses (e.g. Ahearn et al., 2005; Graeber et al., 2012; Wilson and Xenopoulos, 2009) or soil types (Graeber et al., 2012). Another group estimated instream DOM processing via longitudinal sampling (Fellman et al., 2009) or addition studies (Pucher et al., 2021).

However, in order to understand the impacts of agriculture on DOM concentrations, composition and processing in streams, an approach is needed that combines measurements of soil DOM, the corresponding DOM in tributaries and changes in the instream DOM along stream reaches.

The aim of this study therefore is to link spatial and temporal variations of DOC and DOM quality in a stream to the potential terrestrial sources associated with agriculture, the delivery pathways and instream processes. Specifically, we explore (1) how DOM concentrations and composition change from the soil to the tributaries and along the stream to the catchment outlet and (2) which factors control the spatial patterns and seasonal dynamics of DOC and DOM quality of these different ecosystem components.

The study is set in the Hydrological Open Air Laboratory (HOAL) Petzenkirchen (Blöschl et al., 2016), which has mainly agricultural land use, contains diverse flow paths (tile drainages, springs, saturation area flows) within a small area and is well instrumented. It is thus ideally suited for investigating the spatial and temporal variations of DOC concentrations and DOM quality from different land use units (arable, grassland, forest), the corresponding flow paths and instream DOC production. The focus is on base flow conditions as we were mainly interested in the seasonal pattern of instream DOM processing.

## 4.2 Material and Methods

### 4.2.1 Study area

The Hydrological Open Air Laboratory (HOAL) Petzenkirchen (Fig. 4.1) is situated in the western part of Lower Austria (48°9' N, 15°9' E) and has a size of 66 ha. The catchment is drained by the Seitengraben stream, which is 620 m long and has an average flow of 3.93 L s<sup>-1</sup>

(1990-2020). The stream is sustained by eleven tributaries, five of which are perennial (Sys4, Q1, Sys1, Sys2 and Sys3) and two are ephemeral (Frau1, Frau2). The tributaries collect water from different pathways. These include tile drainages from arable areas (Frau1 and Frau2), tile drainages from mixed areas (arable, grassland and forest) (inlet Sys4, Sys3), a tile drainage from the forest (Sys2) and groundwater springs (Q1, Sys1). During low flow episodes, most of the stream water originates from Sys4, the main inlet of the stream, followed by deep aquifer water from spring Q1 and tile drain Sys1. The remaining tributaries contribute only 18 % of the total flow during low flow episodes (Széles et al., 2018). The stream itself interacts with the groundwater, which enables water and nutrient exchange (Exner-Kittridge et al., 2016) and results in diurnal fluctuations of stream flow, caused by transpiration from the riparian vegetation (Széles et al., 2018).

Overall, 87% of the catchment area is arable land, 5% is grassland, 6% is forested and 2% is paved. The dominant soil types are Cambisols (56% of the area), Planosols (21%) and Anthrosols (17 %) (IUSS Working Group WRB. 2015). The climate is humid, with a mean annual temperature of 9.5 °C and a mean annual rainfall of 823 mm yr<sup>-1</sup> (1990–2014). Temperature, rainfall and rainfall intensity peak during summer. The elevation of the catchment ranges from 257 to 325m above sea level. The HOAL is jointly operated by the Federal Agency for Water Management and the Technical University of Vienna with the aim of studying catchment processes using data with high temporal and spatial resolution (Blöschl et al., 2016).

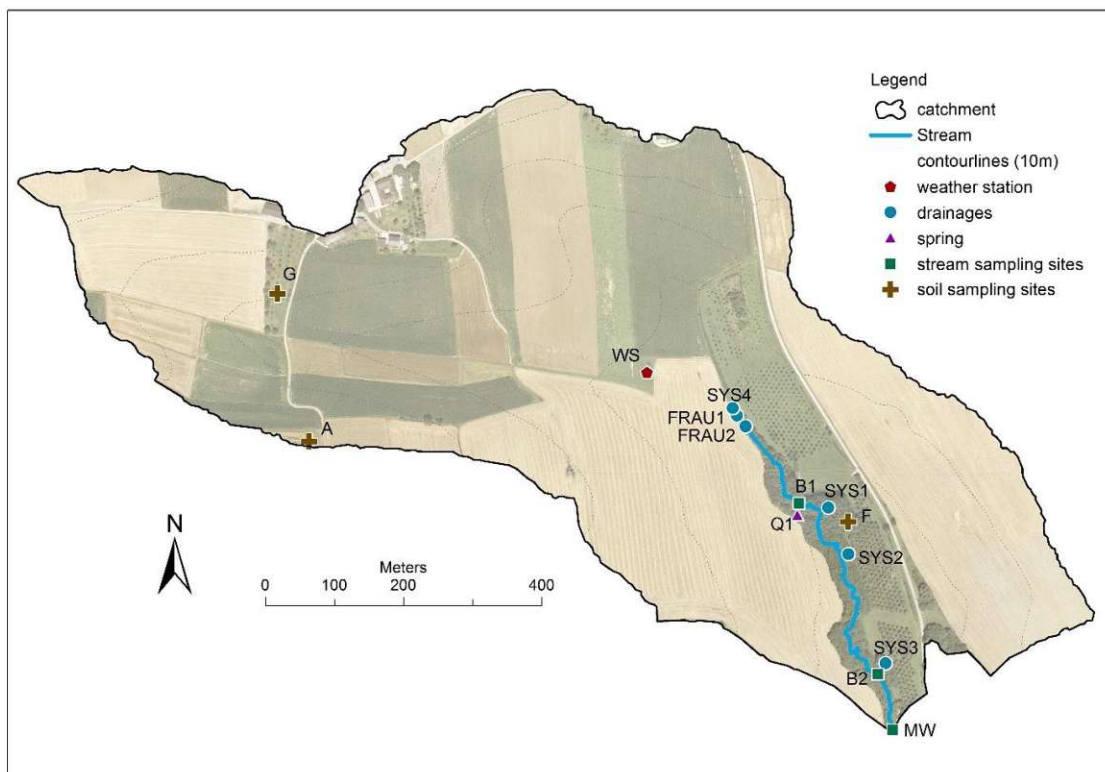


Fig. 4.1: The Hydrological Open Air Laboratory (HOAL) Petzenkirchen with sampling locations. Water sampling sites: tile drains (blue dots), springs (purple triangular) and stream (green quadrats). Soil sampling sites (brown crosses) indicate different land use units (grassland – G; arable land – A; forest –F).

### 4.2.2 Sampling, preparation and analyses

A sampling campaign was conducted during the period January to December in 2017. The year was dryer than normal with a precipitation of 707 mm yr<sup>-1</sup> compared to the long term mean of 785 mm yr<sup>-1</sup> (1990 to 2019).

Stream flow has been measured by calibrated stream gauges (H-flumes and V-notch weirs) in combination with pressure transducers and/or ultra-sonic devices at all relevant tributaries to the stream and at the catchment outlet since 2010 (Fig. 4.1) (Blöschl et al., 2016). Meteorological data are collected at a weather station located approximately in the centre of the catchment. Soil moisture is measured at 33 irregularly distributed sites at 10, 20, 30 and 50 cm depths; those nearest to the soil sampling sites within the same land use unit were used for the analyses.

The sampling strategy for the DOM analyses comprised three compartments. First, we took monthly soil samples from the top soil layer (0-5 cm) in three different land use units (arable, grassland and forest) to obtain information on the DOM sources. At each location we took three replicates, to minimise errors associated with the heterogeneous mixture of soil components and their non-uniform spatial distribution. Since the fluorescence-spectrometer analyses liquids, we produced an eluate from the soil samples. 40 ml of 0.5 mM K<sub>2</sub>SO<sub>4</sub> were added to 20 g of soils and shaken for half an hour at 20°C. After hydro-extraction at 3000 rpm for 15 min at 20°C, the samples were filtered through pre-combusted 0.45 µm glass-fibre filters.

Second, monthly water samples during low flow conditions were taken from all tributaries to the Seitengraben stream and the catchment outlet (MW). Third, additional samples were taken from the stream itself at B1 and B2 to divide the stream into three sections (Sys4 to B1, B1 to B2 and B2 to MW).

All water samples were divided into two parts. One part was used for the DOC/DOM quality analyses, which was immediately filtered through pre-combusted glass-fibre filters with a pore size of 0.7 µm to exclude further microbial activity. The second part was used for the chemical analyses (TOC, nitrate, ammonia, potassium, chloride, electric conductivity, pH-value and suspended sediment concentrations). The probes were stored at 4 °C and processed not later than 3 days after collection.

For the DOM quality analyses, we used spectrophotometric and spectrofluorometric methods. The absorbance measurement was conducted with an UV-VIS spectrometer (UV1700 Pharma Spec, Shimadzu Corporation) with a scanning range from 700 to 200 nm (Chin et al., 1994). Samples were placed in a 5 cm quartz window cuvette (Hella Analytics). Fluorescence was measured with a fluorescence spectrophotometer (Hitachi F-7000, Hitachi High-Technology Corporation) in a range from 250 to 600 nm in 5 nm increments. Due to a scan speed of 1500 nm min<sup>-1</sup> it took 15 min per sample to gather an emission-excitation matrix with a range of 200 to 450 nm for the excitation, and a range of 250 to 600 nm for the emission. Z-values of the matrix represent a light intensity, displayed in Raman Units. Each day, before the start of sample analyses, a sensitivity test with distilled water was performed (S/N Peak to Peak > 250, Drift <2 %). During the analyses, temperature was kept constant at 21 °C.

The Fluorescence and absorbance spectra of DOM were analysed using the “staRdom” package of R (version 3.5; R Core Team, 2020) (Pucher et al., 2019). We conducted a PARAFAC analysis

(Murphy et al., 2013; Pucher et al., 2019) and calculated fluorescence as well as absorbance indices to obtain DOM compositional parameters. We mainly used the relative contribution of the individual PARAFAC components to the total fluorescence gained from the PARAFAC model. The DOM quality analysis was complemented by determining the humification index (HIX; Zsolnay et al., 1999 - higher values indicate more humification) and the biological index (BIX, Huguet et al., 2009 - higher values indicate more autochthonous DOM production). Further we used the absorbance parameters SUVA<sub>254</sub> as a surrogate for aromaticity (Weishaar et al., 2003b) and quantified average molecular size by the peak ratio E2/E3 (Dalrymple et al., 2010). In total, we analysed 384 samples (271 water samples of the tributaries and the stream and 36 soil samples). Inner-filter effects of the fluorescence analysis were corrected, the results were converted to Raman Units, and Raman and Rayleigh scattering of first and second order were removed and interpolated. In the PARAFAC model, seven outliers were removed based on their leverage and later reintroduced in the model with fixed emission and excitation loadings. We verified the PARAFAC model using a split-half analysis and compared the components by Tucker's congruence coefficient (TCC = 0.963; Tucker, 1951). Component spectra were visually checked for plausibility. The final PARAFAC model ( $R^2 = 0.996$ ) resulted in 8 components (Tab. 4.1). The components' spectra were compared with findings from other studies using openfluor.org (Murphy et al., 2014).

Tab. 4.1: Emission and excitation peaks (both in nm) of components with their interpretation according to the literature. The code is used in the further text in addition to component number for better readability.

Component	Emission peak (nm)	Excitation peak(s) (nm)	Description	Code	References
C1	500	<245 (365)	humic-like fluorophore, derived from terrestrial material by photochemical degradation	hum	Murphy et al., 2014; Graeber et al., 2012
C2	436	<245 (340)	Humic-like, terrestrial, identical to syringaldehyde, associated with waters with high organic matter loadings	hum-ter	Murphy et al., 2014; Lambert et al., 2016-1; Peleato et al., 2016
C3	414	<245	humic-like, terrestrial, recalcitrant, very likely was indicative of transformation and degradation of DOM within the lakes	hum-rec	Osburn et al., 2017; Osburn et al., 2011; Osburn et al., 2015
C4	578	<245	Artifact from the fluorometer, has no ecologic implication	-	Yamashita et al., 2010-1; Murphy et al., 2008
C5	390	<245 (320)	humic-like, particularly at sites near terrestrial sources	hum-mic	Murphy et al., 2014; Osburn et al., 2015
C6	340	300 (<245)	protein-like, similar to free and protein bound amino acids tryptophan-like, generated by both microbial communities, periphyton and leachates from higher plants	tryp	Stedmod et al., 2007-1; Murphy et al., 2006; Stedmod et al., 2007-2; Yamashita et al., 2010-2;
C7	334	280	protein-like, tyrosine-like;	tyr	Murphy et al., 2006; Huarong Y et al., 2015; Yamashita et al., 2011
C8	410	300 (<245)	microbial-derived, humic-like, relatively aliphatic, low molecular weight	hum-lab	Lambert et al., 2016-2; Podgorsky et al., 2018;

### 4.2.3 Definition of base flow conditions

Since the focus of the study was on evaluating the seasonal patterns of instream processes rather than events, only periods with baseflow conditions were examined. To identify such periods, a recursive digital filter (Arnold et al., 1995; Nathan and McMahon, 1990) was applied to the streamflow time series of MW on an hourly basis:

$$Q'_t = \beta \cdot Q'_{t-1} + \frac{1+\beta}{2} \cdot (Q_t - Q_{t-1}) \quad (4.1)$$

where  $Q'_t$  is the filtered quick flow (event water) at time step  $t$ . Time steps with  $Q'_t \leq 0$  are considered baseflow conditions.  $Q_t$  is the original stream flow of MW at time step  $t$ . The filter parameter  $\beta$  was set to 0.95 after visual data inspection, to reflect typical subsurface response of the catchment (Eder et al., 2010; Exner-Kittridge et al., 2016).

#### 4.2.4 Exfiltration-infiltration model

In order to estimate the DOC production in the stream, an infiltration model was setup that accounts for diffuse DOC inputs and losses due to water exchange with the subsurface. For each time step of one hour, DOC mass balance gives:

$$F_{prod} = F_{MW} - \sum_{i=1}^n F_i - F_{diff} \quad (4.2)$$

where  $F_{prod}$  is the instream DOC production ( $\text{g h}^{-1}$ , positive if DOC is produced),  $F_{MW}$  is the measured DOC flux at the catchment outlet,  $F_i$  is the measured DOC input flux from tributary  $i$ ,  $n$  is the number of tributaries ( $n=7$ ), and  $F_{diff}$  is the diffusive DOC flux from the groundwater to the stream.

The DOC input flux from the tributaries was estimated as the product of DOC concentrations and stream flow at a time interval of 1 minute. Since DOC concentrations were only measured 12 times during the study period while stream flow was measured every minute, we established a regression between DOC concentrations and the logarithm of flow for each tributary, in order to account for DOC variability between the sampling. These regressions included data from measurements during rainfall-runoff events (data not presented in this study) to render the relationships more robust.

The diffuse DOC flux  $F_{diff}$  was estimated as

$$F_{diff} = Q_{diff} \cdot C_{diff} \quad (4.3)$$

where  $Q_{diff}$  is the diffusive exchange water flux (positive when water infiltrates from the groundwater to the stream) at time step  $t$ , and  $C_{diff}$  is its DOC concentration. Water mass balance for each time step gives

$$Q_{diff} = Q_{MW} - \sum_{i=1}^n Q_i \quad (4.4)$$

where  $Q_{MW}$  and  $Q_i$  are the measured flows at the catchment outlet and at tributary  $i$ , respectively. Evaporation was neglected because most of the stream is shaded by trees. Estimates of daily evaporation from the stream surface were less than 1000 litre per day and thus less than 1.6 percent of daily stream flow on the day with the lowest flow. Infiltrating water

( $Q_{diff} < 0$ ) was assumed to have the DOC concentration of the groundwater, i.e.  $C_{diff} = C_{GW}$  which was set to the mean concentration measured at spring Q1. Exfiltrating water ( $Q_{diff} > 0$ ) was assumed to have the average DOC concentration of the stream water which was estimated as the weighted mean of the DOC concentrations of the tributaries  $C_i$  as

$$C_{diff} = \frac{n}{\sum_{i=1}^n L_i \cdot \sum_{i=1}^n Q_i} \sum_{i=1}^n (Q_i \cdot C_i \cdot L_i) \quad 4.5$$

The weighting was by flow  $Q_i$  as well as by the flow length  $L_i$  from the confluence of the tributary  $i$  with the stream to the catchment outlet.

For the calculation of net production of the individual components (C1-C8) the same model was used but DOC concentrations were replaced by Raman units (RU) of the components. Additionally, instead of a correlation between flow rate and concentration, mean values of the RU at each tributary were used because of the low correlations between flow rate and RU.

## 4.3 Results

### 4.3.1 Spatiotemporal Variations of DOC

#### *Soil*

The lowest DOC values from soil eluate were measured at the arable land site with an annual mean of 0.9 mg L<sup>-1</sup> and a standard deviation of 0.17 mg L<sup>-1</sup> (Tab. 4.2) during the study period. Higher DOC concentrations were observed for the grassland site with a mean of 2.33 (±0.55) mg L<sup>-1</sup>. The forest site soil eluate showed the highest DOC concentrations (4.36 (±1.34) mg L<sup>-1</sup>) in line with the high organic carbon content of the forest soil. TOC contents were 2.0 (±0.35) g kg<sup>-1</sup>, 4.1 (±0.76) g kg<sup>-1</sup> and 9.2 (±0.88) g kg<sup>-1</sup> for the arable land, grassland and forest sites, respectively, suggesting a clear relationship between soil eluate DOC and TOC with a linear regression coefficient of  $r=0.97$ .

In general, soil eluate DOC concentrations varied seasonally, showing slightly increased concentrations at the grassland and forest sites during summer, and high peaks in all soils in October (Fig. 4.2). The peak was especially high in the forest, where DOC concentration almost doubled to the maximum DOC of 7.77 mg L<sup>-1</sup> (Fig. 4.2). This peak occurred at the onset of autumnal leaf fall.

In the arable field, monthly soil DOC changed little throughout the year. During the project period, winter barley was grown (seeding in October 2016) until the harvest in early July. In March and May, mineral fertilizer was applied (2 times 250 kg NAC ha<sup>-1</sup>, which equals 2 times 62.5 kg N ha<sup>-1</sup>). Pesticides were used in April (Husar: Iodosulfuron-Methyl-Natrium and Mefenpyr-Diethyl) and May (Aviator and Atlani: Prothioconazol, Bixafen). At the end of August, pig slurry was distributed on the arable field and incorporated before the seeding of catch crops. These management procedures did, however, not change the soil DOC concentrations much. The higher value in October cannot be directly attributed to any documented

management operation but it may be a delayed effect of the fertilization with pig slurry and its incorporation into the soil in August.

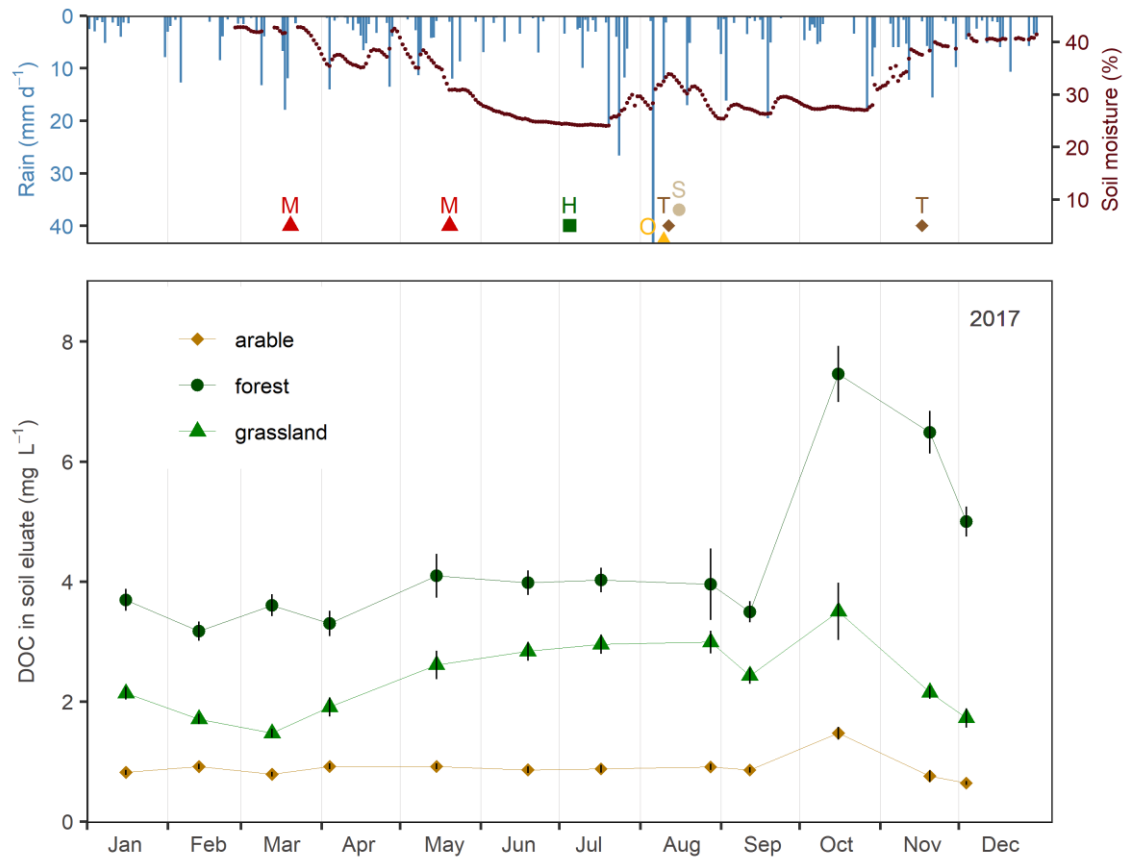


Fig. 4.2: Time series of daily rainfall, soil moisture in 5 cm depth at the arable field and management activities at the arable field (upper panel; M – mineral fertilizer, H – Harvesting, O – organic fertilizer, T – soil treatment, S - seeding). Lower panel shows seasonal fluctuations of DOC concentrations of soil eluate from the three different land uses: arable land (brown diamonds), grassland (green triangles) and forest (dark green circles). Symbols represent the mean of 3 measurements, bars the standard deviations (estimated from both the spatial variability of 3 replicates and the measurement uncertainty of the laboratory device). The first three points (January to March) represent pooled samples, so bars show measurement error only.

### Tributaries

The DOC concentrations of the tributaries show an opposite seasonal variation compared to the soil eluates with the highest concentrations in winter (Fig. 4.3). During base flow conditions, the DOC concentrations from the tributaries ranged between 1.5 and 4.9 mg L<sup>-1</sup>. The highest concentrations were measured in the tributaries that drain the arable land with mean DOC concentrations of 2.8 ± 0.71 mg L<sup>-1</sup> (Frau1) and 2.3 ± 0.66 mg L<sup>-1</sup> (Frau2). DOC concentrations were lowest for the spring Q1 that is groundwater fed (1.50 ± 0.43 mg L<sup>-1</sup>) and Sys4 that has some groundwater contribution (1.55 ± 0.44 mg L<sup>-1</sup>). Surprisingly, the DOC concentrations of Sys2, which drains the forest with the highest DOC in soil eluate, were also low (1.59 ± 0.48 mg L<sup>-1</sup>). During the summer, the DOC concentrations in the tributaries decreased on average by 25% compared to the winter half year.

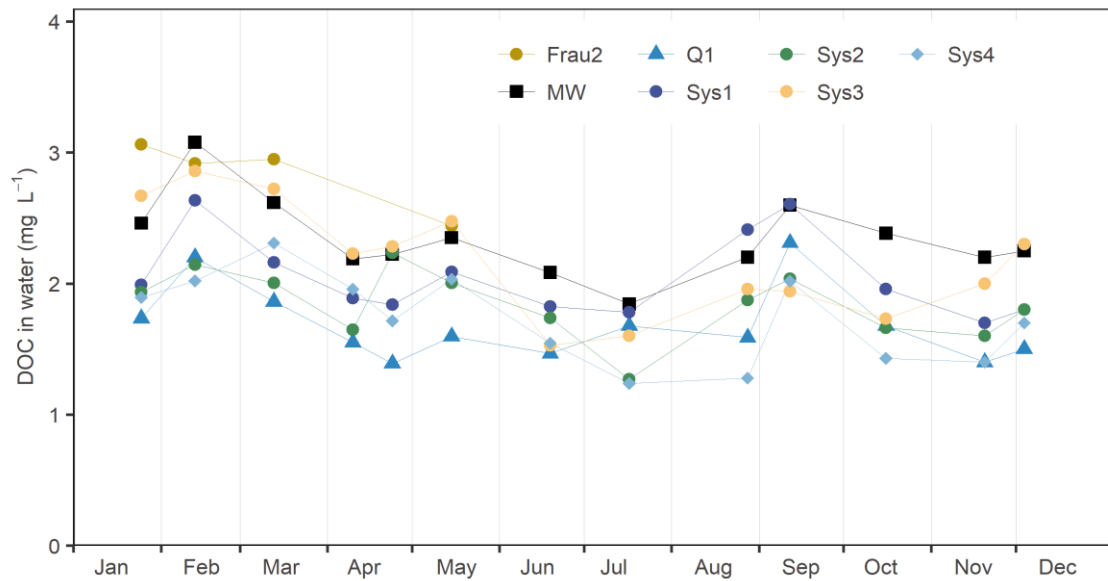


Fig. 4.3: Seasonal fluctuations of DOC concentration for the tributaries and the catchment outlet (MW). The measurement error is 4%, thus is smaller than the symbols. Flow from tile drain draining the arable field (Frau2) only occurred from January to March and in May.

As mentioned earlier, the tributaries show a contrasting seasonal DOC pattern to those of the soil eluates. The flow paths and their sources are well known for the HOAL Petzenkirchen because of the detailed monitoring of all tributaries since 2010 (Blöschl et al., 2016) and additional, hypothesis-driven studies with focus on sediment transport (Eder et al., 2014, 2010), nitrogen transport including groundwater interactions (Exner-Kittridge et al., 2016) and transpiration effects during low flow conditions (Széles et al., 2018). Based on the results of the previous studies and historic drainage maps, it is very likely that Frau1 and Frau2 drain the arable land use unit. While the soil sampling was not conducted in the same field because of logistic reasons, it was conducted in a field where both management and soil type are identical to those of the field drained by the tile drains. Also, the fields are spatially rather uniform in terms of soil characteristics. It was therefore assumed that the soil samples of the arable site are also representative of the area draining Frau1 and Frau2. Sys2 mainly drains the area around the forest on the left bank of the stream and also immediately responds to rainfall.

The comparison of the DOC concentrations of the arable and forest sites and the associated tributaries (arable associated with Frau1 and Frau2, forest associated with Sys2) shows that DOC concentrations in the soil are not aligned with those in the tributaries. At the arable site, the mean DOC concentration of the soil eluate was  $0.87 \text{ mg L}^{-1}$ , but  $2.8$  and  $2.77 \text{ mg L}^{-1}$  in the corresponding tributaries Frau1 and Frau2. In the forest, the mean DOC concentration of the soil eluate was  $3.82 \text{ mg L}^{-1}$ , but  $1.84 \text{ mg L}^{-1}$  in the corresponding tributary Sys2.

Overall, the DOC of the six tributaries (and the stream) were more similar to each other than the DOC of the three land use sites. The mean over the study period ranged between  $1.3$  and  $3.5 \text{ mg L}^{-1}$  for the tributaries, while it ranged between  $0.5$  and  $4.5 \text{ mg L}^{-1}$  for the three soil sites. The temporal standard deviations of the tributaries (maximum standard deviation at Frau1,  $\pm 0.7 \text{ mg L}^{-1}$ ) were also smaller than those of the soil sites (maximum standard deviation in the forest,  $\pm 1.4 \text{ mg L}^{-1}$ ). Both the spatial and temporal patterns of the tributaries show smaller variations

than the soils, suggesting an important role of DOC turnover and buffering along the flow paths from the soil to the stream.

### 4.3.2 DOC: from the tributaries to the catchment outlet

#### *Hydrology and identification of baseflow conditions*

For evaluating budgets of water and DOC the period February 3<sup>rd</sup> to December 31<sup>st</sup> 2017 was used since streamflow data were missing in January 2017 due to frost damages of some pressure transducers. The mean flow at the catchment outlet (MW) in this period was 2.32 L s<sup>-1</sup> and thus less than its long term mean of 4.07 L s<sup>-1</sup>, indicating that the study period was drier than normal. The total flow volume was 85533 m<sup>3</sup>, of which 57570 m<sup>3</sup> (67%) left the catchment during base flow conditions, which occurred 88% of the time.

Over the entire period, the contribution of the inlet (Sys4) to the total flow volume at MW was 29 %. The highest proportion of the water originates from the spring Q1 (40 %). The left bank drainage systems contributed 31% (Sys1: 29%, Sys2: 7%, Sys3: 7%) whereas the right bank drainage systems delivered only about 5% (Frau 1: 0.1%, Frau 2: 5%). During baseflow, the total flow volume contributed by the tributaries was 18 % higher than the total flow volume measured at the catchment outlet, suggesting an important exfiltration flux into the groundwater. This may be related to the relatively dry conditions during the study period (2017) with low groundwater tables. For the period 2013-2015, which was much wetter, Széles et al. (2018) found that 37 % of the total flow volume measured at MW during low flow periods enters the stream laterally. Simultaneous grab control measurements of flow in 2017 confirmed the exfiltration.

#### *DOC mass balance*

As mentioned earlier, the DOC loads of the tributaries were calculated using a regression between flow and DOC concentration. Although the correlation coefficients and the slopes of the regressions varied between tributaries, we found clear relationships for all sites (correlation coefficients between 0.76 and 0.97). Exceptions are the spring Q1 and Frau2, where the correlation coefficients were smaller than 0.5 due to the small flow variability in Q1 and hysteresis effects in Frau2. We therefore used the mean DOC concentrations to calculate loads at Q1 and Frau2.

Although the tributaries draining the arable sites (Frau1 and Frau2) had the highest concentrations, they only made a minor contribution (7%) to the total DOC input of 124 kg (during Feb 3<sup>rd</sup> to Dec 31<sup>st</sup>) into the stream due to their low flow volume (Fig. 4.5). The highest DOC inputs into the stream occurred via the spring Q1 (35 kg DOC, 28 % of total DOC inputs) and Sys1 (34 kg, 28 %), because of their high discharge volumes (24 400 m<sup>3</sup> and 16 400 m<sup>3</sup>, 36 % and 24 % of total flow). The calculated DOC loads clearly show that the DOC inputs were mainly controlled by the flow volume of the respective tributaries (Fig. 4.4).

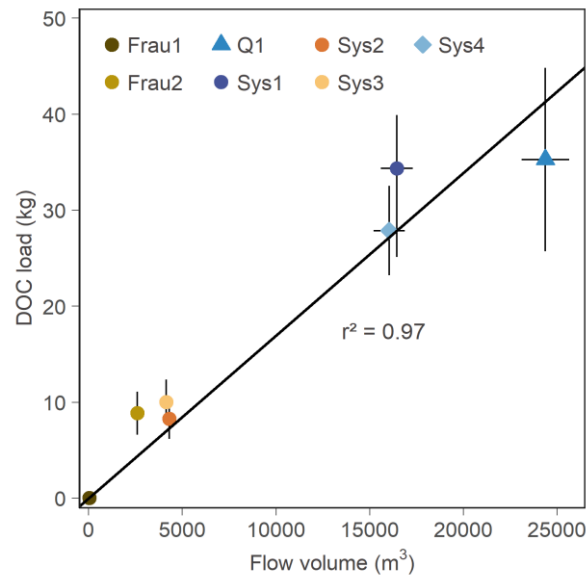


Fig. 4.4: Relationship between DOC load and flow volume for the tributaries during baseflow conditions, February 3rd to December 31st, 2017. Horizontal bars represent the standard deviation of the flow measurements, vertical bars the uncertainty of the DOC load estimation based on the standard errors of the regression coefficients for each tributary.

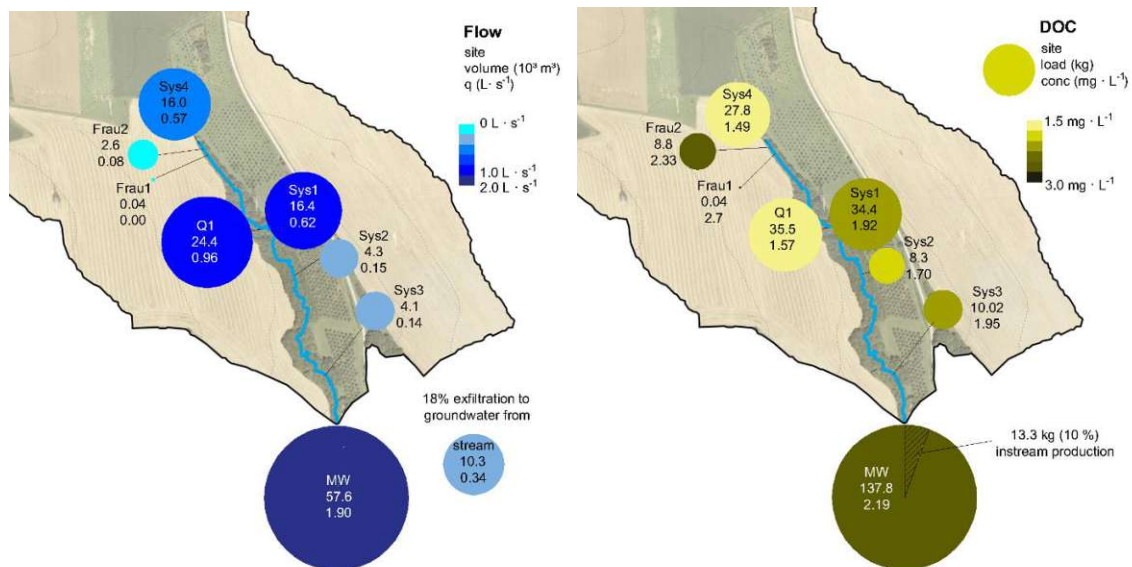


Fig. 4.5: Mass balance of flow (left) and DOC (right) during baseflow conditions from February 3rd to December 31st, 2017. Size of circles represents volume and load, respectively. Colours indicate mean specific discharge  $q$  (flow per area) and mean concentration. The circles at the catchment outlet (MW) represent the measured flow volume (left) and DOC load (right) and the resulting differences due to exfiltration to groundwater and instream DOC production.

### Instream DOC net production

Instream processes were evaluated by comparing the inputs from the tributaries and the outputs at the catchment outlet for both water volume and DOC loads. While over the period from February 3<sup>rd</sup> to December 31<sup>st</sup> 2017 a total loss of water of 10 300 m<sup>3</sup> was measured, there was a DOC load surplus at the catchment outlet of 13.3 kg (Fig. 4.5).

The exfiltration – infiltration model (Eq. 4.2-4.5) applied to the base flow data suggests that, from February 3<sup>rd</sup> to May 15<sup>th</sup>, 2017, 6900 m<sup>3</sup> water infiltrated into the stream and imported 10.4 kg of DOC. On the other hand, the measured water loss during the rest of the year was 17 300 m<sup>3</sup>, which led to an estimated DOC exfiltration of 27.2 kg DOC. The seasonal patterns of water and DOC exchange and the resulting DOC net production are given in Fig. 4.6. During the periods February 3<sup>rd</sup> to Mai 25<sup>th</sup> 2017 and November 20<sup>th</sup> to December 31<sup>st</sup> there was a DOC net production of 39 kg with a maximum production rate of 36 g DOC h<sup>-1</sup>. On May 25<sup>th</sup> the net production turned negative with a minimum of -9 g DOC h<sup>-1</sup>, indicating that more DOC was consumed (incorporated into microbial biomass or respired) than leached or secreted by algae within the stream. In July and August, the net consumption rate slightly increased to -4 g DOC h<sup>-1</sup>, but showed a second low at the beginning of October similar to the one in June (-8 g DOC h<sup>-1</sup>). On November 20<sup>th</sup>, the net production rate turned positive again. Whenever a rainfall runoff event occurred, it caused a temporary peak of DOC production.

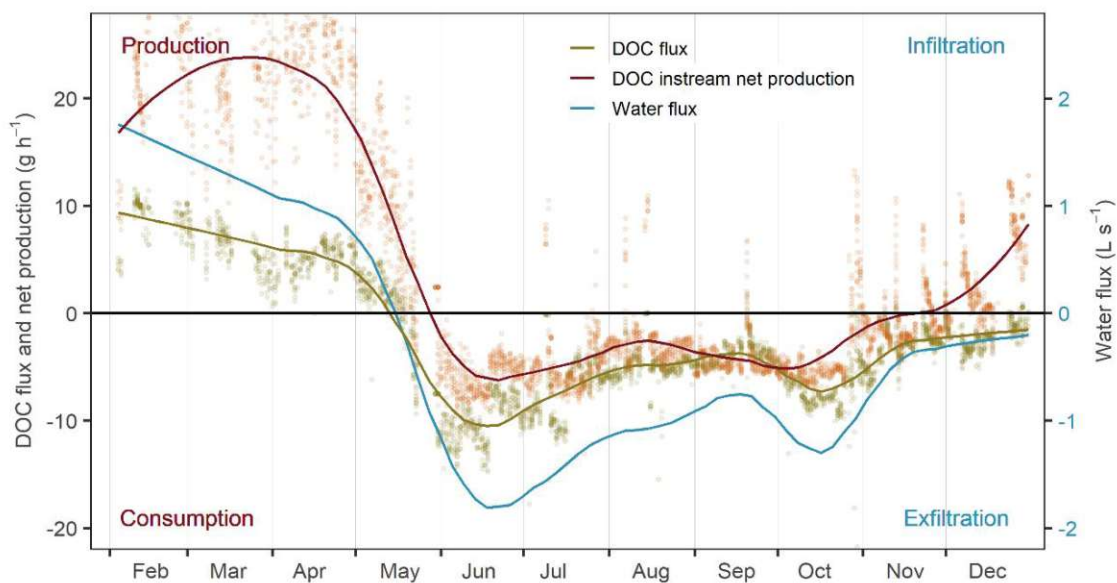


Fig. 4.6: Seasonal patterns (lines) of diffuse infiltration from groundwater to the stream and exfiltration from the stream to groundwater for water (L s<sup>-1</sup>, blue) and DOC fluxes (g h<sup>-1</sup>, green; calculated with the exfiltration-infiltration model) in 2017, from which instream DOC net production (g h<sup>-1</sup>, red) was estimated. The dots represent hourly values for DOC flux (green) and DOC net production (brown). The apparent scatter results from temporal variability and different response times to rainfall of individual tributaries.

### 4.3.3 Spatiotemporal variations of DOM Quality

#### Soil

On average over all soil samples, 68% of fluorescence was caused by refractory, humic-like fluorophores (C1-C3), 18% by protein-like fluorophores (C6 and C7) and 14 % by labile, humic-like fluorophores (C5 and C8), characterised by low molecular weight. Both, land use and season affected the DOM composition (Fig. 4.7). In summer, the forest site showed the highest proportion of refractory humic-like DOM (C1 to C3, 63%), followed by grassland (61%) and the arable site (57%). This decrease of the sum of these components from arable to forest is aligned with an increase of labile, humic-like fluorophores (C5 and C8). The proportion of labile humic-like DOM (C5 and C8) decreased from summer to winter for all land use units. The proportions of protein-like fluorophores (C6 and C7) were similar for all land use units in summer (15% to 16%), but in the winter half year, the mean contribution of C7 (protein-like, tyrosine-like) was 34%, while it was only 13% in summer.

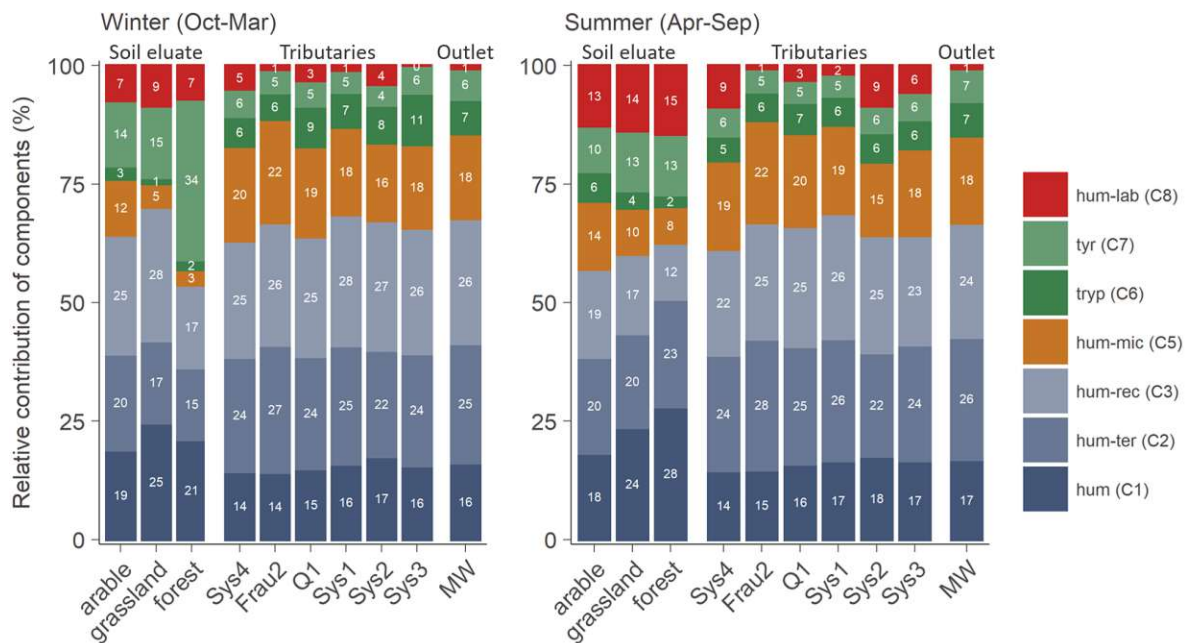


Fig. 4.7: Mean relative contribution of the DOM components to total fluorescence of soil eluates and water samples for the winter (left) and summer (right) half year. Blue: refractory, humic-like (C1-C3); brown: microbial derived, labile, humic-like (C5); green: proteins (tryptophan (C6) and tyrosin (C7)); red (C8): aliphatic with low molecular weight, labile, humic-like.

To understand the differences of the DOM quality of soil eluates at different land use sites, Spearman's rank correlation coefficient between the individual components and DOC concentration, soil temperature and soil moisture were calculated. Significant correlations were found between hum (C7) and DOC (Spearman's rank correlation coefficient  $r_s=0.90$ , significance level of  $p<0.001$ ), hum-lab (C8) and DOC ( $r_s=-0.78$ ,  $p <0.05$ ) and hum-mic (C5) and DOC ( $r_s=-0.73$ ,  $p <0.01$ ). Higher values for measured DOC in the soil eluate were associated with higher relative amounts of hum (C1), and lower relative amounts of hum-mic (C5) and hum-lab (C8) (Fig. 4.8, Panel A).

Soil temperature and soil moisture did not show a significant correlation with any of the components (C1-C8). However, soil temperature was correlated with aromaticity (SUVA, correlation coefficient  $r_s = -0.72$ ,  $p < 0.001$ ) and molecular size (E2/E3,  $r_s = 0.50$ ,  $p < 0.01$ ), indicating that higher temperature has led to less aromatic DOM with low molecular weight. The means of SUVA over the study period were highest at the arable site ( $11.4 \text{ L mg}^{-1} \text{ m}^{-1}$ ), intermediate at the grassland site ( $10.35 \text{ L mg}^{-1} \text{ m}^{-1}$ ), and lowest at the forest site ( $4.77 \text{ L mg}^{-1} \text{ m}^{-1}$ ), but the standard deviation was high for all three land use units (Tab. 4.2). On average over the study period, the molecular size was highest at the forest site (E2/E3=3.4), intermediate at the grassland site (E2/E3=4.6) and lowest at the arable site (E2/E3=4.8).

### *Tributaries*

At the tributaries, refractory humic-like fluorophores (C1 to C3) contributed between 62 % (Sys4) and 68 % (Sys1) to total fluorescence on average over the study period (Fig. 4.7). Protein-like fluorophores (C6 and C7) accounted for 11 % to 12 % of fluorescence for all tributaries with minor differences between the tributaries. Microbial derived, humic-like fluorophores (C5) contributed between 16% (Sys2) and 22 % (Frau2). The remaining 1 % to 7 % were C8, which is described as microbially derived, relatively aliphatic, humic-like fluorophores with low molecular weight. Relevant seasonal changes occur for tryp (C6) and hum-lab (C8); tryp (C6) is lower in summer, while hum-lab (C8) is lower in winter.

We calculated Spearman's rank correlation coefficient between the DOM quality of the tributaries and environmental parameters, in a similar way as for the soil data, but included additional water quality parameters such as nitrate and phosphate concentration. The main explanatory variables of DOM composition were found to be soil moisture in the catchment the tributary is draining, availability of nitrate in the streamflow of the tributary and DOC concentration. Soil moisture is positively correlated with the relative amounts of hum-rec (C3) and negatively with hum-lab (C8) of the tributaries (Fig. 4.8, Panel B). Nitrate was positively correlated with hum-lab (C8) only ( $r_s = 0.38$ ,  $p < 0.01$ ), while higher nitrate concentrations are associated with lower aromaticity (SUVA,  $r_s = -0.36$ ,  $p < 0.01$ ) and smaller molecular size of DOM (E2/E3,  $r_s = 0.55$ ,  $p < 0.001$ ). DOC concentration of the tributaries was positively correlated with hum-mic (C5,  $r_s = 0.38$ ,  $p < 0.01$ ) and negatively correlated with aromaticity (SUVA,  $r_s = -0.51$ ,  $p < 0.001$ ). It appears that increasing DOC concentration has led to less aromatic, labile DOM.

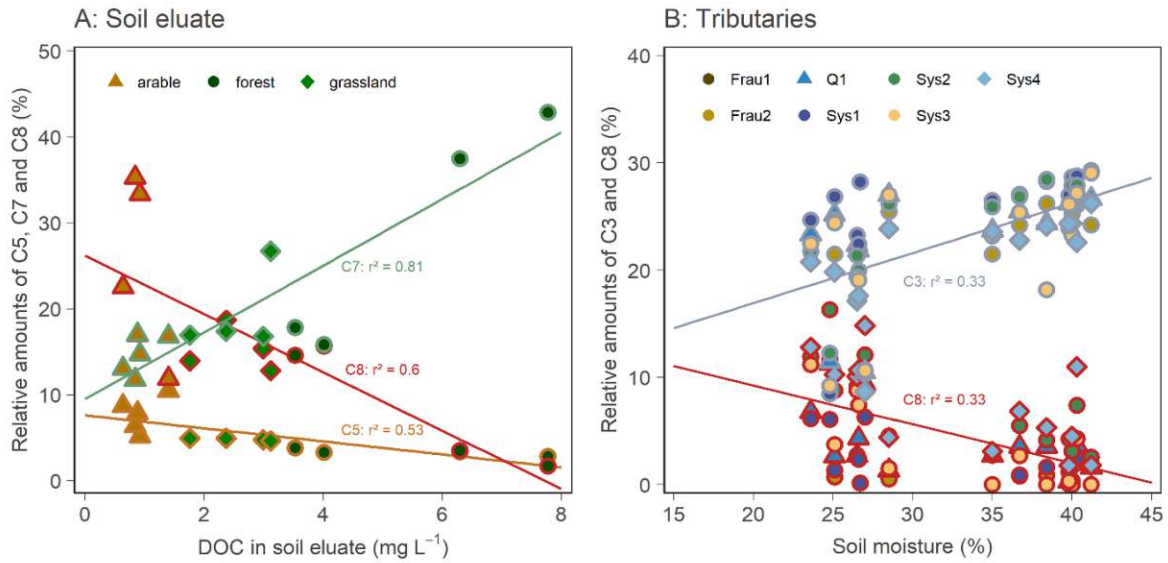


Fig. 4.8: Relative amounts of DOM components in the soil eluate in relation to soil DOC concentration (Panel A) and relative amounts of DOM components in the tributaries in relation to catchment soil moisture (Panel B). Symbols and colour of fill indicate the land use unit and the pathway, respectively. Colour of the symbol borders and regression lines indicate the DOM component.

Tab. 4.2: Mean concentrations of DOC and nitrate and mean values for DOM quality parameters (SUVA, HIX and BIX) including standard deviation for the individual sampling sites. Study period January to December 2017.

	DOC (mg L <sup>-1</sup> )	NO <sub>3</sub> (mg L <sup>-1</sup> )	SUVA (L mg <sup>-1</sup> m <sup>-1</sup> )	E2/E3 (-)	HIX (-)	BIX (-)	
Tributaries	Sys4	1.55 ± 0.44	42.5 ± 3.4	1.51 ± 0.77	7.3 ± 3.1	0.82 ± 0.13	0.89 ± 0.09
	Frau1	2.80 ± 0.71	57.5 ± 12.3	1.35 ± 0.17	7.0 ± 3.6	0.89 ± 0.01	0.90 ± 0.17
	Frau2	2.28 ± 0.67	31.2 ± 6.6	1.91 ± 0.62	7.6 ± 1.2	0.89 ± 0.03	0.89 ± 0.07
	Q1	1.50 ± 0.43	0.5 ± 0.3	3.16 ± 1.74	2.6 ± 1.4	0.84 ± 0.12	0.86 ± 0.05
	Sys1	1.87 ± 0.48	8.4 ± 3.3	2.08 ± 1.19	4.0 ± 1.5	0.84 ± 0.12	0.87 ± 0.11
	Sys2	1.59 ± 0.48	46.0 ± 3.1	1.61 ± 0.84	6.6 ± 1.9	0.83 ± 0.12	0.83 ± 0.05
	Sys3	1.92 ± 0.59	36.7 ± 6.0	1.57 ± 0.78	6.5 ± 2.3	0.79 ± 0.21	1.44 ± 1.68
	MW	2.08 ± 0.48	18.1 ± 4.0	1.96 ± 0.82	5.4 ± 1.7	0.79 ± 0.22	1.38 ± 1.58
Soil eluates	arable	0.90 ± 0.18		11.4 ± 12.7	4.8 ± 1.3	0.69 ± 0.15	1.04 ± 0.78
	grassland	2.33 ± 0.57		10.4 ± 11.5	4.6 ± 0.7	0.77 ± 0.08	0.75 ± 0.35
	fen	4.36 ± 1.41		4.8 ± 3.9	3.4 ± 1.8	0.79 ± 0.06	0.58 ± 0.13

#### 4.3.4 DOM quality: from source to catchment outlet

##### *Soil to tributaries*

The DOM quality differs between soil eluate and tributaries. While the proportions of the more refractory components C1-C3 are comparable between eluates and tributaries (except for the forest soil in winter), the proportions of the more labile fractions vary. The tributaries showed a higher relative proportion of hum-mic (C5, +159%) and trypt (C6, +84%) and a lower proportion of tyr (C7, -62%) and hum-lab (C8, -63%) than the soil eluates (Fig. 4.7). Besides, the seasonal variability of the DOM composition was much lower in the tributaries than in the eluates. Frau 2 (draining the arable field), Sys 1 (groundwater affected), and Sys3 (draining both arable and forested areas) showed lower proportions of hum-lab (C8) in winter than the other tributaries. The lowest seasonal variability occurs at the stream outlet (MW; Fig. 4.7). Similar to Frau 2 and Sys 1, the outlet was characterized by relatively low proportions of hum-lab (C8).

The humification index (HIX) increased from an average of 0.75 in the soil eluate to 0.84 in the tributaries. The ratio E2/E3 was higher in the drainage Frau2 (7.6), Frau1 (7.0) and Sys 2 (6.6) than in the soil eluates of the corresponding arable site (4.8) and forest (3.4) (Tab. 4.2).

##### *Tributaries to catchment outlet*

The instream processes of the individual DOM components were evaluated in an analogous way to DOC based on mass balance including exchanges with the aquifer due to exfiltration and infiltration. During the study period from February 3<sup>rd</sup> to December 31<sup>st</sup>, 2017, all DOM components apart from hum-lab (C8) showed a positive net production (Tab. 4.3). Only hum-lab (C8) was consumed, which almost completely disappeared at the catchment outlet.

Tab. 4.3: Measured flow volumes and calculated DOC and component loads (C1-C8) at the catchment outlet (MW) and as sum of all tributaries including standard deviation ( $\pm$ SD), and instream net production of DOC and the DOM components during the period of DOC net consumption (Mai 25<sup>th</sup> to November 20<sup>th</sup>) and during the period of DOC net production (February 3<sup>rd</sup> to May 24<sup>th</sup> and November 21<sup>st</sup> to December 31<sup>st</sup>, 2017) during baseflow conditions. The calculation of instream net DOC production includes inputs and losses due to water exchange with groundwater based on the Exfiltration-Infiltration model.

	MW	$\Sigma$ Tributaries	Instream production (+) and consumption (-)	
			period of net DOC consumption	period of net DOC production
Flow volume (m <sup>3</sup> )	57582 ( $\pm$ 3598)	67953 ( $\pm$ 2133)	-	-
DOC load (kg)	138 ( $\pm$ 14)	125 ( $\pm$ 15)	-12	+42
C1, hum (RU m <sup>3</sup> )	2462 ( $\pm$ 165)	2359 ( $\pm$ 77)	+183	+285
C2, hum-ter (RU m <sup>3</sup> )	3719 ( $\pm$ 355)	3728 ( $\pm$ 129)	+220	+337
C3, hum-rec (RU m <sup>3</sup> )	3627 ( $\pm$ 664)	3790 ( $\pm$ 458)	+143	+249
C5, hum-mic (RU m <sup>3</sup> )	2666 ( $\pm$ 490)	2885 ( $\pm$ 111)	+74	+123
C6, tyr (RU m <sup>3</sup> )	1064 ( $\pm$ 319)	958 ( $\pm$ 401)	+103	+154
C7, trypt (RU m <sup>3</sup> )	971 ( $\pm$ 670)	761 ( $\pm$ 108)	+144	+202
C8, hum-lab (RU m <sup>3</sup> )	97 ( $\pm$ 155)	508 ( $\pm$ 252)	-149	-211

In addition, changes of DOM quality along the stream were observed at two stream sections. The upstream section 1 was between Sys4 and B1 (190 m) and downstream section 2 between B2 and MW (96 m). For section 1 only periods without stream flow at Frau 1 and Frau 2 were compared. In both sections the relative contributions of hum (C1), hum-ter (C2), hum-rec (C3), tyr (C6) and tryf (C7) increased and hum-lab (C8) decreased according to the upper results provided in Tab. 4.3. Only hum-mic (C5) remained on the same level over the stream course. Molecular size (E2/E3) and aromaticity increased along the stream in both sections, indicating an increasing proportion of more refractory DOM components.

## 4.4 Discussion

### 4.4.1 Land use impacts on DOC and DOM quality

We observed a distinct impact of land use on the DOC concentrations in the soil eluate, showing a decrease from the forest to the grassland and the arable land. DOC concentrations were positively correlated with TOC as was also observed by others (Ghani et al., 2007; Khomutova et al., 2000; Ward et al., 2007; Zhang et al., 2007; Zsolnay, 1996). Marschner and Kalbitz (2003) and Stutter and Billett (2003) suggested that DOC equilibrates between the mobile aqueous phase and the immobile solid phase, indicating that higher TOC leads to higher DOC in the soil. Land use is an important factor controlling the TOC content in the soil and thus also affects DOC concentrations in the soil eluate. The same pattern of decreasing DOC concentrations from forest floor over grassland (A horizon) to arable land (A horizon) was found by Chantigny (2003).

In general, the DOC concentrations in the tributaries measured in the present study area (the HOAL Petzenkirchen) are relatively low, compared to other studies. Vidon et al. (2008) found similar concentrations in tile drains from arable land ( $2.28 \text{ mg L}^{-1}$ ) but almost twice the values in groundwater ( $4.34 \text{ mg L}^{-1}$  and  $3.60 \text{ mg L}^{-1}$ ) and the streams ( $4.78 \text{ mg L}^{-1}$  and  $4.85 \text{ mg L}^{-1}$ ). (Graeber et al., 2012) found even higher DOC concentrations in streams of agricultural catchments ( $7.6 \pm 2.8 \text{ mg L}^{-1}$ ), but forested catchments had approximately the same mean DOC concentration ( $1.5 \pm 0.9 \text{ mg L}^{-1}$ ) as measured in Sys2 draining the forest in the HOAL. Kalbitz et al. (2000) reported that DOM is strongly adsorbed to clay minerals in the mineral soil, resulting in low DOC output from these soils. This process may explain the generally low DOC concentrations in the HOAL where the soil mainly consists of heavy clay material.

Surprisingly, DOC concentrations in the tributaries showed an opposite pattern to the corresponding soils, with increasing DOC concentrations from the tributary draining the forest to the tributary draining the arable field despite similar flow volumes (Sys2 and Frau2 in Fig. 4.5). Higher DOC outputs from the arable fields may be caused by higher microbial degradation due to the surplus of nutrients by fertilization (Chantigny et al., 1999; Frank and Groffman, 2009) or due to soil treatments on the fields such as ploughing (Kalbitz et al., 2000; Steenwerth and Belina, 2008). Fertilizer application lead to a nitrogen surplus, increasing the decomposition rate of organic matter through an improved C/N ratio (Chantigny et al., 1999;

Enowashu et al., 2009; Frank and Groffman, 2009) and thus the potential leaching. The laboratory leaching experiments with soils of the HOAL Petzenkirchen by Tiefenbacher et al. (2020) found that fertilization with both mineral and organic fertilizers reduced DOC leaching for a few weeks. Compared to sandy soils from other regions, less DOC was leached from the clayey soils.

Beside the C/N ratio, the oxygen supply is important for decomposition processes to occur. Bueno and Ladha (2009) found that cultivation and the turnover of soils accelerate the decomposition of plant residues in soils by providing oxygen, thereby resulting also in increased DOM leaching. Tile drains may intensify this process due to the direct linkage of agricultural soils to streams and less retention of DOC in the soil (Blann et al., 2009). This could have been the case in our study area as the field is regularly ploughed and drained.

In addition, an accumulation of organic matter in deeper soil layers during dry periods is possible. During subsequent rain events, this organic matter is leached and may lead to increased DOC concentrations in the corresponding drainage pipes Frau 1 and Frau 2.

In our study, the DOM composition of the soil was only poorly correlated with the DOM composition in the corresponding tributaries. Specifically, the labile DOM fractions (C5-C8) in the soil eluates showed higher proportions of the protein-like components tryp (C6) and tyr (C7) and of the humic-like low-molecular hum-lab C8, while the tributaries were characterised by a higher proportion of the humic-like low-molecular hum-mic C5. Graeber et al. (2012) concluded that seemingly contradicting results from soil and stream studies imply that only a low percentage of the soil organic matter (SOM) lost from agricultural soils is transported to the streams as DOM or that DOM originating from agricultural SOM is rapidly taken up in streams. Besides, the DOM from terrestrial sources is usually subject to a variety of biological, physical, and chemical processes in the soil, which alter its composition (Baldock and Skjemstad, 2000; Qualls and Richardson, 2003; Silveira, 2005). Especially the heavy, clayey soils in the HOAL Petzenkirchen increase the retention time of the soil pore water, thereby altering the DOM composition. Tiefenbacher et al. (2020) also observed differences in DOM composition depending on soil texture. The shift from proteins (C6, C7) and hum-lab (C8) to hum-mic (C5) indicates that hum-mic (C5) is probably a product of the degradation of one of the other components. Such relationships between the degradation of one component and the production of another component have also been observed elsewhere (Pucher et al., 2021 - submitted; Casas - Ruiz et al., 2017; Weigelhofer et al., 2020). The strong modification of DOM during the soil passage in our study is also indicated by the increase of HIX and the strong decrease of SUVA<sub>254</sub> from soil to the tributaries. This is consistent with Fellman et al. (2009), who attributed the decrease of SUVA<sub>254</sub> values to the selective removal of non-aromatic fractions of DOM.

Another explanations for the different patterns of DOC and DOM quality in the soil eluate and the tributaries could be the fact that DOC concentrations of soil eluate represent a potential DOC (Tipping et al., 1999) rather than the material that is leached from the soil under natural conditions. The destruction of the soil aggregates during the analysis and the desorption of organic matter from mineral surfaces by K<sub>2</sub>SO<sub>4</sub> stimulate the leaching of soil organic matter

from the samples (Ewing et al., 2006; Ogle et al., 2005). Under conditions naturally met in the field, water from the fine pores is usually strongly bound and thus not available for transport.

#### 4.4.2 Temporal variations of DOC and DOM quality

We observed no clear influence of agricultural practices on the DOC content of the arable soil eluate. The DOC content in the upper soil layer of the arable fields did not vary much, evidently caused by the limited TOC content ( $2.0 \text{ g kg}^{-1}$ ) compared to grassland ( $4.1 \text{ g kg}^{-1}$ ) and forest ( $9.2 \text{ g kg}^{-1}$ ). Although Kalbitz et al. (2000) found a direct impact of agrotechnical practices on DOC in the arable surface soil layer, causing more frequent fluctuations in the DOC content, we did not observe such changes on an about monthly sampling interval. Similarly, Rosa and Debska (2018) found no direct effect of the organic/natural fertilization on the DOC content in a 2 year arable soil sampling campaign in Poland, and Chantigny (2003) stated that changes in DOC resulting from management activities are generally of short duration. Shorter sampling intervals may provide more detailed insight into this question.

However, we observed clear seasonal patterns in the forest and the grassland, with increased DOC concentrations during the warm summer months and a pronounced DOC peak in late autumn. Again, this pattern was not reflected by the tributaries. In contrast, the tributaries showed a general decline in DOC concentrations during summer, with a small peak in late summer (coinciding with a small decline in the DOC concentrations of the soil eluates) and a larger peak in January and February. These patterns may have been mainly driven by precipitation. The dry weather in summer may have led to an accumulation of potentially leachable organic matter within the soils, resulting also in smaller exports from the terrestrial sources to the tributaries. With increasing rain fall and subsequent increasing moisture content in late summer, part of the accumulated soil organic matter was probably washed out, thereby increasing the DOC concentrations of the tributaries. This may also explain the correlation between soil moisture and DOC concentrations in the tributaries. Soil moisture affects the physical, chemical, and biological processes along the transport of DOM through soil and thus influences DOM export to subsurface and drainage waters (Tiefenbacher et al., 2021; Bolan et al., 2011). It appears that higher soil moisture also stimulates microbial activity (Brockett et al., 2012), leading to the consumption of humic-like fluorophores with low molecular weight (C8) and an increase of the relative amounts of terrestrial, recalcitrant, humic-like components (C3). A relevant input of organic material and thus potentially leachable material is leaf litter in fall. This litter seems to have directly affected soil DOC concentration in the forest in addition to temperature induced seasonal variability. The same phenomenon with less intensity was also observed at the grassland site. These additional TOC inputs seem to be immediately leachable and a metabolizable nutrition for microbes, leading to higher DOC concentrations of the soil eluate. In a long-term litter manipulation experiment Kalbitz et al. (2007) found that a doubling of litter input instantaneously doubled the DOC concentrations. The DOC peak in the forest eluates was accompanied by an increase in protein-like fluorescence from 15 % in summer to 36 % in winter. Fellman et al. (2009) observed similar patterns for protein-like fluorescence at three soils in Alaska, where the relative contribution on total fluorescence decreased from 8 and 10 % in May to approximately 5 and 3 % in July and August. The lower level of protein-like

contribution compared to our results can be explained by the different climate in Alaska, with much colder temperatures and only 5 months of snow free season.

#### 4.4.3 Main drivers of DOC at the catchment outlet

The annual DOC inputs from the tributaries into the stream are largely controlled by water flow, while the DOC source plays a secondary role. Blann et al. (2009) found that the catchment export of DOC was larger with drainages due to higher proportion of total annual precipitation discharged to surface waters relative to the amount that is stored in the soil during the year, evaporated or transpired. However, different land uses affected the DOC export to the stream. The tributaries draining the arable land exhibited higher DOC concentrations than the tributaries draining the mixed or forested land use units.

An important DOC source is the stream itself. During baseflow conditions within the period of positive net production from November to May, instream processes caused 37 % of the total measured DOC load at the catchment outlet. The seasonal patterns of instream DOC production can be explained by changes of temperature, light and availability of nutrients. In March and April, the stream shows a peak in net DOC production. During this time, algae growth and thus primary production are high due to increasing water temperatures and availability of light, thus contributing to instream DOC production (Fasching et al., 2016). Similar short periods of autotrophic production have been observed in other headwater streams (Weigelhofer et al., 2012). In May, the stream gets shaded, leading to a breakdown of algal biomass and a decrease of primary DOC production. High water temperatures and nutrient availability control and stimulate bacterial activity, leading to an increase of instream net consumption due to carbon incorporation into microbial biomass and respiration (Demars et al., 2011; Hill et al., 2000; Rosemond et al., 2014). Interestingly, the stream becomes net productive again already in November, at a time when autotrophic activities are still low. We believe that this net DOC production in winter is mainly due to an increased leaching of leaves within the stream or at the banks (lateral DOC inputs not measured) and generally low heterotrophic activities due to low water temperatures.

Short rainfall runoff events in summer can lead to temporary peaks of net production during a period of general net consumption (shown in Fig. 4.6 by individual positive dots during summer). Such temporary peaks are probably due to lateral inputs of DOC from inundated bank areas and/or resuspension and mixing of stream bed material, encouraging instream leaching. In the same catchment, Eder et al. (2014) found that a small rise of stream water level increased transport capacity and caused the resuspension of bed sediments, which likely affects organic matter leaching. A rise of water level will also increase the water contact area for leaching.

Instream processes also alter DOM composition especially during baseflow (Fasching et al., 2016; Raymond et al., 2016). Hum-lab (C8) almost completely disappeared after 600 m of flow length. Molecular size (E2/E3) and aromaticity (SUVA<sub>254</sub>) increased along the stream indicating bacterial uptake of aliphatic, low molecular weight DOM. This is consistent with the findings of Fellman et al. (2009) for two rivers in Alaska where the protein-rich, labile fraction was selectively removed with passage downstream.

During the period February 3rd to December 31st, 2017, only small rainfall runoff events occurred and thus DOC instream balances were only calculated for baseflow. During high rainfall runoff events, import by tributaries, diffuse lateral inputs from the floodplain, and resuspension will gain in importance, while instream processes will be less significant (Fasching et al., 2016; Raymond et al., 2016). Besides, terrestrial DOM sources for the stream may change in importance.

## 4.5 Summary and Conclusions

Based on a sampling campaign conducted during 2017 in the HOAL Petzenkirchen in Lower Austria we draw the following conclusions:

The DOC concentrations of the soil eluates correlate positively with the TOC contents and are 5 and 1.5 times higher at the forest site and the grassland site, respectively, than at the arable land site. In summer, the soil eluate DOC concentration increases probably due to increased microbial activity and the related faster decomposition of organic material. Additional inputs of organic material such as leaf litter in autumn also increase the DOC concentrations in the soil eluate. In contrast to the soil eluate, the DOC concentrations of the tributaries are lower in summer, probably due to the lower hydraulic connectivity from the source to the tributaries. The strong temporal correlation between DOC load and total flow volume of all seven tributaries ( $r=0.91$ ) indicates that total DOC inputs into the stream are determined by hydrology (i.e. the water fluxes) and land use plays only a secondary role.

Land use and season affect the DOM quality of soil eluate. Leaf litter in winter causes an increase of protein-like DOM. At the tributaries, the impacts of land use and season on the DOM composition are neglectable as processes in the soil alter the DOM quality during transport from the terrestrial source to the stream. Soil moisture correlates with DOM quality, indicating that moisture drives organic matter processing and transport in the soil. High soil moisture leads to an increased share of refractory DOM components and a lower contribution of protein-like and labile humic-like components.

The study also demonstrates that methods of DOC and DOM quality sampling and processing in the soil and the stream are not necessarily comparable. While soil eluates are easy to obtain, they only represent a DOC and DOM quality potential. Even soil pore water collected in the field or from percolation experiments may not represent the DOC and DOM components actually entering the stream, as they are likely modified along the flow path.

Although the catchment of this study is small, relatively homogeneous and dominated by agriculture, the monitoring of the tributaries shows that small forest patches in the immediate vicinity of the stream may play a significant role in the DOC supply. Since flow volumes tend to vary more in space and time than DOC concentrations, the former are more important for determining total DOC loads. Thus, relationships between DOC and DOM quality in the stream and the dominating land use is hard to detect and probably do not fully represent the actual drivers of DOC input into streams. Furthermore, time lags between activities in the catchment and responses in the aquatic DOC need to be accounted for.

Our study also reveals the significance of instream processing of DOC and DOM components, including both production and degradation, complicating the detection of land use impacts and agricultural practises on aquatic carbon characteristics further. In the study period, instream processes increased total DOC export from the catchment by 24 % compared to the DOC inputs from the tributaries. From May 25th to November 20th, 2017, instream net DOC consumption was observed, leading to a loss of 12 kg DOC probably due to bacterial uptake and respiration. Instream processes also alter the DOM quality. The labile humic-like component C8 almost completely disappeared after 600 m of flow length. Molecular size (E2/E3) and aromaticity increased along the stream indicating bacterial uptake of aliphatic, low molecular weight DOM. Future work may be directed towards rainfall runoff events and their impact on DOC inputs from the fields into the stream and the consecutive stimulation of instream processes. Alternative methods for characterising soil DOC and DOM quality may allow the establishment of more direct links across scales. Furthermore, it would be of interest to examine the role of varying levels of DOC loads associated with different land uses for instream DOM processes in streams of different sizes and shapes.



Die approbierte gedruckte Originalversion dieser Dissertation ist an der TU Wien Bibliothek verfügbar.  
The approved original version of this doctoral thesis is available in print at TU Wien Bibliothek.

# Chapter 5

## Indirect nitrogen losses due to leaching

The present chapter corresponds to the following scientific publication in its original form:

*Eder A., G. Blöschl, F. Feichtinger, M. Herndl, G. Klammner, J., Hösch, E. Erhart and P. Strauss, 2015. „Indirect nitrogen losses of managed soils contributing to greenhouse emissions of agricultural areas in Austria: results from lysimeter studies”. Nutr Cycl Agroecosyst 101, pp. 351–364. <https://doi.org/10.1007/s10705-015-9682-9>*

### Abstract

A considerable share of greenhouse gas emissions, especially  $N_2O$ , is caused by agriculture, part of which can be attributed to indirect soil emissions via leaching and runoff. Countries have to report their annual emissions, which are usually calculated by using the default value of 0.3 for  $Frac_{LEACH}$ , a factor that represents the fraction of nitrogen losses compared to total nitrogen inputs and sources. In our study we used 22 lysimeters, covering a wide range of soils, climatic conditions and management practices in Austria, to evaluate nitrogen losses through leaching and to calculate  $Frac_{LEACH}$ . The terms of the nitrogen mass balance of the lysimeters were directly measured for several years. Both grassland and arable land plots gave significantly smaller values of  $Frac_{LEACH}$  than the default value. For grassland,  $Frac_{LEACH}$  values of only 0.02 were found which varied very little over the entire observation period. For arable sites,  $Frac_{LEACH}$  values were higher (around 0.25) and showed significant variability between years due to variations in crop rotation, fertilization rates, and yields.

### 5.1 Introduction

As part of the second commitment period of the Kyoto protocol, 37 countries have agreed to legally binding reductions in their greenhouse gas emissions. To be able to evaluate the progress in achieving the emission reduction goal, annual national inventory reports must be compiled and submitted to the United Nations Framework Convention on Climate Change (UNFCCC). The Intergovernmental Panel on Climate Change (IPCC), which was set up by the World Meteorological Organization (WMO) and the United Nations Environment Program (UNEP), established guidelines which provide internationally agreed methodologies intended for use by countries to calculate greenhouse gas inventories to report to the UNFCCC (IPCC 2006).

One of the listed greenhouse gases is nitrous oxide,  $N_2O$ , which has a global warming potential 296 times higher than carbon dioxide over a 100 year time scale. In Austria, the main sources of nitrous oxide emissions are agriculture, forestry and other land uses with a share of 59 % in the national total nitrous oxide emissions, although these sectors contribute only 9.1 % to the total Austrian greenhouse gas emissions (Environment Agency Austria 2013). 3.69 Gg  $N_2O$  were considered indirect soil emissions via nitrogen leaching, based on the Austrian National Inventory (Environment Agency Austria 2013). In Austria, manure, mineral fertilizer and plant residues are applied to soils, supplying nitrogen as a nutrient for plants. Depending on the environmental conditions, some of the nitrogen is leached as nitrate, nitrite or ammonia. These nitrogen losses can be calculated as a fraction of all nitrogen added to or mineralized in soils, a parameter that is termed  $Frac_{LEACH}$ . A part of the lost nitrogen is transformed to  $N_2O$ .

Mosier et al. (1998) suggested a value of 0.3 for  $Frac_{LEACH}$ , which is the value recommended in the IPCC Guidelines (IPCC 2000, 2006) as a default value. It was largely based on mass balance studies comparing agricultural nitrogen inputs to nitrogen recovered in rivers. According to the IPCC Guidelines 2006 (IPCC 2006)  $Frac_{LEACH}$  should be assumed as zero for dryland regions without irrigation where precipitation is lower than evapotranspiration throughout most of the year and leaching is unlikely to occur. In humid regions  $Frac_{LEACH}$  should range from 0.1 to 0.8 depending on agricultural practices. Lower values than 0.3 for  $Frac_{LEACH}$  can be used if more specific data are available (IPCC 2006). Many countries established country-specific values since research studies usually demonstrate lower values of  $Frac_{LEACH}$  (Tab. 5.1). For example, farm scale studies and larger, catchment based studies in Ireland suggest that approximately ten percent of all applied nitrogen is lost through leaching, i.e.  $Frac_{LEACH} = 0.1$  (Environment Protection Agency Ireland 2011; Del Prado et al. 2006; Ryan et al. 2006; Neill 1989).

Tab. 5.1:  $Frac_{LEACH}$  values smaller than default (0.3) and countries of use

Country	$Frac_{LEACH}$
Belgium	0.12
Canada	0.18
Finland	0.15
Ireland	0.10
Kazakhstan	0.06
Liechtenstein	0.20
Netherlands	0.12
New Zealand	0.07
Norway	0.18
Slovakia	0.14
Switzerland	0.20
Ukraine	0.21

Thomas et al. (2005) found that a  $Frac_{LEACH}$  value of 0.07 is appropriate for New Zealand's dairy and sheep farming systems. In contrast, the calculates for New Zealand's arable and intensive vegetable systems are close to the IPCC default value of 0.3. Switzerland and Liechtenstein use a  $Frac_{LEACH}$  of 0.2, based on Prasuhn and Braun (1994), Braun et al. (1994) and Prasuhn and Mohni (2003) where long-term monitoring and modelling studies were conducted in the canton of Bern.

In Austria, the default value of 0.3 has so far been used as no accurate calculations have been available. However, in the light of the studies in other countries there is reason to believe that this value overcalculates the actual fraction of indirect soil emissions. The purpose of this paper therefore is to calculate values of  $Frac_{LEACH}$  for different land uses and management practices in Austria in order to obtain reliable but upper bound calculates for the entire country.

One attractive way of estimating nitrogen leaching are lysimeters (Kroeze et al. 2003; Williamson et al. 1998; Scholefield et al. 1993; Chichester 1977). In fact, the use of direct lysimetry methods (as opposed to model calculates based on measured water content and soil water tension in different horizons) has increased in popularity in Europe in recent years due to its relatively better accuracy for long term calculations (von Unold and Fank 2008). In Austria various lysimeters are operated on both grassland and crop land which are used here to calculate the nitrogen losses.

## 5.2 Methodology

The IPCC 'Tier 1' method provides a calculation method for estimating  $N_2O$  emissions from leaching and runoff (Eq. 5.1)

$$N_2O_{(L)} - N = (F_{SN} + F_{ON} + F_{PRP} + F_{CR} + F_{SOM}) \cdot Frac_{LEACH} \cdot EF_5 \quad (5.1)$$

where  $N_2O_{(L)} - N$  is the annual amount of  $N_2O$  nitrogen produced by leaching and runoff of nitrogen additions to managed soils ( $kg\ yr^{-1}$ ),  $F_{SN}$  is the annual amount of mineral fertilizer nitrogen applied to soils ( $kg\ yr^{-1}$ ),  $F_{ON}$  is the annual amount of managed animal manure, compost, sewage sludge and other organic nitrogen additions applied to soils ( $kg\ yr^{-1}$ ),  $F_{PRP}$  is the annual amount of urine and dung nitrogen deposited by grazing animals ( $kg\ yr^{-1}$ ),  $F_{CR}$  is the amount of nitrogen in crop residues (above and below ground, including nitrogen fixing crops, and from forage/pasture renewal, returned to soils annually ( $kg\ yr^{-1}$ ),  $F_{SOM}$  is the annual amount of nitrogen mineralised in soils associated with loss of soil carbon from soil organic matter as a result of changes in land use or land management ( $kg\ yr^{-1}$ ),  $Frac_{LEACH}$  is the fraction of all nitrogen added to or mineralised in managed soils that is lost through leaching and runoff in ( $kg\ kg^{-1}$ ) and  $EF_5$  is the emission factor for  $N_2O$  emissions from nitrogen leaching and runoff ( $kg\ kg^{-1}$ ).

In total, 22 lysimeter at seven sites in Austria were used for the mass balance studies in this paper. We use the term lysimeter for a container, filled with disturbed or undisturbed soil, where percolating water is collected either gravimetrically or through suction racks with a negative soil water pressure head ([www.lysimeter.at](http://www.lysimeter.at)). Limitations of lysimeters usually are their inability to deal with lateral pathways of water flow.

The individual terms of Eq. 5.1 were measured as part of the lysimeter setup (Fig. 5.1). In our study, only the ratio of nitrogen leaching losses to the total N inputs was of interest, so no conversion to nitrous oxide was required. No grazing was executed and thus no N inputs of urine and dung ( $F_{PRP}$ ) needs to be taken into account. For our study,  $F_{SOM}$  was kept constant

because no conversion from grassland or forest to arable land was performed and organic carbon content was assumed constant over the observation period. Following our assumptions Eq. 5.1 can then be rewritten in terms of directly measurable quantities (Eq. 5.2).

$$Frac_{LEACH} = N_{(L)} / (F_{SN} + F_{ON} + F_{CR}) \quad (5.2)$$

where  $N(L)$  are the nitrogen losses through leaching. The terms of Eq. 5.2 were calculated from the quantity and quality of the leaching water at the individual sites.

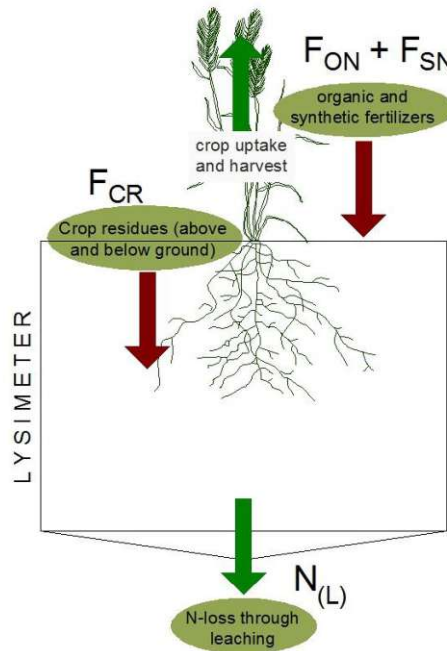


Fig. 5.1: Measured quantities of the nitrogen inputs and outputs (ellipses) of the lysimeters (see Equation 2). Crop uptake and harvest are needed for estimating  $F_{CR}$ .

14 out of the 22 lysimeters are located on arable land. The remaining eight lysimeters are located on grassland. They cover a wide range of soils, climatic conditions and management practices typical of Austrian agricultural land (Fig. 5.2). At some sites more than one lysimeter was available with differences in soil type, land use or land management.

The various lysimeter sites are maintained by different organisations. Therefore, the sizes and measuring principles differ. At some sites, a suction rack is placed at the bottom and used for water collection; at other sites a simple gravity collection of seepage water is performed. Some lysimeters have been filled with disturbed soil at their installation; some are built up of undisturbed soil monoliths. A further distinction is soil depth and therefore the depth of water collection. The terms of the mass balance equation (Eq. 5.2) are all measured and can be used for estimating  $Frac_{LEACH}$ . An exception is  $F_{CR}$ , the plant residues. Because below ground plant residues are not determined every year at each site. They were obtained according to the IPCC guidelines by calculating the root mass as a fraction of yield at sites and years of missing data. Above ground residues are measured at most sites. Root mass as well as N-content of crops was calculated according to IPCC guidelines.

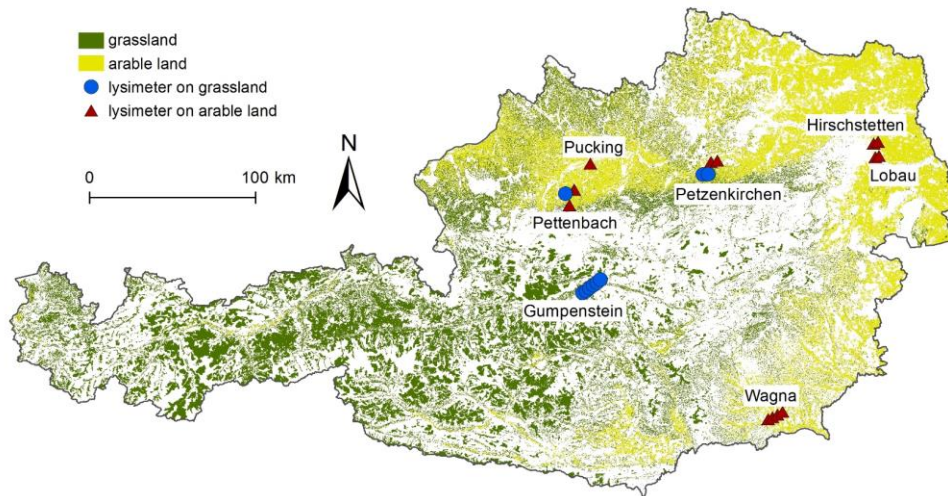


Fig. 5.2: Lysimeter sites and agricultural land use in Austria. Circles show sites on grass land, whereas triangles represent sites on crop land.

### 5.2.1 Site description

The key data of the lysimeter sites are summarized in Tab. 5.2. The description contains number of lysimeters at the site, year of installation, duration of measurement and installation method, surface area, sampling depth and sampling strategy, land use and fertilization, and - if necessary - important site-specific notes.

#### *Petzenkirchen*

In Petzenkirchen two undisturbed lysimeters (Petz and Petz<sub>syn</sub>) were installed in 1989 and operated until 2001. The lysimeters are located at 245 m a.s.l. on a low terrace of the River 'Große Erlauf', soil type is Eutric Cambisol (WRB 2006) from fine sediments above gravel. Typically, the ground water table is four to five meters below surface. Surface area is 0.35 m<sup>2</sup> and seepage water is collected at a depth of 110 cm under gravity conditions and analysed for nitrate and ammonia on a weekly basis (Feichtinger et al. 2004). At the Petzenkirchen site, arable land was turned to fallow in August 1994. On the Petz<sub>syn</sub> site only mineral fertilizer was applied whereas on the Petz site mainly organic fertilizer was used with supplement of mineral fertilizer on demand. In 1995 both lysimeters were converted to fallow management with two cuts a year. Due to the change in land use we split the time series into two periods (1990–1994: Petz 1 and Petz<sub>syn</sub> 1; 1996–2001: Petz 2 and Petz<sub>syn</sub> 2). The year after the change (1995) was not included in the calculation; the effects on nitrogen leaching of the land use changes are discussed in the results section.

Tab. 5.2: Overview of the lysimeter sites used in this paper. Rainfall (P), annual leaching (L), surface area, sampling depth (z), lysimeter type, sampling strategy, soil types and land use are shown.

Site	P (mm yr <sup>-1</sup> )	L (mm yr <sup>-1</sup> )	Surface area (m <sup>2</sup> )	z (cm)	Type	Sampling	Soil type	Land use
Petz 1	723	208	0.35	110	undis.	gravity	Eutric Cambisol	Arable land
Petz <sub>syn</sub> 1	723	297	0.35	110	undis.	gravity	Eutric Cambisol	
Wag <sub>con</sub> 1	914	340	1	70	disturbed	gravity	Dystric Cambisol	Grassland
Wag <sub>con</sub> 2	914	351	1	200	undis.	suction	Dystric Cambisol	
Wag <sub>bio</sub> 1	914	228	1	110	disturbed	gravity	Dystric Cambisol	
Wag <sub>bio</sub> 2	914	337	1	200	undis.	suction	Dystric Cambisol	
Peba 1	1030	307	1	150	undis.	suction	Eutric Cambisol	
Peba 3	1030	362	1	150	undis.	suction	Orthic Luvisol	
Puck 1	753	339	1	150	undis.	suction	Eutric Cambisol	
Lob 1	534	120	1	150	undis.	gravity	Calcaric Fluvisol	
Lob 2	534	120	1	150	undis.	gravity	Calcaric Fluvisol	
Lob 3	534	120	1	150	undis.	gravity	Calcaric Fluvisol	
Hir <sub>s</sub>	520	120	2	250	disturbed	gravity	Chernozem	
Hir <sub>t</sub>	520	120	2	250	disturbed	gravity	Chernozem	
Petz 2	723	173	0.35	110	undis.	gravity	Eutric Cambisol	Grassland
Petz <sub>syn</sub> 2	723	222	0.35	110	undis.	gravity	Eutric Cambisol	
Peba 2	1030	446	1	150	undis.	suction	Eutric Cambisol	
Gump 1	1013	464	1	150	undis.	gravity	Dystric Cambisol	
Gump 2	1013	584	1	150	undis.	gravity	Dystric Cambisol	
Gump 3	1013	1068	1	150	undis.	gravity	Dystric Cambisol	
Gump 4	1013	499	1	150	undis.	gravity	Dystric Cambisol	
Gump 5	1013	508	1	150	undis.	gravity	Dystric Cambisol	

### Wagna

In Wagna two lysimeters were filled in 1989. In 2004, the lysimeter station was renewed and both gravity lysimeters were replaced by undisturbed lysimeters with adjustable suction racks at the bottom (von Unold and Fank 2008). The applied matric potential at the lysimeter bottoms equal the measured matric potential in the undisturbed soil beside the lysimeters. Surface area is 1 m<sup>2</sup> and soil type is Dystric Cambisol on a terrace of Würm ice age. Before the renewal of the lysimeters, seepage water was collected at a depth of 70 and 110 cm, respectively. In 2004 the collection depth was transferred to 2 m. The ground water table is approximately at a depth of 4 m. Management was adapted in order to understand the impact of agricultural practices in three phases. First, the typical crop rotation maize–maize–winter cereal–winter rape was investigated with respect to a regional yield increase. Since 1998 the reduction of N-fertilizers became the primary topic of interest due to increasing nitrate concentrations in the Murtal aquifer. The Murtal aquifer is a significant resource for regional drinking water supply. From 1998, no fertilisation was applied in fall. Additionally, oil pumpkin became more and more attractive in the region. Therefore, oil pumpkin replaced winter rape in the crop rotation. One of the new lysimeters (after 2004) was run according to the guidelines for low N-input farming (BMLFUW 2006), the other one was run according to the guidelines for organic farming (EC 1991). Unfortunately, the biomass of catch crops was not recorded. Left on the fields they add to the mineralisation pool and have to be taken into account for the mass balance (Klammler and Fank 2014). For this reason, the biomass of the catch crop was modelled with Simwaser (Stenitzer 1988), a physically based model that simulates the interplay of soil water and crop development. The model was calibrated on seepage water and crop yield. The time series of Wagna was also split into two periods according to the renovation works and change of

management strategy in 2004 (1990–2003: Wag<sub>con</sub> 1 and Wag<sub>bio</sub> 1; 2005–2012: Wag<sub>con</sub> 2 and Wag<sub>bio</sub> 2).

### *Pettenbach*

In Pettenbach three undisturbed lysimeters were installed in 1995. The identical lysimeters have a surface area of one square meter and are installed at an altitude between 426 and 455 m a.s.l. on deep Eutric Cambisols (Peba 1 and Peba 2) and Ortic Luvisol (Peba 3). Water is collected at a depth of 1.5 m with a double strategy. Free draining water is measured with a tipping bucket. Additionally, a suction rack with a negative potential of approximately field capacity (60 cm water column) gives results that are more typical of field conditions (Murer 2002). The fields where the lysimeters are installed are managed by different farmers. Two of them are placed on arable land (Peba 1 and Peba 3), one is placed on grassland (Peba 2) and the management follows local practice. Additionally to the animal slurry, mineral fertilizer was applied to the Peba 1 site. Peba 2 was subject to the same fertilizer management but was used as grassland. At the Peba 3 site, organic and mineral fertilizer was applied until 1999. Later, only mineral fertilizer was used.

### *Pucking*

In Pucking (Puck 1) a lysimeter identical in size, shape, sampling strategy and depth to those at Pettenbach site was installed in 1995 at an altitude of 288 m a.s.l. The significant difference to the lysimeters in Pettenbach is the very shallow soil (rooting depth of 60 cm). The soil type is an Eutric Cambisol. The field is used as arable land and nitrogen is applied in form of biogas slurry.

### *Gumpenstein*

At site Gumpenstein, five identical lysimeters are in use since 2000 (Herndl et al. 2013). The undisturbed lysimeters are built of Eutric Cambisol on fluvial glacial sediments and have a surface of one square meter. Seepage water is collected in a depth of 1.5 m under gravimetric potential. The application of organic fertilizers from cow excrements was done as slurry and manure and the amount was based on local practice. No mineral fertilizer was applied. The number of cuts depends on the amount of fertilizer added with increasing amount of nitrogen added and number of cuts from Gump 1 to Gump 5.

### *Lobau*

In the Western Marchfeld area, an intensively used agricultural region, three undisturbed lysimeters with a surface area of one square meter has been constructed in 1998. The soil is a Calcaric Fluvisol. Both measuring principles (gravity and suction rack) are used for water collection on a biweekly basis in a depth of 1.5 m. The ground water table is about 2.2–3 m below the surface and may influence the soil water budget in the natural surroundings of the lysimeters. However, the bottom of the lysimeters disconnects the water transfer from the groundwater to the lysimeter. Main goal of the installations was the evaluation of the differences between organic farming (Lob 3) and mineral fertilisation (Lob 2). Lysimeter Lob 1 is used as a control without adding any fertilizer (Erhart et al. 2007). Management and crop

rotation follow the local practice, although application of mineral fertilizer was stopped in 2006. The last nitrogen input by compost was done in 2003.

### *Hirschstetten*

At the Hirschstetten site, data of 18 lysimeters consisting of three soil types in six replicates are available from 1999 to 2002. The lysimeters had been filled horizon-wise according to the natural occurrence of the soils in the Marchfeld area. Very high clay contents and big drying cracks between the lysimeter walls and soil caused a lot of preferential flow for one soil type. This does not reflect natural behaviour and we therefore excluded six of the lysimeters from further calculations. Only two soil types (sandy Chernozem Hir<sub>s</sub> and silty Chernozem Hir<sub>t</sub>) with six lysimeters each were therefore used. Collection of seepage water is done in 2.5 m below ground using gravimetric potential. The surface area is two square meters (Stenitzer and Fank 2008). For this paper, mean values of the six lysimeters were used because management, crop rotation, fertilization and meteorological inputs and therefore results were similar. Only mineral fertilizer is applied.

## 5.3 Results and discussion

Based on the lysimeter results, harvest analyses and various accompanying measurements, the individual terms of the nitrogen mass balance (Fig. 5.1) were either measured directly or calculated indirectly to derive  $Frac_{LEACH}$  (Tab. 5.3).

Tab. 5.3: Nitrogen losses through leaching ( $N_{(L\_tot)}$ ), nitrogen sources ( $F_{SN\_tot}$ ,  $F_{ON\_tot}$ ,  $F_{CR\_tot}$ ) for the whole evaluation period, values for  $Frac_{LEACH}$  calculated for the whole evaluation period ( $Frac_{LEACH\_tot}$ ) and as the mean of annual values ( $Frac_{LEACH\_mean}$ ), standard deviation of annual values (SD), number of years of observation (n).

Site	$N_{(L\_tot)}$ (kg N ha <sup>-1</sup> )	$F_{SN\_tot}$ (kg N ha <sup>-1</sup> )	$F_{ON\_tot}$ (kg N ha <sup>-1</sup> )	$F_{CR\_tot}$ (kg N ha <sup>-1</sup> )	$Frac_{LEACH\_tot}$	$Frac_{LEACH\_mean}$	SD	n	land use
Petz 1	225	908	366	357	<b>0.138</b>	0.288	0.390	5	arable land
Petz <sub>syn</sub> 1	278	0	506	398	<b>0.307</b>	0.565	0.541	5	
Wag <sub>con</sub> 1	638	1608	0	910	<b>0.253</b>	0.261	0.172	10	
Wag <sub>con</sub> 2	164	548	476	1151	<b>0.075</b>	0.121	0.120	8	
Wag <sub>bio</sub> 1	818	1370	293	1077	<b>0.299</b>	0.330	0.278	10	
Wag <sub>bio</sub> 2	270	0	0	1625	<b>0.166</b>	0.309	0.398	8	
Peba 1	479	1571	769	1552	<b>0.123</b>	0.153	0.147	18	
Peba 3	301	116	1888	1568	<b>0.084</b>	0.088	0.059	18	
Puck 1	815	725	793	885	<b>0.921</b>	0.832	1.126	16	
Lob 1	183	0	0	1041	<b>0.176</b>	0.207	0.151	13	
Lob 2	248	0	285	929	<b>0.204</b>	0.230	0.173	13	
Lob 3	241	302	0	1087	<b>0.173</b>	0.240	0.230	13	
Hir <sub>s</sub>	168	0	311	156	<b>0.359</b>	0.416	0.241	4	
Hir <sub>t</sub>	163	0	373	203	<b>0.282</b>	0.320	0.152	4	
Petz 2	36	0	0	2279	<b>0.016</b>	0.018	0.015	6	
Petz <sub>syn</sub> 2	18	0	0	1753	<b>0.011</b>	0.010	0.011	4	
Peba 2	121	955	597	708	<b>0.054</b>	0.057	0.033	6	
Gump 1	3	120	0	201	<b>0.011</b>	0.010	0.012	3	
Gump 2	5	238	0	327	<b>0.008</b>	0.007	0.009	3	
Gump 3	23	214	0	319	<b>0.043</b>	0.038	0.053	3	
Gump 4	4	311	0	377	<b>0.006</b>	0.006	0.002	3	
Gump 5	13	409	0	331	<b>0.017</b>	0.018	0.004	3	

### 5.3.1 Correction of leaching rates

At those sites where the measurements were made by gravity lysimeters, with air pressure acting on the outflow seepage rate may be underestimated, especially in dry regions (Stenitzer and Fank 2008). Therefore, we replaced the leaching rates at sites Hirschstetten and Lobau by a mean annual leaching rate of 120 mm yr<sup>-1</sup>, which was found to be more representative in model simulations studies for this area (Stenitzer and Fank 2008). At the Wagna site, which is wetter, the difference between the two types of lysimeters was calculated as being <10 % (Stenitzer and Fank 2008). To account for this measurement error, the seepage rates at the Wag<sub>con</sub> 1 and Wag<sub>bio</sub> 1 sites were therefore increased by 10 %. The same correction was applied to the other gravity lysimeters in regions with annual rainfall around or higher than 800 mm yr<sup>-1</sup> (Petz 1, Petz<sub>syn</sub> 1, Petz 2, Petz<sub>syn</sub> 2, and Gump 1–Gump 6) following the results of

Stenitzer and Fank (2008) and Dowdell and Webster (1980). Nitrogen concentrations were used as measured. The leaching rates of lysimeters with a suction rack were not corrected.

Due to this correction we artificially enlarged the nitrogen pool, because the nitrogen which is leached in theory is still in the lysimeter. The remaining nitrogen in the lysimeter might have induced higher yields and thus crop residues at the lysimeter compared to the surrounding fields. Percolating water and nitrogen may also be accumulating at the lysimeter bottom, since collection depth of the lysimeters is much higher than rooting depth for cereals (~110 cm), the main crops at Hirschstetten and Lobau. In this case nitrogen will not be taken up by the plants but leached when water content is higher than field capacity. Probably both situations will occur because of the disturbed soil water regime especially at the lysimeter bottom and its interplay with drier soil horizons and plant roots.

However, the errors we cause by correcting leaching rate, are much smaller compared to the errors of the wrongly measured leaching rates. While underestimated leaching rates directly influence  $\text{Frac}_{\text{LEACH}}$  (Eq. 5.2), enlarged nitrogen pools affect  $\text{Frac}_{\text{LEACH}}$  indirectly through increased harvest and thus crop residues which are approximately one-third of harvest nitrogen.

### 5.3.2 Calculation of $\text{Frac}_{\text{LEACH}}$ (only leaching)

We used two different methods for estimating  $\text{Frac}_{\text{LEACH}}$ . The first method was the mass balance of the whole time series of the individual sites. Second, we calculated annual  $\text{Frac}_{\text{LEACH}}$  values and their mean and standard deviation to analyse the annual variability. Of course, the sum of the ratios is not the same as the ratio of the sums, so the second method will be less representative of the long term mean.

In general, the grassland sites show significantly lower values of  $\text{Frac}_{\text{LEACH}}$  compared to those on arable land (Tab. 5.3). The arithmetic mean over all grassland sites is 0.021, while on arable land it is 0.254. The highest single annual value for  $\text{Frac}_{\text{LEACH}}$  on grassland was calculated for the Pettenbach site (0.11 in 1995), where mineral fertilizer was applied in addition to the manure/slurry from pig and cattle. Based on currently valid fertilizer recommendations (BMLFUW 2006) this site was affected by a surplus of fertilizer of 44 % on average.

For grassland, the temporal resolution for the evaluation plays a minor role (annually or over the entire observation period), as the variability between years is small. The annual variability is very low due to similar annual nitrogen requirements of the permanent vegetation in different years. Fluctuations may arise due to rainfall and evaporation, and a different number or different timing of mowing cycles. In Austria most of the grassland is usually grazed either permanently or after a certain number of cuts (for hay production and winter feeding). But grazing does not increase  $\text{Frac}_{\text{LEACH}}$  because additional N input from grazing animals must be considered, when farmers plan their fertilizer management. The Austrian fertilization guideline (BMLFUW 2006) provides thresholds, which must not be exceeded. If farmers let the animals graze, the amount of manure fertilizer must be reduced according to these guidelines. Therefore, dung and urine (from grazing animals is not a surplus but substitute.

The arable sites, generally, show higher values of  $\text{Frac}_{\text{LEACH}}$ . They also exhibit a significant annual variability due to variations in crop rotation and fertilization rate, yields and climate

conditions. In addition, the time factor of the mineralization of plant residues plays an important role (David et al. 1997). In our calculations, the mineralization pool of crop residues has been allocated to the year of harvest, although mineralization and transport will take place over a longer period. Therefore, the annual calculation of  $\text{Frac}_{\text{LEACH}}$  for a single site may not be representative of the longer term mean.

Nevertheless, the annual approach is able to highlight special features of nitrogen leaching. The problem of time delay through mineralization and transport of nitrogen in the soil can be well represented at the Petzenkirchen site, as there was a land use change (Fig. 5.3). After harvesting of maize, the field was converted into permanent fallow in August 1994. The yields of maize in the year of change were very low leaving a large pool of nitrogen remaining in the soil. Thus, in the first months of the following year the highest nitrogen leaching rates were measured with a significant delay.

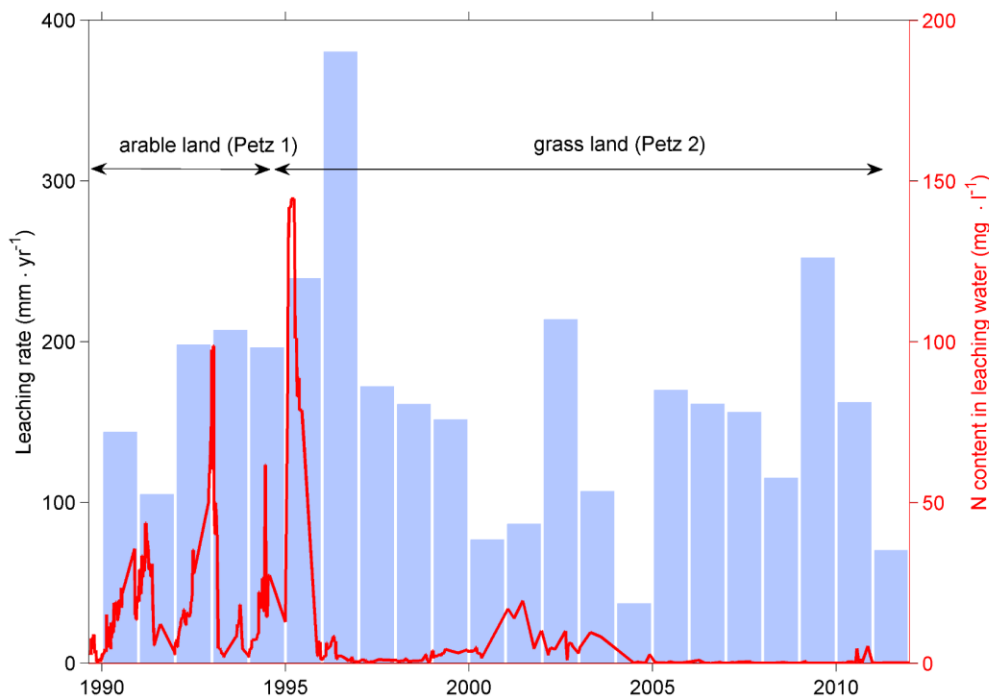


Fig. 5.3: Leaching rates and nitrogen content in seepage water for the Petzenkirchen site.

Individual years can give much larger  $\text{Frac}_{\text{LEACH}}$  values than the long term average due to carry over effects between years. The highest annual values for  $\text{Frac}_{\text{LEACH}}$  of all observation sites were observed at the Pucking site in those years in which soybean was grown with a maximum of  $\text{Frac}_{\text{LEACH}} = 3.60$ . This high value appeared because neither a mineral nor an organic fertilization was applied, which leads to a small denominator in Eq. 5.2. All legumes (Fabacea) tend to show high values of  $\text{Frac}_{\text{LEACH}}$  due to the usually reduced or even absent fertilization.

We conducted a spearman correlation test with the factors rainfall, annual seepage, field capacity, soil depth, sampling depth, yield, N yield, N fertilization and N leached. Texture is represented through field capacity of soil. We left out chemistry which was not sufficiently

available at the different sites. The correlation was done for single years, but also for the means of the entire observation period. Significant correlation is displayed at Tab. 5.4 in the paper.

Tab. 5.4: Correlation coefficient (Spearman) for rainfall (P), annual seepage (L), field capacity (FC), soil depth (d), sampling depth (z), nitrogen export through harvest ( $N_H$ ), nitrogen losses through leaching ( $N_L$ ) and organic fertilizer ( $F_{ON}$ ) influencing  $Frac_{LEACH}$  for single years ( $Frac_{LEACH\_single}$ ) and the means of the entire observation period ( $Frac_{LEACH\_means}$ ).

	P	L	FC	d	z	$N_H$	$N_L$	$F_{ON}$
$Frac_{LEACH\_single}$ (n=136)	0.35	0.65	-0.31	-0.49	-0.22	0.20	0.92	0.21
$Frac_{LEACH\_means}$ (n= 16)	0.23	0.38	-0.50	-0.60	-0.35	0.16	0.86	0.21

As deducible from this table, behaviour of  $Frac_{LEACH}$  is related only to a certain extent to single factors related to the environmental background of a site. Also the relationships between the single factors and  $Frac_{LEACH}$  may be highly nonlinear. In the case of the relationship between  $Frac_{LEACH}$  and field capacity of soil for instance, an exponential relationship was found ( $r^2 = -0.28$ , not shown). We then performed multiple regression including the significant factors drainage, field capacity, soil depth, N yield and N fertilization. This resulted in a  $r^2$  of 0.47. These results indicate that site characteristics alone are only partially responsible for the value of  $Frac_{LEACH}$ . Much more it is depending on the actual management practices at a site as also found by Kirchmann et al. (2002), Feichtinger et al. (2008) and Jia et al. (2014).

### 5.3.3 Nitrogen loss

Although a high  $Frac_{LEACH}$  indicates poor nitrogen uptake it may not necessarily indicate a high absolute nitrogen transport to groundwater. As an example, the nitrogen losses for soybeans in Pucking were only around the average of all crops ( $51 \text{ kg ha}^{-1} \text{ yr}^{-1}$ ).

The highest nitrogen losses took place at the Wagna site during the period when the main focus of research was on increasing yields. The mean nitrogen loss was  $96 \text{ kg ha}^{-1} \text{ yr}^{-1}$  with a maximum for lysimeter  $Wag_{bio} 1$  with  $170 \text{ kg ha}^{-1} \text{ yr}^{-1}$  in 1996. This can be explained by the high input of fertilizer on this site, which was 48 % higher than the N-input recommended by official guidelines from nowadays (BMLFUW 2006). In addition to high amounts of fertilizers, high annual rainfall resulting in high seepage rates increased nitrogen leaching to the groundwater (Fig. 5.4). Although high N losses by leaching were observed at the Wagna site, the average values of  $Frac_{LEACH}$  for the four lysimeters were below (0.25 at  $Wag_{con} 1$ , 0.08 at  $Wag_{con}$  and 0.17 at  $Wag_{bio} 2$ ) or close to the IPCC default value of 0.3 (0.30 at  $Wag_{bio} 1$ ; 0.31 at  $Wag_{bio} 2$ ).

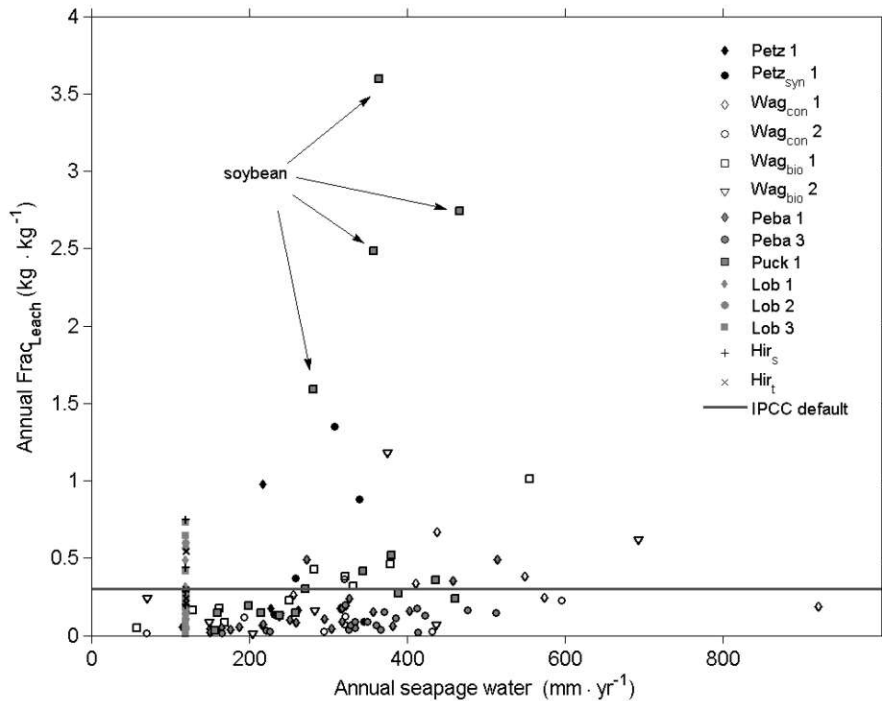


Fig. 5.4: Annual values of  $\text{Frac}_{\text{LEACH}}$  as a function of annual seepage water for the lysimeters analysed. Sites closely located to each other (exhibiting similar meteorological conditions) are displayed in the same design.

In general, high seepage water rates tend to result in both high  $\text{Frac}_{\text{LEACH}}$  values and high nitrogen losses through leaching. A comparison of the sites suggests that deep soil profiles with higher available field capacity produce less nitrogen loss through leaching (see also Tab. 5.4). This can be demonstrated for the Pettenbach and Pucking sites (Fig. 5.5). The lysimeters are close to each other and are subject to the same climatic conditions. The trend line for nitrogen losses of the shallow Pucking site with only 60 cm topsoil (Puck 1) and a field capacity of only 112 mm within these 60 cm of topsoil due to the sandy soil is above the trend lines for Peba 1 and Peba 3 with 150 and 110 cm topsoil and 534 and 396 mm field capacity, respectively. The same annual seepage water led to higher nitrogen losses at the Puck 1 site compared to the Peba 1 and Peba 3 sites although, at Puck 1 site, only 80 % of the recommended amount of fertilizer was applied. In contrast Peba 3 and Peba 1 sites were fertilized with 95 and 122 % of the recommended amount of fertilizer.

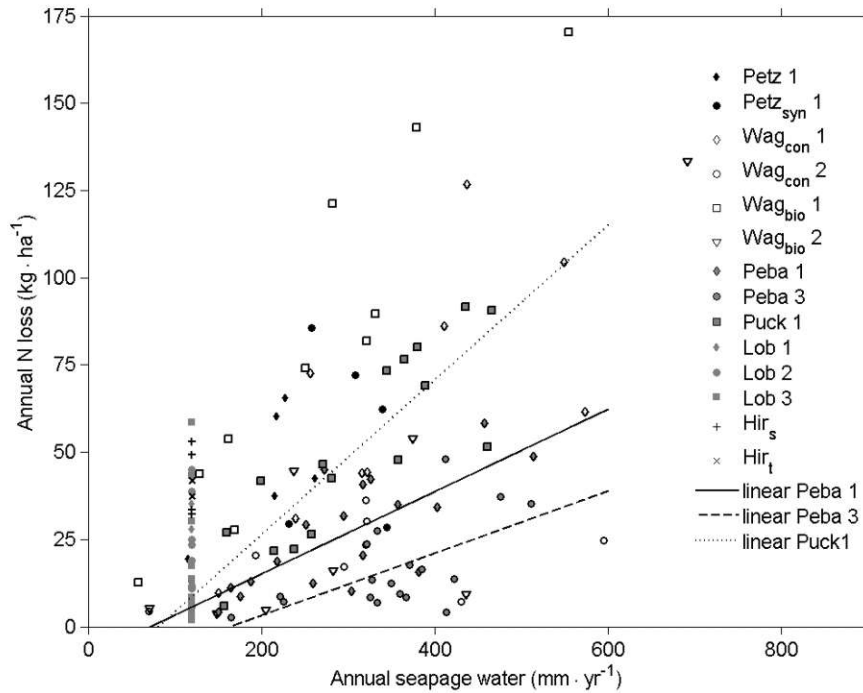


Fig. 5.5: Annual nitrogen losses through leaching as a function of annual seepage water on arable sites. Sites closely located to each other (exhibiting similar meteorological conditions) are displayed in the same design.

Another aspect of exceptionally high nitrogen contents in the leaching water and high values of  $Frac_{LEACH}$  can be related to the nitrogen stock in the soil. On the one hand, a high nitrogen stock in the soil may occur if a lot of above ground and/or below ground plant residues are incorporated into the soil for later mineralization. On the other hand, a poorly developed plant mass of the previous crop in combination with fertilizer supply may leave considerable amounts of nitrogen in the soil. When a poor plant development coincided with rainy periods, high nitrogen losses were measured. This was observed in 2008 at the Lobau site. Although the crop was potatoes which need high nitrogen fertilization, the poor development of green pea in the previous year led to nitrogen losses of  $60 \text{ kg ha}^{-1} \text{ yr}^{-1}$  (Lob2) and  $80 \text{ kg ha}^{-1} \text{ yr}^{-1}$  (Lob3). In addition to the increase of nitrogen in the soil due to incorporation of the green pea biomass, the nitrogen stock in the soil was increased by nitrogen fixation. At the Lob1 site, the zero fertilizer lysimeter at Lobau, only  $20 \text{ kg ha}^{-1} \text{ yr}^{-1}$  nitrogen losses through leaching were measured. However, compared to usual nitrogen losses ( $14 \text{ kg ha}^{-1} \text{ yr}^{-1}$  on average) at this site, the large nitrogen stock in the soil almost doubled the nitrogen losses in 2008.

Consequently, the calculated  $Frac_{LEACH}$  values were significantly lower than those suggested by the IPCC Guidelines (IPCC 2006). However, in the IPCC guidelines nitrogen losses from both leaching and runoff are considered. The latter is not reflected in the lysimeters measurements since they are installed on flat fields and no surface runoff occurs.

### 5.3.4 Calculation of $\text{Frac}_{\text{LEACH}}^a$ (leaching and runoff)

For a mountainous country like Austria, any calculation of a factor  $\text{Frac}_{\text{LEACH}}$  also needs to consider nitrogen losses via lateral pathways (surface runoff, subsurface runoff, drainage) (Tab. 5.5).

Nitrate concentrations of surface runoff and therefore also nitrogen losses through runoff are often small compared to the nitrate losses through leaching (Jackson et al. 1973; Casson et al. 2008). Sharpley et al. (1987) found that 3–9 % of nitrogen fertilizer input was lost to surface runoff for an 8 year monitoring project of 20 catchments in Texas and Oklahoma. However, these results refer to different agroecological environments compared to Austrian conditions. Unfortunately, the data base for calculation of a runoff component for  $\text{Frac}_{\text{LEACH}}$  in Austria is not sufficiently developed yet.

Tab. 5.5: Measured nitrogen losses through leaching ( $N_{(L)\text{leaching}}$ ), estimated nitrogen losses through runoff ( $N_{(L)\text{runoff}}$ ), total nitrogen losses ( $N_{(L)}$ ), nitrogen sources ( $F_{\text{SN}} + F_{\text{ON}} + F_{\text{CR}}$ ), corrected values for  $\text{Frac}_{\text{LEACH}}$  ( $\text{Frac}_{\text{LEACH}}^a$ ) and land use.

Site	$N_{(L)\text{leaching}}$ (kg N ha <sup>-1</sup> )	$N_{(L)\text{runoff}}$ (kg N ha <sup>-1</sup> )	$N_{(L)}^a$ (kg N ha <sup>-1</sup> )	$F_{\text{SN}} + F_{\text{ON}} + F_{\text{CR}}$ (kg N ha <sup>-1</sup> )	$\text{Frac}_{\text{LEACH}}^a$	Land use
Petz 1	225	68	293	1632	0.180	Arable land
Petz <sub>syn</sub> 1	278	83	361	904	0.399	
Wag <sub>con</sub> 1	638	191	830	2518	0.329	
Wag <sub>con</sub> 2	164	49	213	2175	0.098	
Wag <sub>bio</sub> 1	818	245	1064	2740	0.388	
Wag <sub>bio</sub> 2	270	81	351	1625	0.216	
Peba 1	479	144	623	3892	0.160	
Peba 3	301	90	391	3572	0.109	
Puck 1	815	245	1060	2403	0.441	
Lob 1	183	55	238	1041	0.229	
Lob 2	248	74	323	1214	0.266	
Lob 3	241	72	313	1389	0.225	
Hir <sub>s</sub>	168	50	218	467	0.467	
Hir <sub>t</sub>	163	49	211	575	0.367	
Petz 2	36	11	47	2279	0.020	Grassland
Petz <sub>syn</sub> 2	18	6	24	1753	0.014	
Peba 2	121	36	157	2260	0.070	
Gump 1	3	1	4	322	0.014	
Gump 2	5	1	6	564	0.010	
Gump 3	23	7	30	533	0.056	
Gump 4	4	1	5	688	0.008	
Gump 5	13	4	17	740	0.022	

To consider losses by runoff we therefore used results of a simulation study to derive pathways of nitrogen losses at the scale of all of Austria (BMLFUW 2011). We added simulated nitrogen inputs to rivers from overland flow (10,321 t yr<sup>-1</sup>), snow melt (535 t yr<sup>-1</sup>) and drainages (2732 t yr<sup>-1</sup>) and divided this amount with simulated inputs from groundwater (45425 t yr<sup>-1</sup>), resulting in a contribution of 30 % of the total nitrogen losses for pathways related to lateral

flow processes. The number of 30 % can be considered an upper bound of possible losses because BMLFUW (2011) also included emissions from forests, alpine regions and the atmospheric nitrogen input in addition to the input data which would be relevant for the IPCC's indirect soil emissions calculation. Additionally, these nitrogen emissions may not be considered as leaching losses but as inputs to rivers with reduced nitrogen amounts due to the process of denitrification. Unfortunately, denitrification information is not available at present. Including denitrification would further reduce the contribution of lateral pathways.

## 5.4 Conclusions

The evaluation of nitrogen leaching from various lysimeter sites in Austria shows that under local management practices  $\text{Frac}_{\text{LEACH}}$  is smaller than the default value of 0.3 suggested by IPCC rules. In particular, calculated  $\text{Frac}_{\text{LEACH}}$  for grassland is 0.021. For arable sites,  $\text{Frac}_{\text{LEACH}}$  values were around 0.254 (Tab. 5.6). With a ratio of nitrogen losses through runoff to nitrogen losses through leaching of 0.30 (BMLFUW 2008), the modified arithmetic mean for  $\text{Frac}_{\text{LEACH}}$  for arable land and grassland is 0.277 and 0.027, respectively. Arable land and grassland cover 49 and 51 % of the total agricultural area in Austria. Assuming that the results of the lysimeter studies represent management practices, soil properties and climatic conditions that are representative of Austria as a whole, the overall value for  $\text{Frac}_{\text{LEACH}}$  for Austria then is 0.15. This is a considerably smaller value than the default value of  $\text{Frac}_{\text{LEACH}}$  proposed by IPCC.

Tab. 5.6: Mean  $\text{Frac}_{\text{LEACH}}$  (only leaching) and mean modified  $\text{Frac}_{\text{Leach}}^a$  (leaching and runoff) of all arable and grassland sites calculated in this paper from lysimeter data.

	$\text{Frac}_{\text{LEACH}}$	$\text{Frac}_{\text{LEACH}}^a$
Arable land	0.254	0.277
Grassland	0.021	0.027
Austria overall	0.135	0.150

This calculation of the nitrogen losses through leaching and runoff may certainly be further improved by upscaling of site results using more detailed regional characteristics of land management and soil properties. A comparison of  $\text{Frac}_{\text{Leach}}$  to main environmental parameters has revealed that the complexity of the interactions between these parameters is the main driver of changing values for  $\text{Frac}_{\text{Leach}}$ . As a basis for an upscaling of the results obtained, process based models may be employed which are able to deal with a large variety of different climate–soil–land management interactions. These models may be calibrated using results of this lysimeter study. Further research is also necessary for hilly land, where nitrogen losses occur through a combination of seepage, subsurface flow and surface flow.

# Chapter 6

## Summary of the results and overall conclusions

This thesis contributes in both methodological and practical ways to the current state of knowledge of transport and transformation processes of sediments, carbon and nitrogen in agricultural systems.

Chapter 2 proposes a new method for more accurately estimating sediment concentrations and loads. The method is very relevant for evaluating erosion protection measures and land management in general.

In the study, quasi-continuous turbidity measurements and additional water sampling was found as the best available representation of instantaneous sediment concentrations in the stream draining the Petzenkirchen catchment, Austria. The transport of suspended sediment in streams is influenced by a wide range of highly variable factors, causing enormous variation of the sediment concentrations – stream flow relationship in this study and therefore biased sediment concentrations estimates of up to 150% when using a generalised rating curve. More accurate results were obtained with rating curves on an event basis, but omitting hysteresis effects still misrepresented instantaneous sediment concentration estimates. For reliably estimating total loads of suspended sediment, application of a single event rating approach was sufficient, as evaluated against the observed benchmark turbidity data.

Variable rainfall intensities, antecedent soil water content and event runoff volume were identified as most relevant for the hysteresis direction. Large clockwise hysteresis loops were caused by long events with low intensities and higher initial soil moisture. Small but intense events and drier soil conditions entailed counter clockwise hysteresis. Eight-shaped hysteresis loops are mixed forms that happened during events with medium rainfall intensity and medium initial soil water content, but total runoff had to be very low.

In Chapter 3 provided more detailed insight into one part of the sediment transport processes represented in Chapter 2. Specifically, Chapter 3 investigated the resuspension of stream-bed sediments. Two artificial flooding experiments with sediment free water in the stream draining the HOAL clearly indicate resuspension of fine sediments from the streambed. During the first experiment, suspended sediment load decreased from 16.2 kg to 2.2 kg along the stream in line with the decrease of stream flow. During the second experiment less sediment was resuspended and transported through the different sections of the stream (12.6 kg to 0.6 kg along the stream) due to the depletion of easily available sediments from the streambed. The evaluation of flow and travel times indicates that the first peak of the sedigraphs of natural events in this stream is indeed caused by the resuspension of streambed sediments, which contributes between 0.1 and 6% of the total sediment load of natural events, depending on total flow volume. While this is not a large fraction it is a relevant component explaining the space-time patterns of sediment concentrations in streams.

Moving from (particulate) sediments to (dissolved) carbon, Chapter 4 sheds light on the dissolved organic carbon (DOC)-related processes within the same catchment. The chapter also

identifies the drivers for DOC export from the land surface into the stream and the modification of its quality.

The results suggest that, in summer, the soil eluate DOC concentration increases due to increased microbial activity and the related faster decomposition of organic material. Additional inputs of organic material such as leaf litter in autumn also increase the DOC concentrations in the soil eluate. In contrast to the soil eluate, the DOC concentrations of the tributaries are lower in summer, probably due to the lower hydraulic connectivity from the source to the tributaries. The strong temporal correlation between DOC load and total flow volume of all seven tributaries ( $r=0.91$ ) indicates that total DOC inputs into the stream are determined by hydrology (i.e. the water fluxes) and land use plays only a secondary role.

At the tributaries, the impacts of land use and season on the DOM composition are negligible as processes in the soil substantially alter the DOM composition during transport from the terrestrial source to the stream. Soil moisture correlates with DOM composition, indicating that moisture drives organic matter processing and transport in the soil.

This thesis also reveals the significance of instream processing of DOC and DOM components, including both production and degradation. In the study period, instream processes increased total DOC export from the catchment by 24 % compared to the DOC inputs from the tributaries. From May 25th to November 20th, 2017, instream net DOC consumption was observed, leading to a loss of 12 kg DOC probably due to bacterial uptake and respiration. Instream processes led to a disappearance of the labile humic-like component C8. Molecular size (E2/E3) and aromaticity increased along the stream indicating bacterial uptake of aliphatic, low molecular weight DOM.

In Chapter 5 the indirect nitrogen losses from agricultural areas and their contribution to greenhouse gases emission were evaluated by using 22 lysimeter sites in Austria.

Under local management practices the values of  $Frac_{LEACH}$  found here are smaller than the default value of 0.3 suggested by IPCC rules. In particular,  $Frac_{LEACH}$  for grassland was estimated as 0.021. For arable sites,  $Frac_{LEACH}$  values were around 0.254. Arable land and grassland cover 49 and 51 % of the total agricultural area in Austria. Assuming that the results of the lysimeter studies represent management practices, soil properties and climatic conditions that are representative of Austria as a whole, the overall value for  $Frac_{LEACH}$  for Austria is estimated as 0.15.

Based on the work in this thesis, a new  $Frac_{LEACH}$  for Austria was proposed, which has been in use since 2016 for the preparation of National Inventory Report, submitted annually to the International Panel on Climate Change (IPCC). The new  $Frac_{LEACH}$  of 0.15, compared to the initial 0.3, reduces the Austrian indirect soil emissions by 50% to 1,46 Gg  $N_2O$ , which is equivalent to 435 Gg  $CO_{2eq}$ .

Overall, this thesis shows that the transport via different flow paths also requires consideration of the different time scales associated with the processes. Sediments are usually transported with surface runoff or in the stream which, in small catchments, responds quickly to changes in rainfall intensity and thus makes the transport processes highly variable. Thus, the temporal dynamics are in the minute range. The activation of streambed sediments occurs immediately as streamflow increases. Its importance has not been fully appreciated before. Here we find that

the temporal scale of these processes requires commensurate measurements. Fortunately, high resolution devices for many parameters have been developed in recent years in order to record the temporal dynamics of transport processes more easily. Nevertheless, some element of calibration is still required, as illustrated in this work.

On the other hand, the pathways from the fields through the soil towards groundwater or the tile drainage systems are on a temporal scale of days (drainages) to years (groundwater). The substances transported via this path are subject to a large number of processes, especially under agricultural land use. Their transport is buffered, less dynamic and allows measurements on longer temporal scales. The processes within the carbon and nitrogen cycle in the soil compartment are very complex, leaving room for more research, and, likewise, the instream processes are not fully understood. Notwithstanding these complexities, this thesis has demonstrated clear patterns of the seasonal dynamics of substance fluxes in the landscape. By evaluating the budgets of sediments, carbon and nitrogen at various scales we have illustrated the relative roles of soil processes and instream processes, relating measurements across scales.

The availability of the Hydrological Open Air Laboratory has been a major asset in these analyses because of the heavy instrumentation and the prior research at the site. Similarly, the well-defined boundary conditions of the lysimeters have been instrumental in identifying the role and magnitude of component processes as the basis for developing a better understanding of transport processes across scales.



Die approbierte gedruckte Originalversion dieser Dissertation ist an der TU Wien Bibliothek verfügbar.  
The approved original version of this doctoral thesis is available in print at TU Wien Bibliothek.

# Acknowledgements

Financial support from the Austrian Science Funds (FWF) as part of the Vienna Doctoral Programme on Water Resource Systems (DK-plus W1219-N22).

Funding of part of the equipment in the Hydrology Open Air Laboratory (HOAL) through the Innovative Projects Programme of the Vienna University of Technology.

Funding of part of the equipment in the HOAL by the Federal Agency for Water Management.

Funding by the Provincial Government of Lower Austria, NFB, within the Science Call 2015 (SC15-002; project ORCA, Chapter 4).



Die approbierte gedruckte Originalversion dieser Dissertation ist an der TU Wien Bibliothek verfügbar.  
The approved original version of this doctoral thesis is available in print at TU Wien Bibliothek.

# Bibliography

- Ahearn D.S., R.W. Sheibley, R.A. Dahlgren, M. Anderson, J. Johnson and K.W. Tate, 2005. Land use and land cover influence on water quality in the last free-flowing river draining the western Sierra Nevada, California. *J. Hydrol.* 313, 234–247. <https://doi.org/10.1016/j.jhydrol.2005.02.038>
- Arnold J.G., P.M. Allen, R. Muttiah and G. Bernhardt, 1995. Automated Base Flow Separation and Recession Analysis Techniques, *Ground Water*, 33, 1010-1018. <https://doi.org/10.1111/j.1745-6584.1995.tb00046.x>
- Asselman N.E.M., 2000: Fitting and interpretation of sediment rating curves, *Journal of Hydrology* 234, 228-248. [https://doi.org/10.1016/S0022-1694\(00\)00253-5](https://doi.org/10.1016/S0022-1694(00)00253-5)
- Baker A., R. Inverarity, M Charlton and S. Richmond, 2003. Detecting river pollution using fluorescence spectrophotometry: Case studies from the Ouseburn, NE England. *Environ. Pollut.* 124, 57–70. [https://doi.org/10.1016/S0269-7491\(02\)00408-6](https://doi.org/10.1016/S0269-7491(02)00408-6)
- Baldock J.A. and J. O. Skjemstad, 2000. Role of the soil matrix and minerals in protecting natural organic materials against biological attack, in: *Organic Geochemistry*. Pergamon, pp. 697–710. [https://doi.org/10.1016/S0146-6380\(00\)00049-8](https://doi.org/10.1016/S0146-6380(00)00049-8)
- Blann, K.L., J.L Anderson, G.R Sands, and B. Vondracek, 2009. Effects of Agricultural Drainage on Aquatic Ecosystems: A Review. *Crit. Rev. Environ. Sci. Technol.* 39, 909–1001. <https://doi.org/https://doi.org/10.1080/10643380801977966>
- Blöschl, G. and E. Zehe, 2005. On hydrological predictability. *Hydrological Processes*, 19 (19), 3923-3929. <https://doi.org/10.1002/hyp.6075>
- Blöschl, G., A.P. Blaschke, M. Broer, C. Bucher, G. Carr, X. Chen, A. Eder, M. Exner-Kittridge, A. Farnleitner, A. Flores-Orozco, P. Haas, P. Hogan, A. Kazemi Amiri, M. Oismüller, J. Parajka, R. Silasari, P. Stadler, P. Strauss, M. Vreugdenhil, W. Wagner, and M. Zessner, 2016. The Hydrological Open Air Laboratory (HOAL) in Petzenkirchen: A hypothesis-driven observatory. *Hydrol. Earth Syst. Sci.* 20, 227–255. <https://doi.org/10.5194/hess-20-227-2016>
- BMLFUW - Bundesministerium für Land- und Forstwirtschaft, Umwelt und Wasser, 2006. Richtlinien für die Sachgerechte Düngung. Anleitung zur Interpretation von Bodenuntersuchungsergebnissen in der Landwirtschaft. 6. Auflage, Bundesministerium für Land- und Forstwirtschaft, Umwelt und Wasser , 79 S., Wien
- BMLFUW - Bundesministerium für Land- und Forstwirtschaft, Umwelt und Wasser, 2011. Stoffbilanzmodellierung für Nährstoffe auf Einzugsgebietsebene als Grundlage für Bewirtschaftungspläne und Maßnahmenprogramme. Bundesministerium für Land- und Forstwirtschaft, Umwelt und Wasser, 190 S., Wien. BMLFUW-UW.3.1.2/0029-VII/1/2008
- Bolan, N.S., D.C. Adriano and M. de-la-Luz, 2004. Dynamics and environmental significance of dissolved organic matter in soil. *SuperSoil 2004 3rd Aust. New Zeal. Soils Conf.* 5–9.
- Bolan, N.S., D.C. Adriano, A. Kunhikrishnan, T. James, R. McDowell and N. Senesi, 2011. Dissolved Organic Matter. *Biogeochemistry, Dynamics, and Environmental Significance in*

Soils., *Advances in Agronomy*. Academic Press. <https://doi.org/10.1016/B978-0-12-385531-2.00001-3>

- Braun M., P. Hurni P and E. Spiess, 1994. Phosphor- und Stickstoffüberschüsse in der Landwirtschaft und Para-Landwirtschaft: Abschätzung für die Schweiz und das Rheineinzugsgebiet der Schweiz unterhalb der Seen. Schriftenreihe der FAC Liebefeld 18, Bern. ISSN-1013-154X
- Brasington, J. and K. Richards, 2000: Turbidity and suspended sediment dynamics in small catchments in the Nepal Middle Hills, *Hydrological Processes* 14, 2559-2574. [https://doi.org/10.1002/1099-1085\(20001015\)14:14<2559::AID-HYP114>3.0.CO;2-E](https://doi.org/10.1002/1099-1085(20001015)14:14<2559::AID-HYP114>3.0.CO;2-E)
- Brockett, B.F.T., C.E. Prescott and S.J. Grayston, 2012. Soil moisture is the major factor influencing microbial community structure and enzyme activities across seven biogeoclimatic zones in western Canada. *Soil Biol. Biochem.* 44, 9–20. <https://doi.org/10.1016/j.soilbio.2011.09.003>
- Bryan, R. B. and S.E. Brun, 1999. Laboratory experiments on sequential scour/deposition and their application to the development of banded vegetation. *Catena* 37, 147–63.
- Bueno, C.S. and J.K. Ladha, 2009. Comparison of soil properties between continuously cultivated and adjacent uncultivated soils in rice-based systems. *Biol. Fertil. Soils* 45, 499–509. <https://doi.org/10.1007/s00374-009-0358-y>
- Campbell, F.B. and H.A. Bauder, 1940. A rating-curve method for determining silt-discharge of streams, *Transactions of the American Geophysical Union* 21, 603-607. <https://doi.org/10.1029/TR021i002p00603>
- Casson J.P., B.M. Olson, J.L. Little and S.C. Nolan, 2008. Assessment of Environmental Sustainability in Alberta's Agricultural Watersheds Project. Volume 4: Nitrogen loss in surface runoff. Alberta Agriculture and Rural Development, 71 pp, Lethbridge, Alberta, Canada.
- Chantigny M.H., 2003. Dissolved and water-extractable organic matter in soils: A review on the influence of land use and management practices, in: *Geoderma*. Elsevier, pp. 357–380. [https://doi.org/10.1016/S0016-7061\(02\)00370-1](https://doi.org/10.1016/S0016-7061(02)00370-1)
- Chantigny M.H., D.A. Angers, D. Prévost, R.R. Simard and F.P. Chalifour, 1999. Dynamics of soluble organic C and C mineralization in cultivated soils with varying N fertilization. *Soil Biol. Biochem.* 31, 543–550. [https://doi.org/10.1016/S0038-0717\(98\)00139-4](https://doi.org/10.1016/S0038-0717(98)00139-4)
- Chen, W., P. Westerhoff, J.A. Leenheer and K. Booksh, 2003. Fluorescence Excitation-Emission Matrix Regional Integration to Quantify Spectra for Dissolved Organic Matter. *Environ. Sci. Technol.* 37, 5701–5710. <https://doi.org/10.1021/es034354c>
- Chin, Y., G.R. Aiken and E. O'Loughlin, 1994. Molecular weight, polydispersity, and spectroscopic properties of aquatic humic substances. *Environ. Sci. ...* 28, 1853–1858. <https://doi.org/10.1021/es00060a015>
- Chikita, K.A., R. Kemnitz, R., Kumai, 2002. Characteristics of sediment discharge in the subarctic Yukon River, Alaska, *Catena* 48, 235-253. [https://doi.org/10.1016/S0341-8162\(02\)00032-2](https://doi.org/10.1016/S0341-8162(02)00032-2)
- FAO, ISRIC and ISSS, World reference base of soil resources, 1998: World Soil Resources Report, 84, Rome. ISBN 92-5-104141-5

- Chichester F.W., 1977. Effects of increased fertilizer rates on nitrogen content of runoff and percolate from monolith lysimeters. *J Environ Qual* 6: 211-217. doi:10.2134/jeq1977.00472425000600020023x
- Cronan, C.S. and G.R. Aiken, 1985. Chemistry and transport of soluble humic substances in forested watersheds of the Adirondack Park, New York. *Geochim. Cosmochim. Acta* 49, 1697–1705. [https://doi.org/10.1016/0016-7037\(85\)90140-1](https://doi.org/10.1016/0016-7037(85)90140-1)
- Dalrymple, R.M., A.K. Carfagno and C.M. Sharpless, 2010. Correlations between dissolved organic matter optical properties and quantum yields of singlet oxygen and hydrogen peroxide. *Environ. Sci. Technol.* 44, 5824–5829. <https://doi.org/10.1021/es101005u>
- David M.B., L.E. Gentry, D.A. Kovacic, and K.M. Smith, 1997. Nitrogen balance in and export from an agricultural watershed. *J Environ Qual.* 26: 1038-1048. doi:10.2134/jeq1997.00472425002600040015x
- Demars, B.O.L., J. Russell Manson, J.S. Ólafsson, G.M. Gíslason, R. Gudmundsdóttir, G. Woodward, J. Reiss, D.E. Pichler, J.J. Rasmussen and N. Friberg, 2011. Temperature and the metabolic balance of streams. *Freshw. Biol.* 56, 1106–1121. <https://doi.org/10.1111/j.1365-2427.2010.02554.x>
- Del Prado A., L. Brown, R. Schulte, M. Ryan and D. Scholefield, 2006. Principles of development of a mass balance N cycle model for temperate grasslands: an Irish case study. *Nutr Cyc Agroecosys* 74: 115–131. Doi:10.1007/s10705-005-5769-z
- DeRose R.C., I.P. Prosser, M. Weisse and A.O. Hughes, 2003. Patterns of Erosion and Sediment and Nutrient Transport in the Murray-Darling Basin. CSIRO Land and Water Technical Report 32/03.
- Dowdell, R.J. and C.P. Webster, 1980. A lysimeter study using nitrogen-15 on the uptake of fertilizer nitrogen by perennial ryegrass swards and losses by leaching. *Eur J Soil Sci* 31: 65-75. doi:10.1111/j.1365-2389.1980.tb02065.x
- EC (European Council), 1991. Council regulation No 2092/91 of June 1991 on organic production of agricultural products and indications referring thereto on agricultural products and foodstuff. <http://eurex.europa.eu/LexUriServ/LexUriServ.do?uri=CONSLEG:1991R2092:20080514:EN:PDF>, accessed on April 07, 2014
- Eder A., M. Exner-Kittridge, P. Strauss and G. Blöschl, 2014. Re-suspension of bed sediment in a small stream &ndash; Results from two flushing experiments. *Hydrol. Earth Syst. Sci.* 18, 1043–1052. <https://doi.org/10.5194/hess-18-1043-2014>
- Eder A., P. Strauss, T. Krueger and J.N. Quinton, 2010. Comparative calculation of suspended sediment loads with respect to hysteresis effects (in the Petzenkirchen catchment, Austria). *J. Hydrol.* 389, 168–176. <https://doi.org/10.1016/j.jhydrol.2010.05.043>
- Enowashu E., C. Poll, N. Lamersdorf and E. Kandeler, 2009. Microbial biomass and enzyme activities under reduced nitrogen deposition in a spruce forest soil. *Appl. Soil Ecol.* 43, 11–21. <https://doi.org/10.1016/j.apsoil.2009.05.003>
- Environment Agency Austria, 2013. Austria's National Inventory Report 2013 – Agriculture (CRF Sector 4), 260-322. Environment Agency Austria, Vienna

- Environmental Protection Agency Ireland. National inventory report 2011, Greenhouse gas emissions 1990-2009 reported to the UPFCCC, Wexford, Ireland
- Erhart E., F. Feichinger and W. Hartl, 2007. Nitrogen leaching losses under crops fertilized with biowaste compost compared with mineral fertilization. *J Plant Nutr Soil Sci* 170: 608–614. doi:10.1002/jpln.20062518
- Ewing S.A., J. Sanderman, W.T. Baisden, Y. Wang, R. Amundson, 2006. Role of large-scale soil structure in organic carbon turnover: Evidence from California grassland soils. *J. Geophys. Res. Biogeosciences* 111, 3012. <https://doi.org/10.1029/2006JG000174>
- Exner-Kittridge M., P. Strauss, G. Blöschl, A. Eder, E. Saracevic and M., Zessner, 2016. The seasonal dynamics of the stream sources and input flow paths of water and nitrogen of an Austrian headwater agricultural catchment. *Sci. Total Environ.* 542, 935–945. <https://doi.org/10.1016/j.scitotenv.2015.10.151>
- Fasching, C. and T.J. Battin, 2012. Exposure of dissolved organic matter to UV-radiation increases bacterial growth efficiency in a clear-water Alpine stream and its adjacent groundwater. *Aquat. Sci.* 74, 143–153. <https://doi.org/10.1007/s00027-011-0205-8>
- Fasching, C., A.J. Ulseth, J. Schelker, G. Steniczka and T.J., Battin, 2016. Hydrology controls dissolved organic matter export and composition in an Alpine stream and its hyporheic zone. *Limnol. Oceanogr.* 61, 558–571. <https://doi.org/10.1002/lno.10232>
- Feichtinger F., J. Dorner and F. Aigner, 2004. Durchschnittliche Versickerungsmengen und bewirtschaftungsbedingte Stickstoffausträge im Alpenvorland Niederösterreichs. *Schriftenreihe des Bundesamt für Wasserwirtschaft*, Vol 20: 79-90
- Feichtinger F., P. Strauss, J.M. Lescot, M. Kaljonen and G. Hofmayer, 2008: Integrated assesment of groundwater protection using Agricultural Best Management Practices – a nitrogen case study. *Die Bodenkultur* 59, 1-4: 149-164
- Fellman, J.B., E. Hood, D.V. D'Amore, R.T. Edwards and D. White, 2009. Seasonal changes in the chemical quality and biodegradability of dissolved organic matter exported from soils to streams in coastal temperate rainforest watersheds. *Biogeochemistry* 95, 277–293. <https://doi.org/10.1007/s10533-009-9336-6>
- Fellman, J.B., E. Hood and R.G.M. Spencer, 2010. Fluorescence spectroscopy opens new windows into dissolved organic matter dynamics in freshwater ecosystems: A review. *Limnol. Oceanogr.* <https://doi.org/10.4319/lo.2010.55.6.2452>
- Findlay, S., J.M. Quinn, C.W. Hickey, G. Burrell and M. Downes, 2001. Effects of land use and riparian flowpath on delivery of dissolved organic carbon to streams. *Limnol. Oceanogr.* 46, 345–355. <https://doi.org/10.4319/lo.2001.46.2.0345>
- Findlay S.E.G., R.L. Sinsabaugh, W.V. Sobczak, and M. Hoostal, 2003. Metabolic and structural response of hyporheic microbial communities to variations in supply of dissolved organic matter. *Limnol. Oceanogr.* 48, 1608–1617. <https://doi.org/10.4319/lo.2003.48.4.1608>
- Frank, D.A. and P.M. Groffman, 2009. Plant rhizospheric N processes: what we don't know and why we should care. *Ecology* 90, 1512–1519. <https://doi.org/https://doi.org/10.1890/08-0789.1>
- Ghani, A., M. Dexter, R.A. Carran and P.W. Theobald, 2007. Dissolved organic nitrogen and carbon in pastoral soils: the New Zealand experience. *Eur. J. Soil Sci.* 56, 832–843.

- Giménez, R., J. Casalí, I. Grande, J. Díez, M.A. Campo, J. Álvarez-Mozos and M. Goñi, 2012. Factors controlling sediment export in a small agricultural watershed in Navarre (Spain), *Agricultural Water Management*, 110, 1–8. <https://doi.org/10.1016/j.agwat.2012.03.007>
- Gippel, C.J., 1995. Potential of turbidity monitoring for measuring the transport of suspended solids in streams, *Hydrological Processes*, 9, 83-97. <https://doi.org/10.1002/hyp.3360090108>
- Gooseff, M. N., R. O. Hall Jr. and J. L. Tank, 2007. Relating transient storage to channel complexity in streams of varying land use in Jackson Hole, Wyoming, *Water Resour. Res.*, 43, W01417. <https://doi.org/10.1029/2005WR004626>
- Grayson, R.B., B.L. Finlayson, C.J. Gippel, B.T. Hart, 1996. The Potential of Field Turbidity Measurements for the Computation of Total Phosphorus and Suspended Solids Loads, *Journal of Environmental Management* 47, 257-267. <https://doi.org/10.1006/jema.1996.0051>
- Graeber, D., J. Gelbrecht, M.T. Pusch, C. Anlanger, and D. von Schiller, D., 2012. Agriculture has changed the amount and composition of dissolved organic matter in Central European headwater streams. *Sci. Total Environ.* 438, 435–446. <https://doi.org/10.1016/j.scitotenv.2012.08.087>
- Gurnell, A.M., 1987. Suspended Sediment, in: A.M. Gurnell, M.J. Clark (Eds.), *Clacio-Fluvial Sediment Transfer*, Wiley, Chichester, pp. 305-354. <https://doi.org/10.1002/esp.3290130611>
- House, W.A. and M.S. Warwick, 1998. Hysteresis of the solute concentration/discharge relationship in rivers during storms, *Water Resources* 32, 2279-2290. DOI:10.1016/S0043-1354(97)00473-9
- Herndl M., M. Schink, M. Kandolf, A. Böhner and K. Buchgraber, 2013. Nährstoffauswaschung im Grünland in Abhängigkeit vom Wirtschaftsdüngungs- und Nutzungssystem, Conference Proceeding: 15. Dumpensteiner Lysimetertagung 2013, Raumberg-Gumpenstein, 25-30, ISBN: 978-3-902559-90-6
- Hill B.H., R.K. Hall, P. Husby, A.T. Herlihy and M. Dunne, 2000. Interregional comparisons of sediment microbial respiration in streams. *Freshw. Biol.* 44, 213–222. <https://doi.org/10.1046/j.1365-2427.2000.00555.x>
- Hudson, N., A. Baker and D. Reynolds, 2007. Fluorescence analysis of dissolved organic matter in natural, waste and polluted waters - A review. *River Res. Appl.* <https://doi.org/10.1002/rra.1005>
- Huguet, A., L. Vacher, S. Relexans, S. Saubusse, J.M. Froidefond and E. Parlanti, 2009. Properties of fluorescent dissolved organic matter in the Gironde Estuary. *Org. Geochem.* 40, 706–719. <https://doi.org/10.1016/j.orggeochem.2009.03.002>
- Ide J.H., H. Haga, M. Chiwa and K. Otsuki, 2008. Effects of antecedent rain history on particulate phosphorus loss from a small forested watershed of Japanese cypress (*Chamaecyparis obtusa*), *Journal of Hydrology* 352 (3-4), 322-335. doi:10.1016/j.jhydrol.2008.01.012

- IPCC, 2006. IPCC Guidelines for National Greenhouse Gas Inventories, Prepared by the National Greenhouse Gas Inventories Programme, H.S. Eggleston, L. Buendia, K. Miwa, T. Ngara and K. Tanabe (Eds). IGES, Japan, ISBN 4-88788-032-4
- IPCC, 2000. Good Practice Guidelines and Uncertainty Management in National Greenhouse Gas Inventories. Prepared by the National Greenhouse Gas Inventories Programme, J. Penman, D. Kruger, I. Galbally, T. Hiraishi, B. Nyenzi, S. Emmanul, L. Buendia, R. Hoppaus, T. Martinsen, J. Meijer, K. Miwa and K. Tanabe (Eds). IGES, Japan, ISBN 4-88788-000-6
- IUSS Working Group WRB. 2015. World Reference Base for Soil Resources 2014, update 2015. International soil classification system for naming soils and creating legends for soil maps. World Soil Resources Reports No. 106. FAO, Rome. ISBN 978-92-5-108369-7
- Jackson W.A., I.E. Asmussen, E.W. Hauser and A.W. White, 1973. Nitrate in surface and subsurface flow from a small agricultural watershed. *J Environ Qual* 2: 480-482. doi:10.2134/jeq1973.00472425000200040017x
- Jia X.C., L.J. Sha, P. Liu, B.Q. Zhao, L.M. Gu, S.T. Dong, S.H. Bing, J.W. Zhang and B. Zhao, 2014. Effect of different nitrogen and irrigation treatments on yield and nitrate leaching of summer maize (*Zea mays* L.) under lysimeter conditions. *Agr Water Manage* 137: 92-103
- Kalbitz K., A. Meyer, R. Yang and P. Gerstberger, P., 2007. Response of dissolved organic matter in the forest floor to long-term manipulation of litter and throughfall inputs. *Biogeochemistry* 86, 301–318. <https://doi.org/10.1007/s10533-007-9161-8>
- Kalbitz, K., S. Solinger, J.H. Park, B. Michalzik and E. Matzner, 2000. Controls on the dynamics of dissolved organic matter in soils: a review. *Soil Sci.* 165, 277–304.
- Khomutova, T.E., L.T. Shirshova, S. Tinz, W. Rolland and J. Richter, 2000. Mobilization of DOC from sandy loamy soils under different land use (Lower Saxony, Germany), *Plant and Soil*.
- Kirchmann H., A.E.J. Johnston and L.F. Bergstrom, 2002: Possibilities for reducing nitrate leaching from agricultural land. *AMBIO* 31, 5: 404-408
- Klammler G. and J. Fank, 2014. Determining water and nitrogen balances for beneficial management practices using lysimeters at Wagna test site (Austria). *Sci Total Environ* 449: 448-462. doi:10.1016/j.scitotenv.2014.06.009
- Kovacs, A., M. Honti, A. Eder, M. Zessner, A. Clement and G. Blöschl, 2012. Identification of phosphorus emission hotspots in agricultural catchments. *Science of the Total Environment*, 433, 74–88. <https://doi.org/10.1016/j.scitotenv.2012.06.024>
- Kroeze C, R. Aerts, N. van Breemen, D. van Dam, K. van der Hoek, P. Hofschreuder, M. Hoosbee, J. de Klein, H. Kros, H. van Oene, A. Tietema, R. van der Veeren, and W. de Vries, 2003. Uncertainties in the fate of nitrogen I: An overview of sources of uncertainty illustrated with a Dutch case study. *Nutr Cyc Agroecosys* 66: 43-69. doi:10.1023/A:1023339106213
- Kronvang B., A. Laubel and R. Grant, 1997. Suspended sediment and particulate phosphorus transport and delivery pathways in an arable catchment, Gelbaek stream, Denmark, *Hydrological Processes* 11, 627-642. doi:10.1016/j.jhydrol.2008.01.012
- Krueger T., J.N. Quinton, J. Freer, C.J.A. Macleod, G.S. Bilotta, R.E. Brazier, P. Butler and P.M. Haygarth, 2009. Uncertainties in data and models to describe event dynamics of agricultural

sediment and phosphorus transfer. *Journal of Environmental Quality* 38 (3), 1137-1148. <https://doi.org/10.2134/jeq2008.0179>

Lana-Renault N. and D. Regüés, 2009. Seasonal patterns of suspended sediment transport in an abandoned farmland catchment in the Central Spanish Pyrenees. *Earth Surf. Process. Landforms* 34, 1291-1301. <https://doi.org/10.1002/esp.1825>

Lenzi, M.A. and L. Marchi, 2000. Suspended Sediment Load During Floods in a Small Stream of the Dolomites (Northeastern Italy), *Catena* 39, 267-282. [https://doi.org/10.1016/S0341-8162\(00\)00079-5](https://doi.org/10.1016/S0341-8162(00)00079-5)

Lewis, J., 1996. Turbidity controlled suspended sediment sampling for runoff-event load estimation, *Water Resources Research* 32, 2299-2310. <https://doi.org/10.1029/96WR00991>

Marschner B. and K. Kalbitz, 2003. Controls of bioavailability and biodegradability of dissolved organic matter in soils, in: *Geoderma*. Elsevier, pp. 211-235. [https://doi.org/10.1016/S0016-7061\(02\)00362-2](https://doi.org/10.1016/S0016-7061(02)00362-2)

Merritt W.S., R.A. Letcher, A.J. Jakeman, 2003. A review of erosion and sediment transport models, *Environmental Modelling & Software* 18, 761-799. [https://doi.org/10.1016/S1364-8152\(03\)00078-1](https://doi.org/10.1016/S1364-8152(03)00078-1)

Millington A.C., 1981: Relationship between three scales of erosion measurement on two small basins in Sierra Leone. In: *Erosion and Sediment Transport Measurement, Proc. Florence Symposium*, 485-492.

Mosier A., C. Kroeze, C. Nevison, O. Oenema, S. Seitzinger, O. van Cleemput, 1998. Closing the global N<sub>2</sub>O budget: nitrous oxide emissions through the agricultural nitrogen cycle – OECD/IPCC/IEA phase II development of IPCC guidelines for national greenhouse gas inventory methodology. *Nutr Cycl Agroecosy*, 52: 225-248. doi: 10.1023/A:1009740530221

MURER E., 2002. Erfassung und Bewertung der Sickerwasserquantität und -qualität im Pilotprojekt zur Grundwassersanierung in Oberösterreich. *Monolithische Feldlysimeter. Schriftenreihe des Bundesamtes für Wasserwirtschaft, Vol 16: 112-139*

Murphy K.R., C.A. Stedmon, D. Graeber and R. Bro, 2013. Fluorescence spectroscopy and multi-way techniques. *PARAFAC. Anal. Methods*. <https://doi.org/10.1039/c3ay41160e>

Murphy K.R., C.A. Stedmon, P. Wenig and R. Bro, 2014. OpenFluor-an online spectral library of auto-fluorescence by organic compounds in the environment †. <https://doi.org/10.1039/c3ay41935e>

Nash, J.E. and J.E. Sutcliffe, 1970. River Flow Forecasting Through Conceptual Models. Part I. A Discussion of Principles, *Journal of Hydrology* 10, 282-290. [https://doi.org/10.1016/0022-1694\(70\)90255-6](https://doi.org/10.1016/0022-1694(70)90255-6).

Nathan R.J. and T.A. 1990. McMahon, Evaluation of Automated Techniques for Base Flow and Recession Analyses, *Water Resources Research* 26, 1465-1473. <https://doi.org/10.1029/WR026i007p01465>

Neill M., 1989. Nitrate concentrations in river waters in the south-east of Ireland and their relationship with agricultural practice. *Wat Res* 23: 1339-1355. doi:10.1016/0043-1354(89)90073-0

- Nistor C.J. and M. Church, 2005. Suspended sediment transport regime in a debris-flow gully on Vancouver Island, British Columbia, *Hydrological Processes* 19, 861-885. DOI: 10.1002/hyp.5549
- Ogle S.M., F.J. Breidt and K. Paustian, 2005. Agricultural management impacts on soil organic carbon storage under moist and dry climatic conditions of temperate and tropical regions. *Biogeochemistry* 72, 87-121. <https://doi.org/10.1007/s10533-004-0360-2>
- Osburn C.L., N.J. Anderson, C.A. Stedmon, M.E. Giles, E.J. Whiteford, T.J. McGenity, A.J. Dumbrell and G.J.C. Underwood, 2017. Shifts in the Source and Composition of Dissolved Organic Matter in Southwest Greenland Lakes Along a Regional Hydro-climatic Gradient. *J. Geophys. Res. Biogeosciences* 122, 3431-3445. <https://doi.org/10.1002/2017JG003999>
- Paustian, S.J. and R. L. Beschta, 1979. Suspended sediment regime of an Oregon coast range stream, *Water Resources Bulletin* 15 (1), 144-154. <https://doi.org/10.1111/j.1752-1688.1979.tb00295.x>
- Parsons A. J. and G.L. Stromberg, 1998. Experimental analysis of size and distance of travel of unconstrained particles in interill flow. *Water Resources Research* 34, 2377-81. <https://doi.org/10.1029/98WR01471>
- Petticrew E.L., A. Krein and D.E. Walling, 2007. Evaluating fine sediment mobilization and storage in a gravel-bed river using controlled reservoir releases, *Hydrological Processes* 21, 198-210. <https://doi.org/10.1002/hyp.6183>
- Piscart C., R. Genoel, S. Doledec, E. Chauvet and P. Marmonier, 2009. Effects of intense agricultural practices on heterotrophic processes in streams. *Environ. Pollut.* 157, 1011-1018. <https://doi.org/10.1016/j.envpol.2008.10.010>
- Prasuhn V. and M. Braun, 1994. Abschätzung der Phosphor- und Stickstoffverluste aus diffusen Quellen in die Gewässer des Kantons Bern. Schriftenreihe der FAC Liebefeld 17. Bern
- Prasuhn V. and R. Mohni, 2003. GIS-gestützte Abschätzung der Phosphor- und Stickstoffeinträge aus diffusen Quellen in die Gewässer des Kantons Bern. FAL, interner Bericht z.H. Amt für Gewässerschutz und Abfallwirtschaft, Kanton Bern. Zürich-Reckenholz.
- Prosser I.P., I.D. Rutherford, J.M. Olley, W.J Young, P.J. Wallbrink, C.J. Moran 2001a. Large-scale patterns of erosion and sediment transport in river networks, with examples from Australia. *Marine and Freshwater Research* 52, 81-99. <https://doi.org/10.1.1.458.6303>
- Pucher M., U. Wunsch, G. Weigelhofer, K. Murphy, T. Hein and D. Graeber, 2019. StaRdom: Versatile software for analyzing spectroscopic data of dissolved organic matter in R. *Water (Switzerland)* 11. <https://doi.org/10.3390/w11112366>
- Qualls, R.G. and C.J. Richardson, 2003. Factors controlling concentration, export, and decomposition of dissolved organic nutrients in the Everglades of Florida, *Biogeochemistry*.
- Quinton J.A., P. Strauss, N. Miller, E. Azazoglu, M.Yli-Halla, and R. Uusitalo, 2003. The potential for soil phosphorus tests to predict phosphorus losses in overland flow. *J. Plant Nutrition and Soil Science*, 166, 4, 432-437. <https://doi.org/10.1002/jpln.200321122>
- Raymond P.A., J.E. Saiers and W.V. Sobczak, 2016. Hydrological and biogeochemical controls on watershed dissolved organic matter transport: pulse-shunt concept. *Ecology* 97, 5-16. <https://doi.org/10.1890/14-1684.1>

- Rosa, E. and B. Debska, 2018. Seasonal changes in the content of dissolved organic matter in arable soils. *J. Soils Sediments* 18, 2703–2714. <https://doi.org/10.1007/s11368-017-1797-y>
- Rosemond A.D., J.P. Benstead, P.M. Bumpers, V. Gulis, J.S. Kominoski, D.W.P. Manning, K. Suberkropp and J.B. Wallace, 2014. Experimental nutrient additions accelerate terrestrial carbon loss from stream ecosystems, *Science* 347, 6226, 1142-1145. DOI: 10.1126/science.aaa1958
- Ryan M., C. Brophy, J. Connollym K. McNamara and O.T. Carton, 2006. Monitoring of nitrogen leaching on a dairy farm during four drainage seasons. *Irish J Agr Food Res* 45: 115-134. <http://www.jstor.org/stable/25562571>. Accessed 28 August 2014
- Scholefield D., K.C. Tyson, E.A. Garwood, A.C. Armstrong, J. Hawkins and A.C. Stone, 1993. Nitrate leaching from grazed grassland lysimeters: effects of fertilizer input, field drainage, age of sward and patterns of weather. *Eur J Soil Sci* 44: 553-749. doi: 10.1111/j.1365-2389.1993.tb02325.x
- Seeger M., M.P. Errea, S. Begueria, J. Arnaez, C. Marti and J.M Carcia-Ruiz, 2004. Catchment soil moisture and rainfall characteristics as determinant factors for discharge/suspended sediment hysteretic loops in a small headwater catchment in the Spanish Pyrenees, *Journal of Hydrology* 288, 299-311. <https://doi.org/10.1016/j.jhydrol.2003.10.012>
- Sharpley A.N., S.J. Smith, and J.W. Naney, 1987. Environmental impact of agricultural nitrogen and phosphorus use. *J Agric Food Chem* 35: 812-817. <https://doi.org/10.1021/jf00077a043>
- Silveira M.L.A., 2005. Dissolved organic carbon and bioavailability of N and P as indicators of soil quality. *Sci. Agric.* 62, 502–508. <https://doi.org/10.1590/S0103-90162005000500017>
- Steenwerth K. and K.M. Belina, 2008. Cover crops enhance soil organic matter, carbon dynamics and microbiological function in a vineyard agroecosystem. *Appl. Soil Ecol.* 40, 359–369. <https://doi.org/10.1016/j.apsoil.2008.06.006>
- Stenitzer E., 1988: Simwasser - A numerical model for simulation of soilmoisture regimes and of crop yield. *Mitteilungen aus der Bundesanstalt für Kulturtechnik und Bodenwasserhaushalt, Petzenkirchen.*
- Stenitzer E. and J. Fank, 2008. Schwerkraft- versus Unterdrucklysimeter - eine Simulationsstudie. In *diffuse Einträge in das Grundwasser: Monitoring - Modellierung - Management. Landwirtschaft und Wasserwirtschaft im Fokus zu erwartender Herausforderungen. Beiträge zur Hydrogeologie* 56: 114-118. Graz.
- Stutter M.I. and M.F. Billett, 2003. Biogeochemical controls on streamwater and soil solution chemistry in a High Arctic environment. *Geoderma* 113, 127–146. [https://doi.org/10.1016/S0016-7061\(02\)00335-X](https://doi.org/10.1016/S0016-7061(02)00335-X)
- Sun H.Y., P. Koal, G. Gerl, R. Schroll, R.G. Joergensen and J.C. Munch, 2017. Water-extractable organic matter and its fluorescence fractions in response to minimum tillage and organic farming in a Cambisol. *Chem. Biol. Technol. Agric.* 4, 15. <https://doi.org/10.1186/s40538-017-0097-5>
- Széles, B., M. Broer, J. Parajka, P. Hogan, A. Eder, P. Strauss and G. Blöschl, 2018. Separation of Scales in Transpiration Effects on Low Flows: A Spatial Analysis in the Hydrological Open

Air Laboratory. Water Resour. Res. 54, 6168–6188.  
<https://doi.org/10.1029/2017WR022037>

- Soler M., J. Latron and F. Gallart, 2008: Relationships between suspended sediment concentrations and discharge in two small research basins in a mountainous Mediterranean area (Vallcebre, Eastern Pyrenees). *Geomorphology* 98, 143–152.  
<https://doi.org/10.1016/j.geomorph.2007.02.032>
- Stubblefield A.P., J.E. Reuter, R.A. Dahlgren and C.R. Goldman, 2007. Use of turbidometry to characterize suspended sediment and phosphorus fluxes in the Lake Tahoe basin, California, USA, *Hydrological Processes* 21, 281–291. DOI: 10.1002/hyp.6234
- Terajima, T., Y. Sakamoto, Y. Nakai and K. Kitamura, 1997. Suspended sediment discharge in subsurface flow from the head hollow of a small forested watershed, northern Japan, *Earth Surface Processes and Landforms* 22 (11), 987–1000. [https://doi.org/10.1002/\(SICI\)1096-9837\(199711\)22:11<987::AID-ESP790>3.0.CO;2-X](https://doi.org/10.1002/(SICI)1096-9837(199711)22:11<987::AID-ESP790>3.0.CO;2-X)
- Thomas S.M., S.F. Ledgard and G.S. Francis, 2005. Improving calculates of nitrate leaching for quantifying New Zealand’s indirect nitrous oxide emissions. *Nutr Cyc Agroecosys* 73: 213–226. doi:10.1007/s10705-005-2476-8
- Tiefenbacher A., G. Weigelhofer, A. Klik, M. Pucher, J. Santner, W. Wenzel, A. Eder and P. Strauss, 2020. Short-term effects of fertilization on dissolved organic matter in soil leachate. *Water (Switzerland)* 12. <https://doi.org/10.3390/w12061617>
- Tipping E., C. Woof, E. Rigg, A.F. Harrison, P. Ineson, K. Taylor, D. Benham, J. Poskitt, A.P. Rowland, R. Bol and D.D. Harkness, 1999. Climatic influences on the leaching of dissolved organic matter from upland UK moorland soils, investigated by a field manipulation experiment. *Environ. Int.* 25, 83–95. [https://doi.org/10.1016/S0160-4120\(98\)00098-1](https://doi.org/10.1016/S0160-4120(98)00098-1)
- Tucker L.R., 1951. A method for synthesis of factor analysis studies. Washington, DC: Department of the Army. Pers. Res. Sect. Rep. No. 984.
- Vidon P., L.E. Wagner and E. Soyeux, 2008. Changes in the character of DOC in streams during storms in two Midwestern watersheds with contrasting land uses. *Biogeochemistry* 88, 257–270. <https://doi.org/10.1007/s10533-008-9207-6>
- Vinther F.P., E.M. Hansen and J. Eriksen, 2006. Leaching of soil organic carbon and nitrogen in sandy soils after cultivating grass-clover swards. *Biol. Fertil. Soils* 43, 12–19. <https://doi.org/10.1007/s00374-005-0055-4>
- vonUnold G. and J. Fank, 2008. Modular design of field lysimeters for specific application needs. *Water Air Soil Pollut. Focus* 8:233–242. doi:10.1007/s11267-007-9172-4
- Walling D.E. and A. Teed, 1971. A simple pumping sampler for research into suspended sediment transport in small catchments, *Journal of Hydrology* 13, 325–337. [https://doi.org/10.1016/0022-1694\(71\)90251-4](https://doi.org/10.1016/0022-1694(71)90251-4)
- Walling D.E., 1988. Erosion and sediment yield research – some recent perspectives. *Journal of Hydrology*, 100, 113–141. [https://doi.org/10.1016/0022-1694\(88\)90183-7](https://doi.org/10.1016/0022-1694(88)90183-7)
- Ward P.D., G.H. Garrison, K.H. Williford, D.A. Kring, D. Goodwin, M.J. Beattie and C.A. McRoberts, 2007. The organic carbon isotopic and paleontological record across the Triassic-Jurassic boundary at the candidate GSSP section at Ferguson Hill, Muller Canyon, Nevada, USA.

- Palaeogeogr. Palaeoclimatol. Palaeoecol. 244, 281–289.  
<https://doi.org/10.1016/j.palaeo.2006.06.042>
- Wass P.D. and G.J.L. Leeks, 1999. Suspended sediment fluxes in the Humber catchment, UK, *Hydrological Processes* 13, 935-953. [https://doi.org/10.1002/\(SICI\)1099-1085\(199905\)13:7<935::AID-HYP783>3.0.CO;2-L](https://doi.org/10.1002/(SICI)1099-1085(199905)13:7<935::AID-HYP783>3.0.CO;2-L)
- Weigelhofer, G., J. Fuchsberger, B. Teufl, N. Welti and T. Hein, 2012. Effects of Riparian Forest Buffers on In-Stream Nutrient Retention in Agricultural Catchments. *J. Environ. Qual.* 41, 373–379. <https://doi.org/10.2134/jeq2010.0436>
- Weishaar, J.L., G.R. Aiken, B.A. Bergamaschi, M.S. Fram, R. Fujii and K. Mopper, 2003a. Evaluation of specific ultraviolet absorbance as an indicator of the chemical composition and reactivity of dissolved organic carbon. *Environ. Sci. Technol.* 37, 4702–4708. <https://doi.org/10.1021/es030360x>
- Weishaar J.L. G.R. Aiken, B.A. Bergamaschi, M.S. Fram, R. Fujii and K. Mopper, 2003b. Evaluation of specific ultraviolet absorbance as an indicator of the chemical composition and reactivity of dissolved organic carbon. *Environ. Sci. Technol.* 37, 4702–4708. <https://doi.org/10.1021/es030360x>
- Williams C.J., A.B. Scott, H.F. Wilson and M.A. Xenopoulos, 2012. Effects of land use on water column bacterial activity and enzyme stoichiometry in stream ecosystems. *Aquat. Sci.* 74, 483–494. <https://doi.org/10.1007/s00027-011-0242-3>
- Williams, C.J., Y. Yamashita, H.F. Wilson, R. Jaffe and M.A. Xenopoulos, 2010. Unravelling the role of land use and microbial activity in shaping dissolved organic matter characteristics in stream ecosystems. *Limnol. Oceanogr.* 55, 1159–1171. <https://doi.org/10.4319/lo.2010.55.3.1159>
- Williams G.P., 1989. Sediment concentration versus water discharge during single hydrological events in rivers, *Journal of Hydrology* 111, 89-106. [https://doi.org/10.1016/0022-1694\(89\)90254-0](https://doi.org/10.1016/0022-1694(89)90254-0)
- Williamson J.C., T.D. Taylor, R.S. Torrens and M. Vojvodic-Vukovic, 1998. Reducing nitrogen leaching from dairy farm effluent-irrigated pasture using dicyandiamide: a lysimeter study. *Agr, Ecosys and Environ* 69: 81-88. doi: 10.1016/S0167-8809(98)00099-1
- Wilson H. and M.A. Xenopoulos, 2009. Effects of agricultural land use on the composition of fluvial dissolved organic matter. *Nat. Geosci.* 37–41. <https://doi.org/https://doi.org/10.1038/ngeo391>
- Wondzell S.M., M. N. Gooseff and B. L. McGlynn, 2010. An analysis of alternative conceptual models relating hyporheic exchange flow to diel fluctuations in discharge during baseflow recession. *Hydrol. Process.* 24, 686-694. <https://doi.org/10.1002/hyp.7507>
- Worrall F. and T.P. Burt, 2007. Trends in DOC concentration in Great Britain. *J. Hydrol.* 346, 81–92. <https://doi.org/10.1016/j.jhydrol.2007.08.021>
- Yeshaneh, E., A. Eder and G. Blöschl, 2013. Temporal variation of Suspended Sediment transport in the Koga Catchment, North Western Ethiopia and environmental implications. *Hydrol. Process.*, 28, 24, 5972-5984. <https://doi.org/10.1002/hyp.10090>

- Zhang, J., Y. Wu, T.C. Jennerjahn, V. Ittekkot and Q. He, 2007. Distribution of organic matter in the Changjiang (Yangtze River) Estuary and their stable carbon and nitrogen isotopic ratios: Implications for source discrimination and sedimentary dynamics. <https://doi.org/10.1016/j.marchem.2007.02.003>
- Zsolnay A., 1996. Dissolved Humus in Soil Waters, in: Humic Substances in Terrestrial Ecosystems. Elsevier, pp. 171–223. <https://doi.org/10.1016/b978-044481516-3/50005-0>
- Zsolnay A., E. Baigar, M. Jimenez, B. Steinweg and F. Saccomandi, 1999. Differentiating with fluorescence spectroscopy the sources of dissolved organic matter in soils subjected to drying. *Chemosphere* 38, 45–50. [https://doi.org/10.1016/S0045-6535\(98\)00166-0](https://doi.org/10.1016/S0045-6535(98)00166-0)